AD-A186 905 ACOUSTIC BACKSCATTERING FROM BOTTOM SEDIMENT AT NORMAL INCIDENCE IN THE LABORATORY(U) NAVAL POSTGRADUATE SCHOOL MONTEREY CA T YU SEP 87 1/2

UNCLASSIFIED F/G 20/1 NL

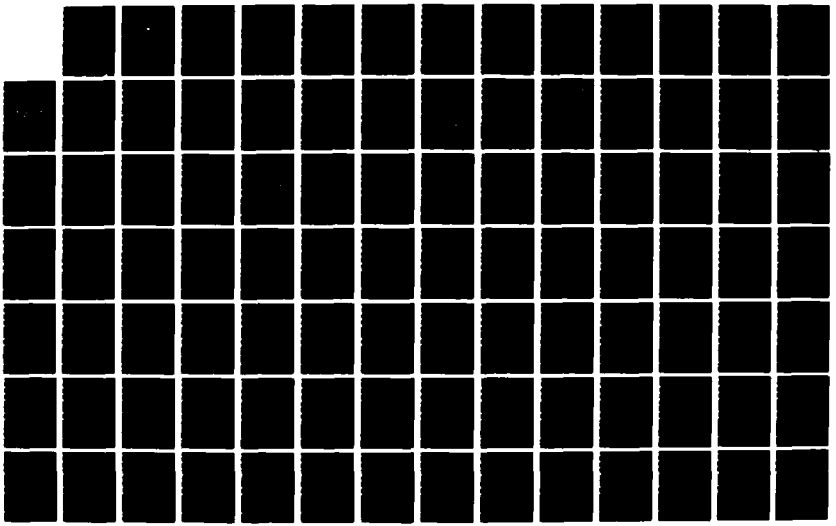

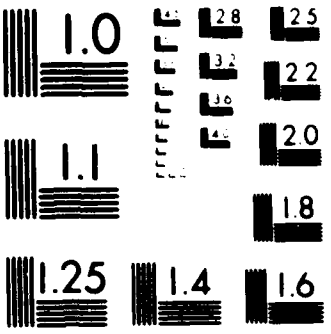

MICROCOPY RESOLUTION TEST CHART
NATIONAL BUREAU OF STANDARDS-1963-A

DTIC FILE COPY

(2)

AD-A186 905

NAVAL POSTGRADUATE SCHOOL

Monterey, California

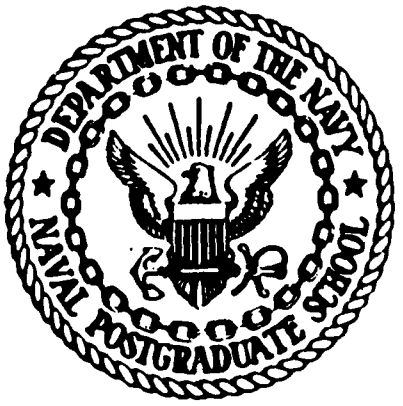

DTIC
ELECTE
DEC 2 8 1987
S D
H

THESIS

ACOUSTIC BACKSCATTERING FROM BOTTOM SEDIMENT AT NORMAL INCIDENCE IN THE LABORATORY

by

Yu, Ta-Te

September 1987

Co-Advisor	James V. Sanders
Co-Advisor	Alan B. Coppens
Co-Advisor	Stevens P. Tucker

Approved for public release; distribution is unlimited.

87 12 14 148

SECURITY CLASSIFICATION OF THIS PAGE

REPORT DOCUMENTATION PAGE

1a REPORT SECURITY CLASSIFICATION Unclassified	1b RESTRICTIVE MARKINGS
2a SECURITY CLASSIFICATION AUTHORITY	3 DISTRIBUTION/AVAILABILITY OF REPORT Approved for public release; distribution is unlimited
2b DECLASSIFICATION/DOWNGRADING SCHEDULE	
4 PERFORMING ORGANIZATION REPORT NUMBER(S)	5 MONITORING ORGANIZATION REPORT NUMBER(S)
6a NAME OF PERFORMING ORGANIZATION Naval Postgraduate School 6b OFFICE SYMBOL (If applicable) code 68	7a NAME OF MONITORING ORGANIZATION Naval Postgraduate School
6c ADDRESS (City, State, and ZIP Code) Monterey, California 93943-5000	7b ADDRESS (City, State, and ZIP Code) Monterey, California 93943-5000
8a NAME OF FUNDING/SPONSORING ORGANIZATION 8b OFFICE SYMBOL (If applicable)	9 PROCUREMENT INSTRUMENT IDENTIFICATION NUMBER
8c ADDRESS (City, State, and ZIP Code)	10 SOURCE OF FUNDING NUMBERS PROGRAM ELEMENT NO / PROJECT NO / TASK NO / WORK UNIT ACCESSION NO

11 TITLE (Include Security Classification)
Acoustic Backscattering From Bottom Sediment At Normal Incidence In The Laboratory

12 PERSONAL AUTHOR(S)
Yu, Ta-Te

13a TYPE OF REPORT	13b TIME COVERED	14 DATE OF REPORT (Year, Month, Day)	15 PAGE COUNT
Master's Thesis	FROM _____ TO _____	1987 September	100

16 SUPPLEMENTARY NOTATION

17 COSATI CODES			18 SUBJECT TERMS (Continue on reverse if necessary and identify by block number)
FIELD	GROUP	SUB-GROUP	volume reverberation, waveform envelope, scattering coefficient, decay constant, sediment

19 ABSTRACT (Continue on reverse if necessary and identify by block number)

Normally incident sound pulses were used to investigate sediment types in the laboratory. Materials of five different grain sizes, ranging in diameter from 0.16 to 5.30 mm, were used to find acoustic volume reverberation at three frequencies. An acoustic volume reverberation model was used to test the experimental data and to determine the scattering coefficients for the individual sediments.

It was found that different sediments have different volume reverberations. From the slope of the trailing edge of the volume reverberation, the sediment type can be determined roughly. Different frequencies were used to find the relationship between volume reverberation and frequency, and the results showed that with increase in frequency the volume reverberation of the sediment will be decreased.

20 DISTRIBUTION/AVAILABILITY OF ABSTRACT	21 ABSTRACT SECURITY CLASSIFICATION	
☐ UNCLASSIFIED/UNLIMITED ☐ SAME AS RPT ☐ DTIC USERS	unclassified	
22a NAME OF RESPONSIBLE INDIVIDUAL Stevens P. Tucker	22b TELEPHONE (Include Area Code) (408) 646-3269	22c OFFICE SYMBOL code 68Tx

DD FORM 1473, 84 MAR 83 APR edition may be used until exhausted
All other editions are obsolete

SECURITY CLASSIFICATION OF THIS PAGE

Approved for public release; distribution is unlimited.

Acoustic Backscattering From Bottom Sediment At Normal Incidence In The Laboratory

by

Yu, Ta-Te
Lieutenant Commander, Republic Of China Navy
B.S., Chung-Cheng Institute Of Technology, 1979

Submitted in partial fulfillment of the

MASTER OF SCIENCE IN HYDROGRAPHIC SCIENCES

from the

NAVAL POSTGRADUATE SCHOOL
September 1987

Author: Yu, Ta-Te 17/9
YU, TA-TE

Approved by: James V. Sanders per GBC
James V. Sanders, Co-Advisor

Alan B. Coppens 18 Sept '87
Alan B. Coppens, Co-Advisor

Stevens P. Tucker
Stevens P. Tucker, Co-Advisor

Curtis A. Collins
Curtis A. Collins, Chairman,
Department of Oceanography

G E Schacher
Gordon E. Schacher,
Dean of Science and Engineering

ABSTRACT

Normally incident sound pulses were used to investigate sediment types in the laboratory. Materials of five different grain sizes ranging in diameter from 0.16 to 5.30 mm were used to find acoustic volume reverberation at three frequencies. An acoustic volume reverberation model was used to test the experimental data and to determine the scattering coefficients for the individual sediments.

It was found that different sediments have different volume reverberations. From the slope of the trailing edge of the volume reverberation, the sediment type can be determined roughly. Different frequencies were used to find the relationship between volume reverberation and frequency, and the results showed that with increase in frequency the volume reverberation of the sediment decreases.

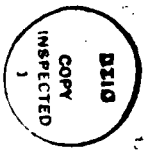

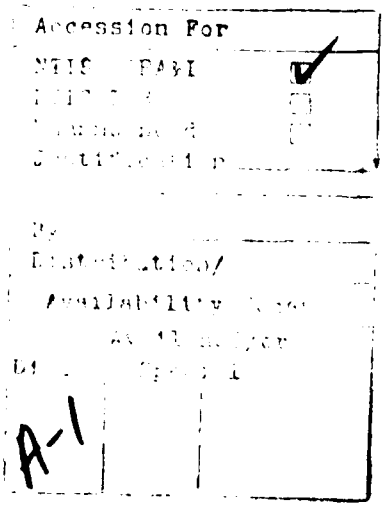

TABLE OF CONTENTS

LIST OF TABLES

LIST OF FIGURES

ACKNOWLEDGEMENT

The author expresses his appreciation to Dr. James V. Sanders, Dr. Alan B. Coppens, and Dr. Stevens P. Tucker for their technical advice. I also want to thank Mr. Dale Garlowitz, Lt. F. Rossman, Lt. R. Koehler for their help and AMOL Ocean Acoustics Division, Miami, of the National Oceanic and Atmosphereric Administration (NOAA) for provided the transducer.

Also, I would like to express my sincere appreciation to my parents, my wife and my son for their encouragement and understanding.

I. INTRODUCTION

The underwater echo-sounder is used mainly for sounding purposes and has become an essential part of the equipment used by hydrographers. But sounding is not the only role for echo-sounders; it may also serve as a fish-finder for fishermen, sub-bottom profiler for marine geologists, etc.

To provide nautical charts containing information about the bottom type, acoustic techniques can provide a rapid remote method for the examination of the sea-bed and sub-bottom. It has been and continues to be the aim of many workers to apply acoustic methods to the quantitative classification of sedimentary sea-bottoms.

A sound beam projected onto to the sea-bottom interacts with the water-sediment interface, the nature of its echo will depend on the bottom type and roughness. For plane fluid reflectors, the amplitude of an acoustic wave echo is governed by the Rayleigh reflection coefficient (Bezdek, 1973). The coefficient is an explicit function of the properties of the two mediums, i.e. their densities, sound speeds, and the angle of incidence.

However, if the boundary is not plane, instead acting as a scattering surface, scattering will affect the value of the apparent reflection coefficient; the degree that it does depends on the scale of the boundary irregularities relative to the acoustic wavelength (Huang, 1971). In this situation the result is that some energy will be scattered backward from the interface and some will penetrate into the bottom, where it is both absorbed and scattered. The backscattered energy from within the bottom is manifested as bottom reverberation. This is illustrated in Figure 1.1 which shows sound impinging on a rough bottom where reflection occurs at the interface before and after it is scattered by volume inhomogeneities in the sediment.

Since different sediments have different grain sizes, they have different surface and volume reverberation characteristics. How to use this simple but important fact to classify the materials forming the surface of a sea-bed is the subject of this research.

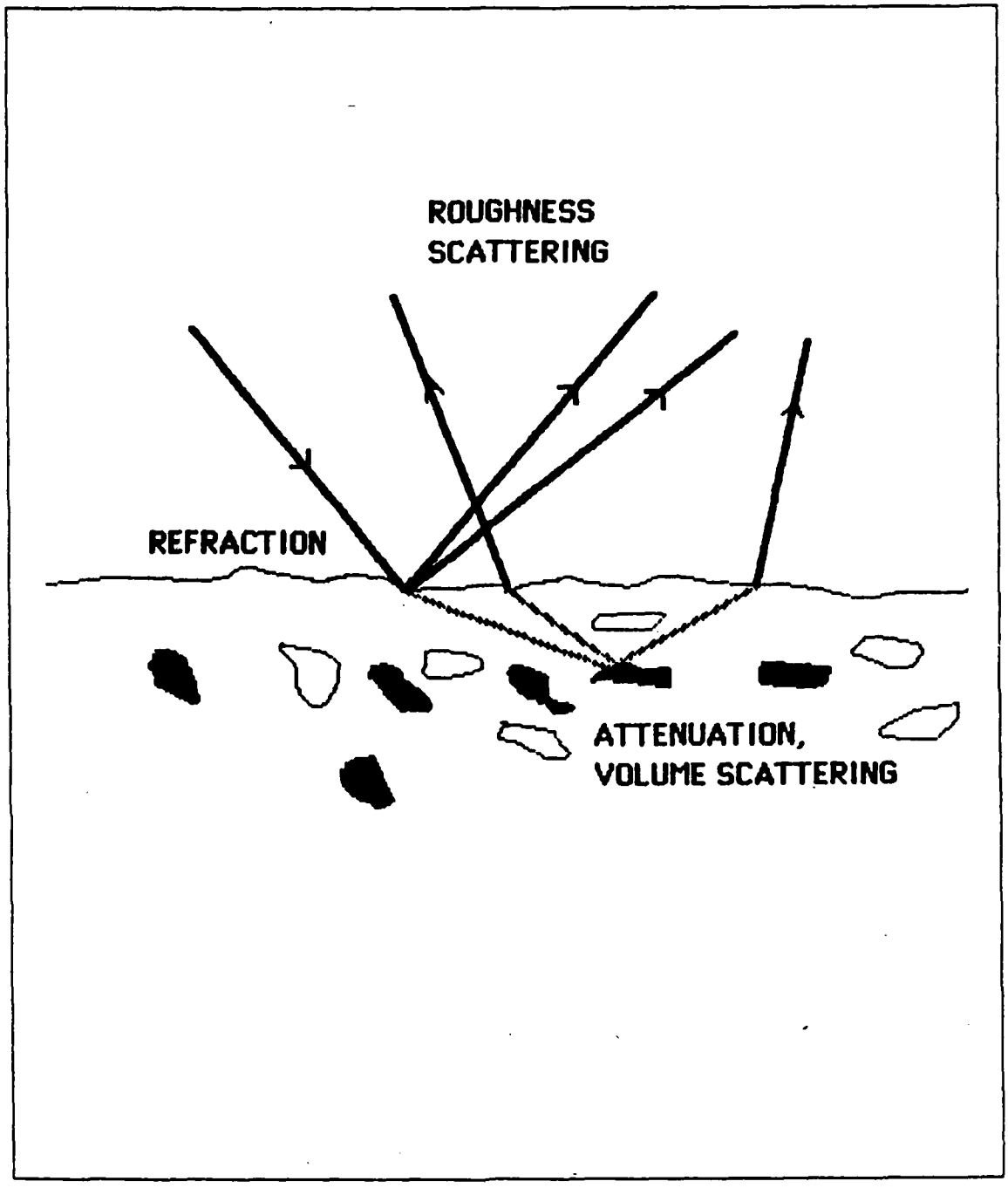

Figure 1.1 Bottom acoustic scattering mechanisms.

II. BACKGROUND AND LITERATURE REVIEW

To provide an understanding of this experiment some background information relevant to the interaction of sound with the water column and sea-bed is provided.

A. REVERBERATION

In an empty room or in a mountain valley it is not unusual for a sound to persist even though its source has been cut off. This reverberation usually decreases rapidly in intensity with time. When distinct echoes are not heard, the reverberation may be considered as a blending of a large number of echoes.

Similarly, when a sound beam is projected into the ocean from a sound projector, a persistence of sound is observed either when the projector serves also as a hydrophone (monostatic case), or when a separate hydrophone is used (bistatic case). But since the ocean is really not a closed volume like a room, and the medium is also different, the explanation of ocean reverberation must differ from that for room reverberation.

In the ocean the roughness of the surface and bottom, air bubbles, suspended solid matter, and organic matter such as plankton and fish cause inhomogeneities. These "targets" scatter sound back to the hydrophone as a large number of weak echoes which are observed as reverberation or backscattering (Eyring, 1948).

In an ocean environment the reverberation may be one of three types according to where the scatterers are located. One type of scattering occurs in the volume of the sea, or in the volume of the sea sediment, and produces volume reverberation. Sea-surface reverberation is produced by scatterers located on or near the the sea surface, and bottom reverberation originates at scatterers on or near the sea bottom. The last two types of reverberation may be considered together as surface reverberation, since a two-dimensional distribution of scatterers is involved (Urick, 1983).

B. HISTORICAL PERSPECTIVE

The investigation of sound scattering by the ocean bottom began during the Second World War and was carried out both in shallow and in deep water (Bunchuk and Zhitkovskii, 1980). The earliest attempts to use backscattered sound to classify sediment types were at both normal angles of incidence and at different grazing angles. Frequencies used were mostly below 200 kHZ (Gurcan, Creasey and Gazey, 1981).

Descriptions of the backscattering fall into two categories: One approach is to attribute the backscattering to surface roughness, while the other is to consider that the bottom backscattering is due to volume backscattering (Eckart, 1953; Horton and Muir, 1967).

A different approach was followed by Pace and Ceen (1982) who showed on the basis of the time spreading of rectified returns that sea-bottoms of mud, sand, fine gravel, coarse gravel may be distinguished one from another. Gurcan, Creasey and Gazey (1981) found the power spectrum of backscattered sound to exhibit harmonically-related resonance peaks. From their positions and spacings these resonances can be used for classification purposes.

Other important work was done by Breslau (1967), McLeroy (1972), Dodds (1984), and Meng and Dinghua (1984). Breslau was concerned with interference based on the reflection coefficient of the bottom; McLeroy and Meng and Dinghua were concerned with extracting information from the echo waveform. Dodds company, Huntec, Ltd., has developed the Deep Tow System which uses a broadband acoustic source (1-10 kHZ) to remotely classify the bottom with some success. Recent work done by Diaz (1986), Chang (1986), and Facada (1987), used high-frequency (181 kHZ) tone-burst signals at normal incidence to show that the volume reverberation of sediment is proportional to grain sizes.

III. MODEL DEVELOPMENT

Since sound waves interact with the water-sediment interface, the backscattering energy from the interface is dependent not only on the surface roughness but on the sediment volume scattering as well. The theoretical considerations of this experiment therefore should include both surface and volume reverberation from the sediment. For this reason some basic surface and volume scattering theory will be discussed, and finally, a simple model will be developed.

A. SCATTERING STRENGTH AND REVERBERATION LEVEL

1. Scattering Strength

The physical property upon which reverberation depends is called the surface or volume scattering strength. It is defined to be

$$S_{s,v} = 10 \log (I_{scat}/I_{inc}) \tag{3.1}$$

In this parameter the unit is decibel, I_{scat} is the intensity of the sound scattered by a unit area or volume refer to a unit distance, and I_{inc} is the incident plane wave intensity. If the direction of scattering is back to the source, the quantity S is termed backscattering strength. The scattering strength for volume and surface reverberation are illustrated in Figures 3.1a and 3.1b (Urick, 1983). It is customary to use the backscattering cross section of a unit area or volume as the basic parameter involving scattering; it is given the symbols m_v and m_s and is the ratio of scattered power, refered to unit distance, to the intensity incident on a unit volume or area. Thus,

$$I_{scat} = m_{s,v}/\text{area or volume} \tag{3.2}$$

If it is assumed that the scattering is uniformly distributed over a sphere, or a hemisphere, Equations (3.1) and (3.2) give

$$S_V = 10 \log (m_V/4\pi) \tag{3.3}$$

$$S_S = 10 \log (m_S/2\pi) \tag{3.4}$$

2. Reverberation Level And Assumptions

In the sonar equation, the term RL refers to the "equivalent plane-wave reverberation level". This is the level of the axially incident plane wave which produces the same hydrophone voltage across the hydrophone terminals as that produced by the received reverberation.

To find an explicit expression for RL, some simplifying assumptions are needed:

1. Straight-line propagation paths, with all sources of attenuation other than spherical spreading neglected.

2. A random, homogeneous distribution of scatterers throughout the area or volume producing reverberation at any one instant of time.

3. A density of scatterers so large that a large number of scatterers occur in an elemental volume dV or dA.

4. A pulse length short enough for propagation effects over the range extension of the elemental volume or area to be neglected.

5. An absence of multiple scattering, that is, the reverberation produced by reverberation is negligible.

B. SURFACE SCATTERING THEORY

Surface scattering means scattering produced by scatterers distributed over a nearly plane surface rather than throughout a volume. In terms of decibels the reverberation level can be expressed as

$$RL_S = 10 \log [(I_0/r^4)u_S \int b(\theta,\varphi)\, b'(\theta,\varphi)dA] \tag{3.5}$$

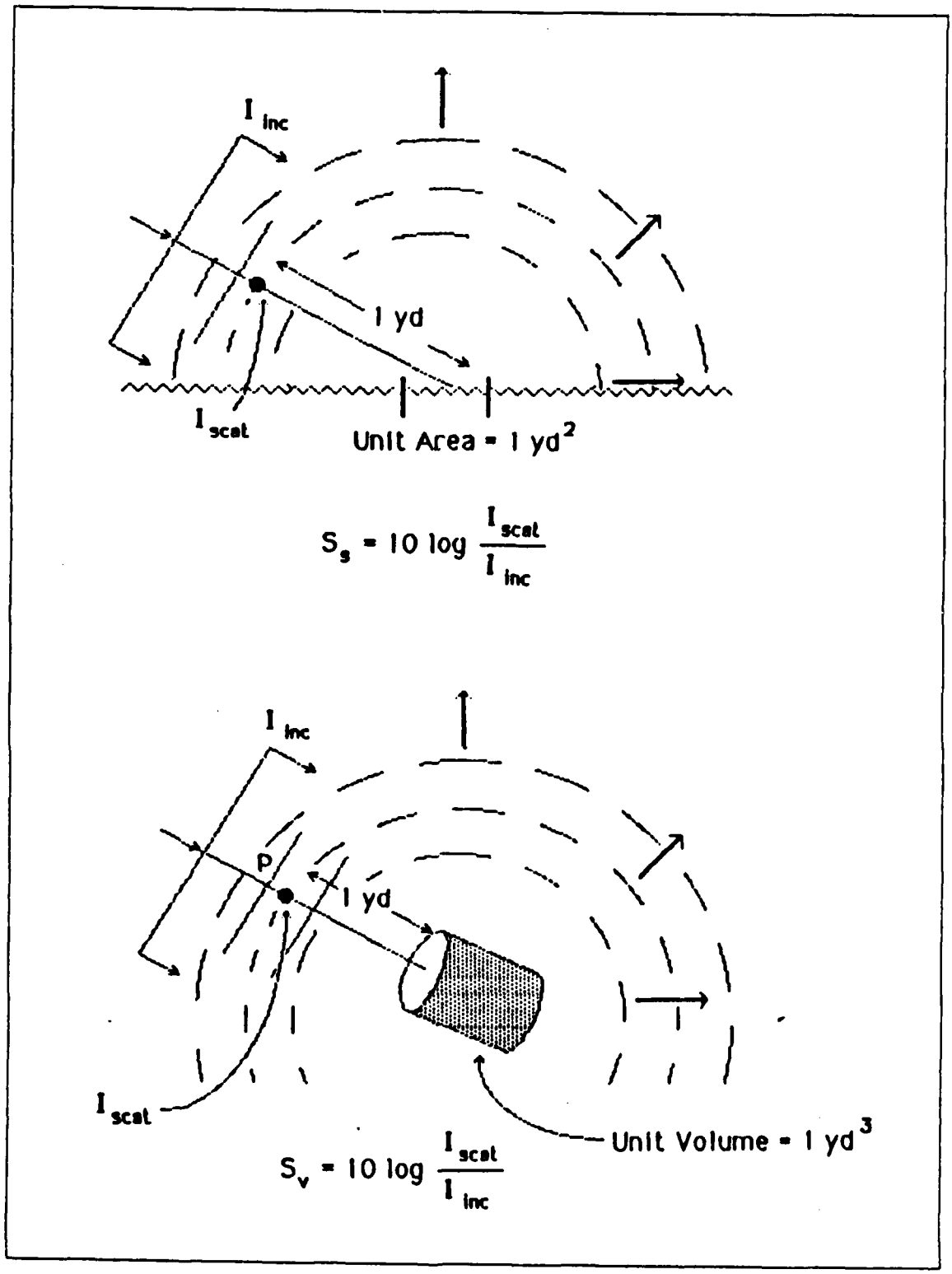

Figure 3.1 scattering strength for volume and surface scattering.

Where

dA = elemental area of the scattering surface.

I_o = axial intensity at unit distance from source.

r = distance between transducer and scattering surface.

$10 \log u_s = S_s$ is the scattering strength for surface reverberation.

$b(\theta,\varphi)$ = beam pattern function of the projector.

$b'(\theta,\varphi)$ = beam pattern function of the hydrophone.

θ = vertical beam angle (normally small)

φ = horizontal beam angle.

$b(\theta,\varphi)$ is the beam pattern function which acts to define the projector's major lobe. On the beam center $b(\theta,\varphi) = 1$, but it drops to 0.707 at the 1/2 power point, i.e. I_o is reduced by 3 dB. In monostatic sonar the same transducer is used both for projection and reception, and we can assume that transmitted and received patterns are the same; but in practice they need not be.

If dA is taken as a portion of a circular annulus in the plane of the scatterers, according to Figure. 3.2 we may then write

$$dA = (c\tau/2)r d\Theta \tag{3.6}$$

Then reverberation level becomes

$$RL_s = 10 \log (I_o/r^4) u_s (c\tau/2) r \int b(\theta,\varphi) b'(\theta,\varphi) d\Theta \tag{3.7}$$

For near grazing incidence, the axis of the beam is only slightly inclined toward the scattering surface, so that

$$\int b(\theta,\varphi) b'(\theta,\varphi) d\varphi = \int b^2(\theta,\varphi) d\varphi = \Phi \tag{3.8}$$

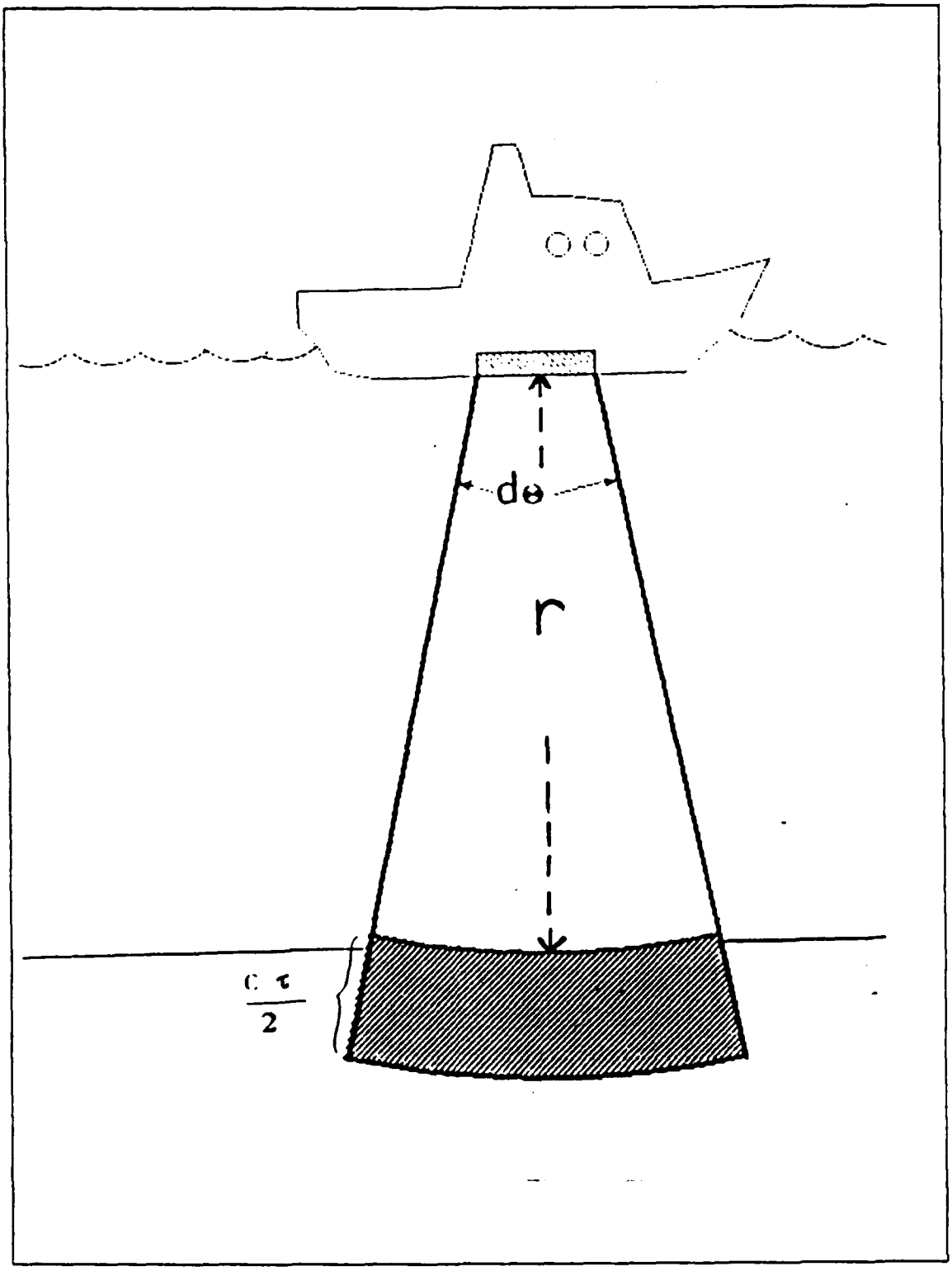

Figure 3.2 Elemental area of the scattering surface.

Where Φ is the effective horizontal beam width of the transmitting/receiving transducer, therefore

$$RL_s = 10 \log [(I_o/r^4)u_s(c\tau/2)r\Phi] \qquad (3.9)$$

$$= SL - 2TL + S_s + 10 \log A$$

Where

$10 \log I_o = SL$

$10 \log 1/r^4 = -2TL$

$10 \log u_s = S_s$

$(c\tau/2)r\Phi = A$

C. VOLUME SCATTERING THEORY

Due to inhomogeneities within the ocean volume, sound is scattered in all directions, and the portion of scattering which returns to transducer is known as backscattering or reverberation. Sound which has penetrated into sediment and is scattered back is also considered as volume reverberation. Volume scattering is illustrated in Figure 3.2a and 3.2b.

The volume reverberation can be expressed as

$$RL_v = 10 \log [(I_o/r^4)u_v \int b(\theta,\varphi)b'(\theta,\varphi)dV)] \qquad (3.10)$$

Individual terms have the same definition as used for surface reverberation except for the exchange of S_v for S_s and dV for dS. Here $10 \log u_v$ is the backscattering strength for volume reverberation and is denoted by the symbol S_v. The elemental volumes according to Figure 3.3 are

$$dV = r^2(c\tau/2)d\Omega \qquad (3.11)$$

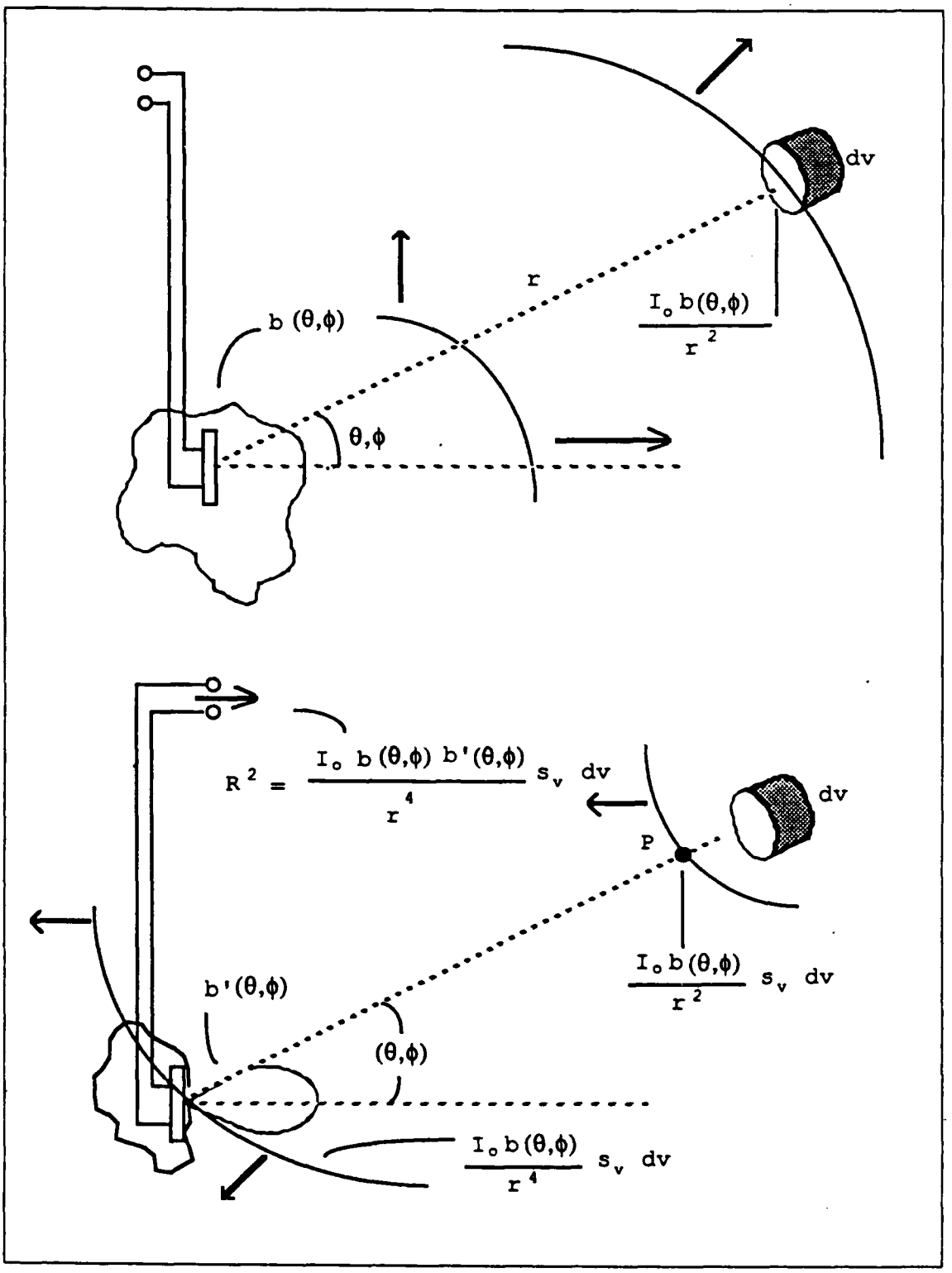

Figure 3.3 Geometric view of volume scattering.

Where τ is pulse length, c is the velocity of sound, and $d\Omega$ is the elemental solid angle subtended by dV at the source. The volume reverberation is

$$RL_V = 10 \log [(I_o/r^4)\, r^2(c\tau/2)S_V \int bb' d\Omega] \qquad (3.12)$$

Let the actual two-way beam pattern bb′ be replaced by an ideal pattern as shown in Figure 3.4. Then the width Ψ of this ideal beam is given by

$$\int bb' d\Omega = \int 1 \times 1 \, d\Omega = \Psi \qquad (3.13)$$

In terms of Ψ the reverberation level becomes

$$RL_V = 10 \log [(I_o/r^4)u_V(c\tau/2)\Psi r^2] \qquad (3.14)$$

$$= SL - 2TL + S_V + 10 \log V$$

where

$10 \log I_o = SL$

$10 \log 1/r^4 = -2TL$

$10 \log u_V = S_V$

$(c\tau/2)\Psi r^2 = V$

In summary the reverberation levels for surface and volume are

$RL_V = SL - 40 \log r + S_V + 10 \log V \qquad V = (c\tau/2)\Psi r^2$

$RL_S = SL - 40 \log r + S_S + 10 \log A \qquad A = (c\tau/2)\Phi r$

The most complicated terms in these two equations are the scattering strength S_V and S_S, in which

$S_V = 10 \log u_V \qquad S_S = 10 \log u_S$

The quantities of u_V and u_S can depend on the grazing angle of the incident wave relative to the bottom, the frequency, the scattering angle, and the surface relief and structure of the bottom (Buhchuk and Zhitkovskii, 1980).

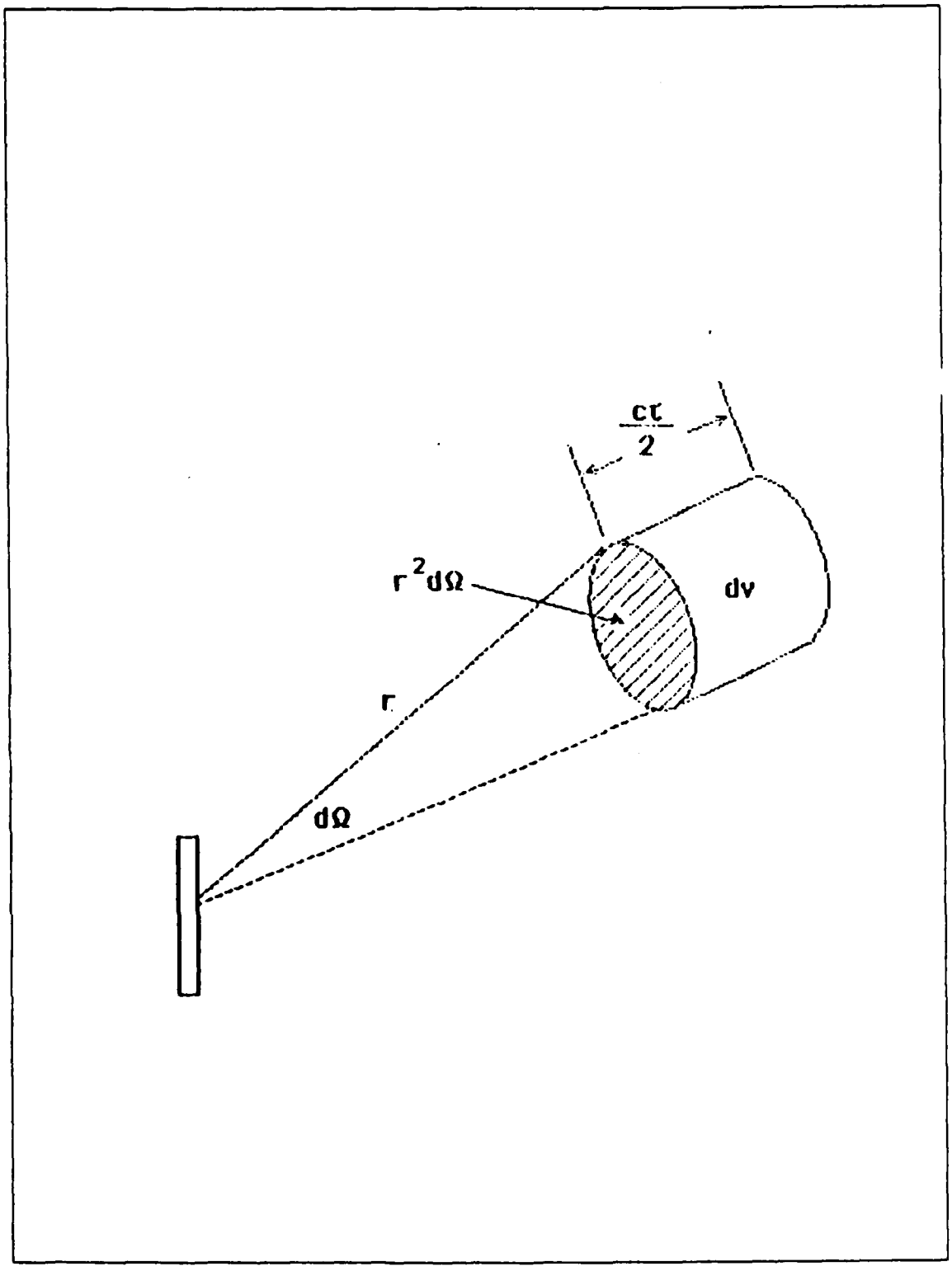

Figure 3.4 The elemental volume for volume scattering.

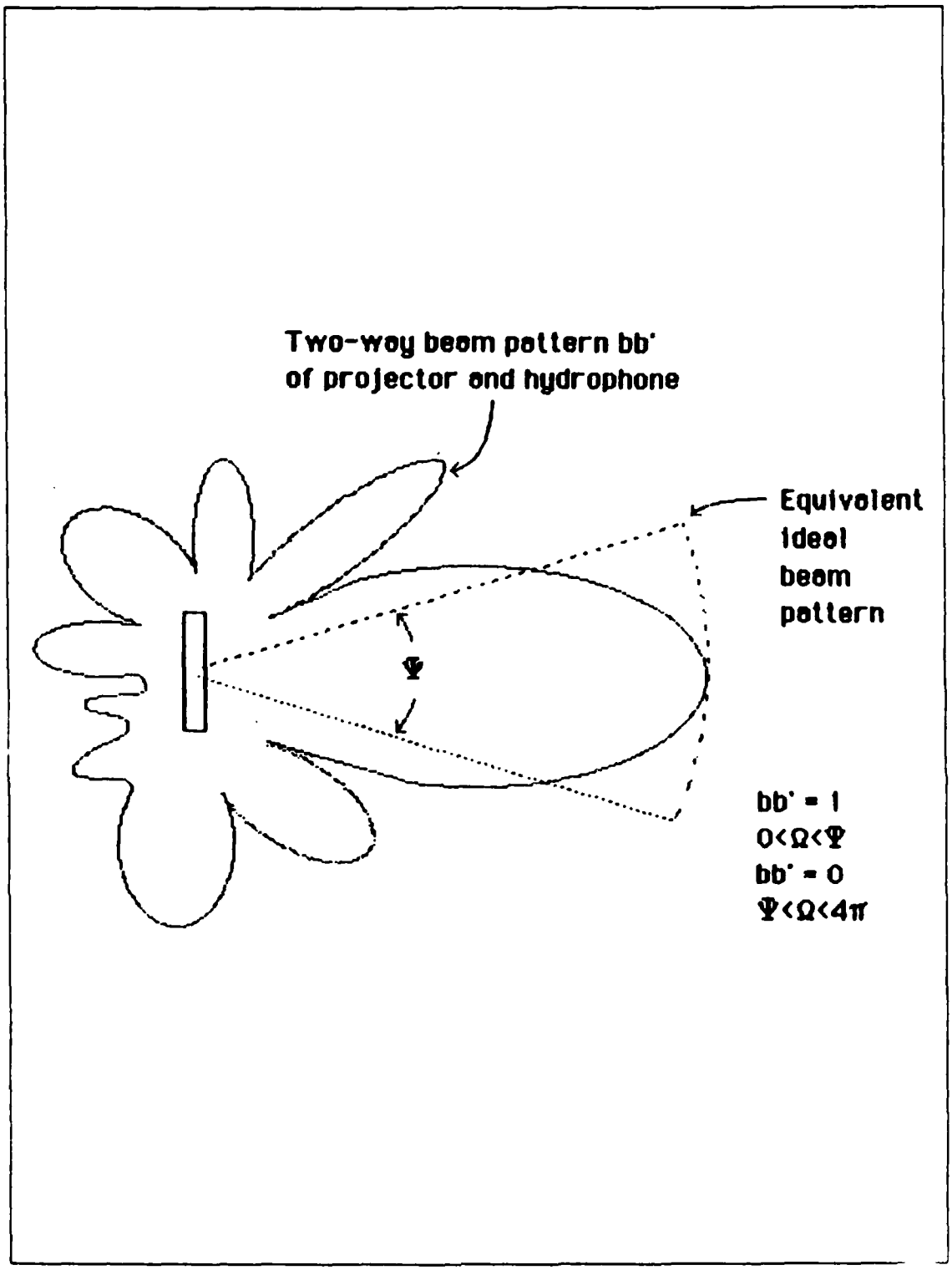

Figure 3.5 Actual and equivalent beam patterns.

D. MODEL OF ACOUSTIC BACKSCATTERING

The model of Sanders and Coppens (1986) was used for this experiment. It is as follows

The square pulse used to excite the transmitting transducer can be described by the unit step function, H.

$$V(t) = V_0[H(t) - H(t-\tau)] \tag{3.15}$$

where V(t) is the voltage at time t, V_0 is the maximum voltage, and τ is the pulse length.

$$H(t) = \begin{cases} 0 & t < 0 \\ 1 & t \geq 0 \end{cases}$$

$$H(t-\tau) = \begin{cases} 0 & t-\tau < 0 \\ 1 & t-\tau \geq 0 \end{cases}$$

The square electrical pulse is transformed by the transducer into an acoustic pulse with an exponential rise, an approximately flattened top, and an exponential decay. This shape of waveform can be described as

$$f(t) = (1-e^{-\alpha t})\, H(t) - (1-e^{-\alpha(t-\tau)})H(t-\tau) \tag{3.16}$$

where t is the time measured from the beginning of the pulse and α is the rise and decay constant (assumed to be the same).

For a transducer located in the water and sending out a sound pulse to a smooth sediment surface, the reflected pulse received by same transducer will have an intensity

$$I = [\int T_i^2 s_v e^{-\beta\xi} I_o f(t-2\xi/c)d\xi/(r+\xi)^2 + R_i f(t)/r^2]/r^2 \quad (3.17)$$

where

T_i = intensity transmission coefficient

s_v = volume scattering coefficient

β = absorption coefficient in sediment

ξ = affected sediment depth

R_i = intensity reflection coefficient

r = distance between transducer and sediment

From (eqn 3.17), the intensity contributed by scattering is

$$I_s = \int T_i^2 s_v e^{-\beta\xi} I_o f(t-2\xi/c)d\xi/(r+\xi)^2/r^2 \quad (3.18)$$

and the intensity contributed by the reflection is

$$I_r = R_i I_o f(t)/r^4 \quad (3.19)$$

If we assume $r > > \xi$, then

$$I_s = (T_i^2 s_v I_o/r^4) \int e^{-\beta\xi} f(t-2\xi/c)d\xi \quad (3.20)$$

where

$$f(t-2\xi/c) = (1-e^{-\alpha(t-2\xi/c)})H(t-2\xi/c)-(1-e^{-\alpha(t-\tau-2\xi/c)})H(t-\tau-2\xi/c) \quad (3.21)$$

The lower limit of ξ is zero; the upper limit is $ct/2$ for $H(t-2\xi/c)$ and $c(t-\tau)/2$ for $H(t-\tau-2\xi/c)$. Here only the decay portion, $t \geq \tau$, of interest. After integration we have

$$I_s = A\,[(1-e^{-c\beta t/2})/\beta - (e^{-c\beta t/2}-e^{-\alpha t})/(-\beta+2\alpha/c) \qquad (3.22)$$

$$+ (e^{-c\beta(t-\tau)/2}-1)/\beta + (e^{-c\beta(t-\tau)/2}-e^{-\alpha(t-\tau)})/(-\beta+2\alpha/c)]$$

where

$$A = T_i^2\, s_v\, I_o /r^4 \qquad (3.23)$$

with f(t) from Equation 3.16, I_r becomes

$$I_r = I_o\, R_i\, (e^{\alpha\tau}-1)e^{-\alpha t}/r^4 \qquad (3.24)$$

Adding two components I_r and I_s gives the total intensity received by the transducer:

$$I = N\{T_i^2 s_v/\beta[e^{-c\beta t/2}(e^{c\beta\tau/2}-1)] + T_i^2 s_v/(-\beta+2\alpha/c) \qquad (3.25)$$

$$[e^{-c\beta t/2}(e^{c\beta\tau/2}-1) + e^{-\alpha t}(1-e^{\alpha\tau})] + R_i(e^{\alpha\tau}-1)e^{-\alpha t}\}$$

where $N = I_o/r^4$

This formula looks quite complex, but all the variables in this expression are known except s_v . For this reason, trying different s_v values to get one to fit the experimental data for different kinds of sediments is an important goal of this research.

IV. EXPERIMENTAL DESIGN AND PROCEDURES

A. EQUIPMENT AND ACCESSORIES OF EXPERIMENT

1. Material Selection

In this experiment, five different sediments were used: Monterey fine sand #30, Monterey Aquarium #2, aggregate, and two sizes of glass beads. The sizes of the materials varies from 0.2 mm to 5.3 mm (Facada, 1987) and are listed in Table 1. Since the natural sediments used are inhomogeneous in composition and shape, a "sediment" composed of homogeneous particles (spherical glass beads) was chosen for some experiments.

The various materials were added to water and left in the test tank for two or three days to allow the water to completely saturate the sediment and to let air bubbles dissolve. To help remove air bubbles, a water jet or hand stirring was used until no further bubbles could be seen rising from the sediment. Bleach was added to the water to control biologic growth.

2. Experimental Tank

Two glass tanks, each measuring 70 cm × 70 cm × 60 cm, were filled with 24 cm of fine sand, aquarium sand, or aggregate sand, and 36 cm of water was added above the sand. Because of the limited volume of glass beads available, a plastic bucket was placed in the tank to contain them.

3. Electronic Equipment

A block diagram showing the equipment configuration is shown in Figure 4.1. The output from a General Radio Model 1310 oscillator with a frequency range of a 2 Hz to 2 MHz was simultaneously fed into a Hewlett- Packard HP 5233L frequency counter and a General Radio Type 396-A tone burst generator which was used to generate either 8- or 16-cycle pulses. The signal output passed through a Hewlett-Packard HP 467-A power amplifier, into a Datasonic Transmit/Receive (T/R) switch, then to the transducer. The output signal was also used to trigger a Tektronix Type RM 503 analog oscilloscope and a Nicolet Model 3091 digital oscilloscope.

The signal return from the sediment was received by the transducer, amplified 20 dB by a Hewlett-Packard 465-A pre-amplifier, and then passed through a Spencer Kennedy, Inc., Model 302 variable electronic filter which serves as a high-pass filter to eliminate low frequency noise before going to the oscilloscope.

TABLE 1
PHYSICAL PROPERTIES OF SEDIMENT

	FINE SAND	AGGREGATE SAND	AQUARIUM SAND	COARSE GLASS BEADS	FINE GLASS BEADS
a (mm)	0.3	5.3	1.72	1.7	0.16
ρ (g/cm^3)	2.69	2.64	2.59	2.50	2.48
ρ_{mix} (g/cm^3)	1.98	1.97	2.02	1.91	1.90
C (m/s)	1680	1555	1588	1822	1878
R_m	0.36	0.36	0.36	0.53	0.48
R_c	0.38	0.52	0.38	0.41	0.42

Three different transducers were used in the experiment. A Naval Research Laboratory F-41 circular-piston type had a 8.8 cm diameter active face and a thickness of 4.4 cm. Its resonance frequency was 185 kHz (Diaz, 1986). The second, a Ross transducer, was borrowed from the Acoustic Division of the Atlantic Meteorological and Oceanographic Laboratory (AMOL), Miami, of the National Oceanic and Atmospheric Administration (NOAA). This seven-element transducer has a frequency range from 20 kHz to 150 kHz with resonance frequencies at 62 kHz and 108 kHz; the -3 dB beamwidth at 62 kHz is 10 degrees, and at 108 kHz it is 5.5 degrees (AMOL/Ocean Acoustics Division, 1979). The third transducer, a Celesco Industries Type LC10 hydrophone, was used to measure the sound speed in the sediments. The LC10 is a small (0.97-cm diameter by 2.87-cm long) cylinder with a receiving range of 0.1 to 120 kHz.

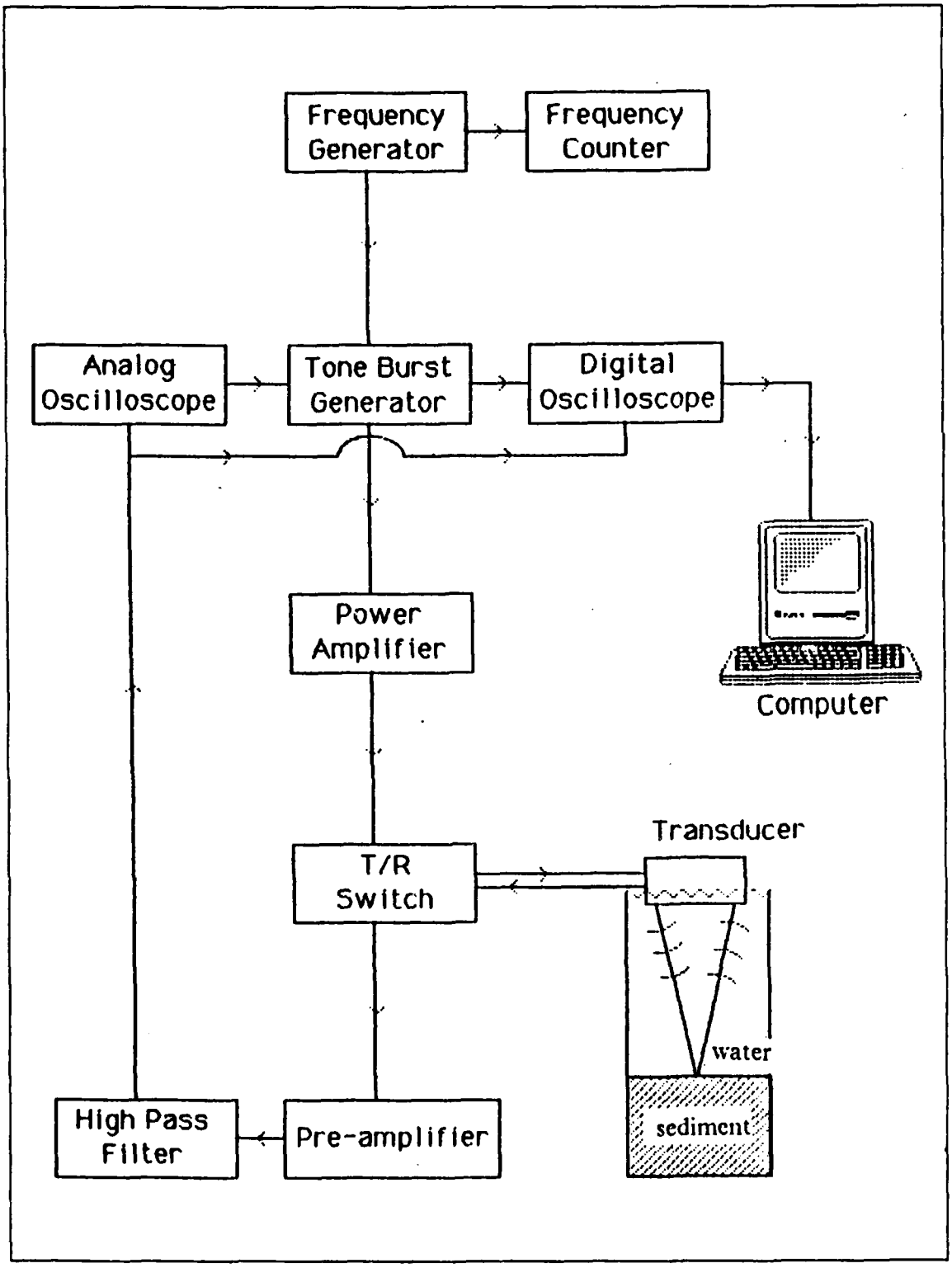

Figure 4.1 Schematic of the equipment configuration.

The waveform of the return signal was displayed on the digital oscilloscope and sent as a stream of characters to a HP-86 computer. To reduce manual operations a HP-3421A Data Acquisition and Control Unit was used to receive commands from the computer and then automatically control the digital oscilloscope.

B. MATERIAL PROPERTY MEASUREMENT

The physical properties of the sediments were measured for later use in computations.

1. Density

The water-saturated and dry densities of the different sediments were measured separately. The dry density was measured by filling a 100-ml graduated cylinder and weighting. After subtracting the weight of the empty cylinder to find the net weight of material, division by the volume gives the density. Water-saturated density was measured using the same method. The density measurement results are summarized in Table 4.1.

2. Speed of sound

The speed of sound was measured by using three LC-10 transducers inside the tank, one acting as source, the other two as receivers. The three LC-10s were inserted at the same depth in the sediments. One LC-10 was placed 15 cm away from the source, and the second LC-10 was moved along the straight line defined by the source and first receiver. The two signals shown on the digital oscilloscope (Figure. 4.2) allow measurement of the travel time over the known distance between two LC-10 receivers. From this the speed of sound in the sediment can be calculated.

3. Reflection coefficient

The normal-incidence pressure reflection and transmission coefficients were measured to check the computed value. The ratio of maximum measured voltage for signals returned from the sediment and from the water/air interface at same distance gives the reflection coefficient,

$$R_m = V_s/V_w \tag{4.1}$$

where

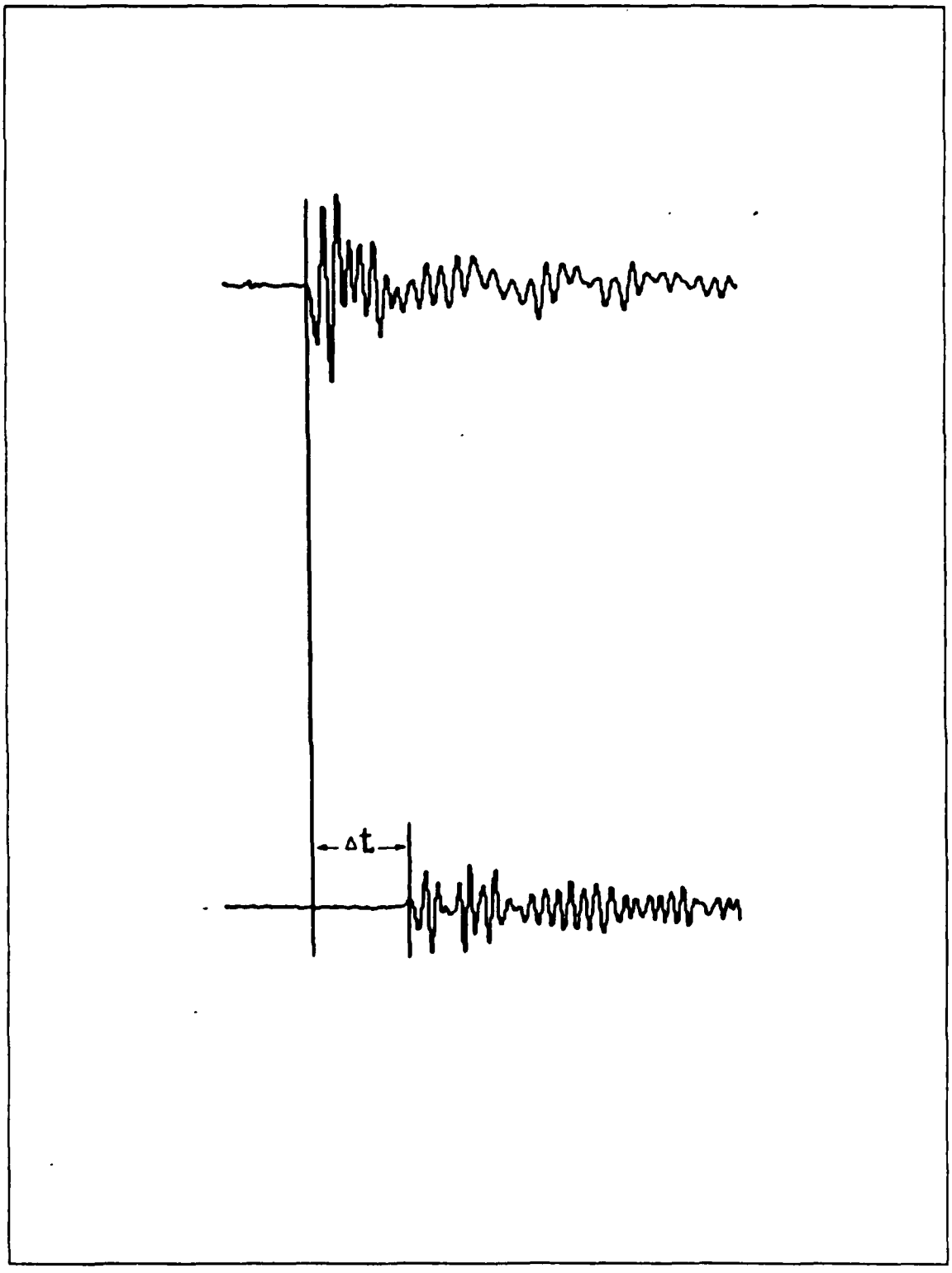

Figure 4.2 Two echos received on the digital oscilloscope.

V_w = maximum voltage of signal return from water/air interface.

V_s = maximum voltage of signal return from sediment.

Since the densities and sound speeds are known, the normal reflection coefficients of the different sediments can also be computed from

$$R_c = (r_2 - r_1)/(r_2 + r_1) \tag{4.2}$$

where

$r_1 = \rho_1 c_1$ is the specific acoustic impedance of water.
$r_2 = \rho_2 c_2$ is the specific acoustic impendance of sediment.

The measured and computed reflection coefficients are listed in Table 1.

C. EXPERIMENTAL DESIGN CONSIDERATIONS

1. Fundamental concept of experiment

The original hypothesis of this experiment was that the different sediments must have different volume reverberation characteristics and that there should exist a relationship between the sediment properties and their volume reverberations.

Let a transducer located in the water send out a sound pulse to the water/air interface. If the interface is smooth, the received echo waveform is purely reflection. If the interface is not smooth, then the amplitude of the received waveform is reduced because the sound energy scattered at the rough surface. Suppose the scattering is first order and the surface has the same roughness everywhere; then the echo is a combination of reflected and scattered energy, and its amplitude is reduced in relation to the purely reflected echo amplitude. In Figure 4.3(a) the solid line represents a purely reflected waveform, and the dashed line represents the combined reflected and scattered waveform.

If the echo is returned from a water/sediment interface instead of the water/air interface, the echo amplitude in the tail should be increased because additional energy

is scattered back from within the volume of sediment. In Figure 4.3(b) the dotted line represents the echo from the sediment, while the solid and dashed lines represent the purely-reflected water/air interface amplitude and the combined reflected and scattered amplitudes from the water/air interface.

2. **Experimental Considerations**

Some necessary considerations are required to ensure the success of this experiment. Some of these effects were studied by Diaz (1986) and Chang (1986).

a. Effects of the transmitting electronics

The the electrical signal from the tone burst generator applied to the transducer showed that the signal envelope was a clean square wave. This demonstrated that the transmitting electronics had a negligible effect on the received signal.

b. Effects Of Sampling Rate

The fastest sampling rate of the digital oscilloscope was 1 μs. and is not enough to give a precise reproduction of the echo waveform at the high frequencies used for this experiment. However, observation showed that there was natural "jitter" in the triggering of the scope, so that for consecutive pulses, the scope would sample different parts of the waveform. To obtain an accurate waveform, a large number of waveforms were sampled and averaged. If sufficient "jitter" were present, the voltage measured in a given sampling bin should vary between the maximum and minimum values in the vicinity of the corresponding time. Since the sine wave varied between negative and positive, these voltage values were squared before averaging in order to get an accurate shape of the waveform envelope.

To determine the minimum number of samples required for good reproduction of the shape of the waveform envelope, the water/air interface was measured with different number of samples by Diaz (1986) and Chang (1986). Their results showed that 50 samples for each data set were enough to give a true echo waveform.

c. Effects Of Water/Air Interface Interference

In an ideal situation the transducer should be far away from all unwanted surfaces to avoid interference. If the transducer is located close to the water surface and projects a pulse to the sediment surface below it, most of the energy will be sent to the sediment surface, but nevertheless some energy will be transmitted to the water surface and then reflected back toward the sediment. Restricted by the size of the test

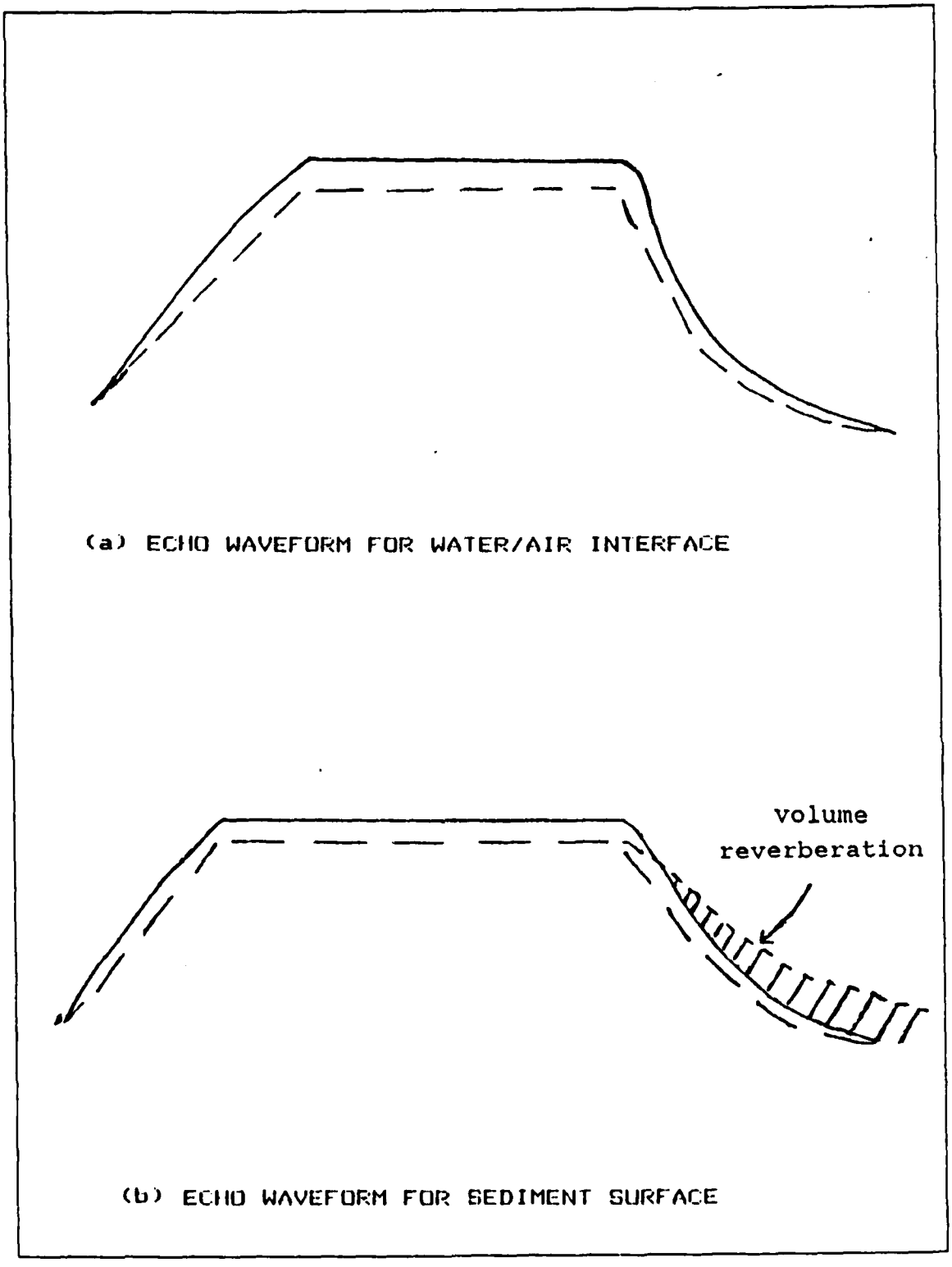

Figure 4.3 Theoretical echo waveform from water and sediment.

tank, the transducer had to be located close to the water surface. To find out the magnitude of this interference, the water surface was agitated by hand to alter the amount of reflection from the water surface. The observed waveform was not changed during the ruffling. It was concluded that this interference is negligible.

d. Effects Of Bottom Reflection Interference

To find out if the sediment in the test tank was thick enough to avoid reflection from the bottom of the tank, a simple computation is sufficient. For a 16-cycle signal with a frequency of 181 kHz, the pulse duration is 88 μs, and the decay time approximately 100 μs; the echo from the smooth water/air interface has the same decay time. For sound pulses in the sediment the decay time should be longer because of volume reverberation. For the fine sand the decay time is 152 μs, for a total time interval of 240 μs. With a sound speed of 1680 m/s for the fine sand, and a sediment depth of 25 cm, the echo from the bottom of the tank comes back to the surface of sediment 286 μs after the incident pulse begins reflecting from the surface of the sediment, too late to interfere with the reflected pulse. For the other sediments the depth was deep enough to prevent any bottom reflection interference.

e. Effects Of Side Lobe

Since the test tank was too small to avoid the interference, if any, caused by the side lobes, a test was necessary to find out if this is important. The half-beamwidth (-3 dB) for the F-41 transducer was measured to be 10.0° (Chang, 1986); for the Ross transducer the half beamwidth at 108 kHz it was 5.5° and at 62 kHz it was 10.0° (AMOL, 1979). For a 30-cm distance from transducer, the sediment surface insonified by the major lobe is a circular area of radius about 5.3 cm. Since the test tank dimensions were 70 cm × 70 cm × 60 cm, if the transducer is located at the center of tank, the major lobe will not strike the sides of the tank. To test this, Diaz (1986) and Chang (1986) disturbed the surface of the sediment outside the center 30 cm × 30 cm square area. Waveforms returning from the sediment were compared before and after the disturbance. They were indentical, indicating that the effect of the side lobe was negligible. For the Ross transducer the same measurement was made, resulting in the same conclusion.

f. Effects Of Sediment Inhomogeneity

The experiments of Diaz (1986) and Chang (1986) were bothered by a drastic change in the echo waveforms whenever the transducer was moved parallel to the smoothed aggregate or fine sand sediment surfaces. It was assumed that the

waveform fluctuations were caused by inhomogeneities in the sediment. Facada (1987) tried to use more homogeneous glass beads as sediment to prove this assumption, but the results did not satisfy him; the inconsistencies between echo waveforms from different pulses still existed. He concluded that the variations in the shape of the pulse tails increase as the grain size of the sediment increases and that changes in the echo waveforms resulted not from volume reverberation but from surface scattering.

To avoid particulate scattering the wave lengths should be at least three times longer than the grain size (Bradshw, 1981). To meet this criterion three different frequencies were used. For fine sand, since the largest grain size is 0.6 mm, a wavelength equal to 9.3 mm (181 kHz) readily qualifies. Two other frequencies, 108 kHz and 62 kHz, are applied to aquarium and aggregate sand, respectively.

g. Effects Of Gas Bubbles In The Sediment

Since we are only interested in the decay constant of the sediment itself, gas bubbles trapped inside the sediment should be removed before the experiment. To help remove gas bubbles a water jet was used to stir the sediments before each set of data measurements.

h. Effects of Gas Bubbles on the Active Face of the Transducer

When a cloud of gas bubbles collects on the active face of the transducer, the sound waves will be affected and the amplitude of the echo will be reduced. This may be seen on the oscilloscope. It was very important to remove these bubbles from time to time during the experiment by means of a small brush.

D. PROGRAMMING

The computer programs used in this experiment were prepared by Chang (1986). To acquire and analyze the data three programs are available.

1. **Program "THESIS3"**

This program converts the waveform data from the Nicolet 3091 Digital Oscilloscope into voltage and time value. The Nicolet is controled by the HP-3041 Data Acquisition and Control Unit. The program squares the voltage and then takes the average of 50 sets of readings. To insure the data are not lost, the data are stored on disk after each 10 sets are acquired.

2. **Program "MAXIMUM"**

This program reads the squared voltage data and the corresponding time data stored on disk and then determines local maxima. The square-roots of the maxima were taken and stored on the disk in a separate data file.

3. Program "PLOT3"

This program plots the envelope of the echo waveforms. The voltage is converted to log values and plotted vs. time. A least-square method is used to find the best fitting straight line, which is then plotted. The slope of this line and its correlation coefficient are then printed.

V. RESULTS AND DISCUSSIONS

One of the significant features of this experiment is the measurement of volume reverberation for different sediments. The theoretical echo waveforms for water and sediment can be seen in Figures 4.4(a) and (b). Actual echo waveforms from water and sediment are shown for comparison in Figure 5.1.

Since the observed volume reverberation in sediments is quite sensitive to inhomogeneities in both bottom surface and composition, the echo waveforms vary not only from sediment to sediment but also between individual measurements on the same sediment. For this reason, 50 samples for each data set and 10 data sets for each sediment type were taken to get the average shapes of the echo waveforms.

The slopes of the trailing edges of the echos for the various sediments were measured, and a relationship between grain size and the echo decay slopes at different frequencies was determined. Finally, a simple model of backscattering was used to determine the scattering coefficient for each sediment.

A. DECAY OF VOLUME REVERBERATION

1. Fine Sand

Ten sets measurements were made at 181 kHz for fine sand (ka = 0.11) and the individual echo decay slopes found along with their correlation coefficients (Table 2).

The decay slopes for fine sand varied from -0.0310 to -0.0378 Np μs. The average slope of all ten sets was -0.0344 Np/μs. Compared to the decay constant for purely-reflected (water/air interface) pulses, α = -0.0377 Np/μs, volume reverberation is seen to be present.

Since the fine sand was the most homogeneous sediment used and its surface was smooth, the variation in its decay constant was smaller than for the others.

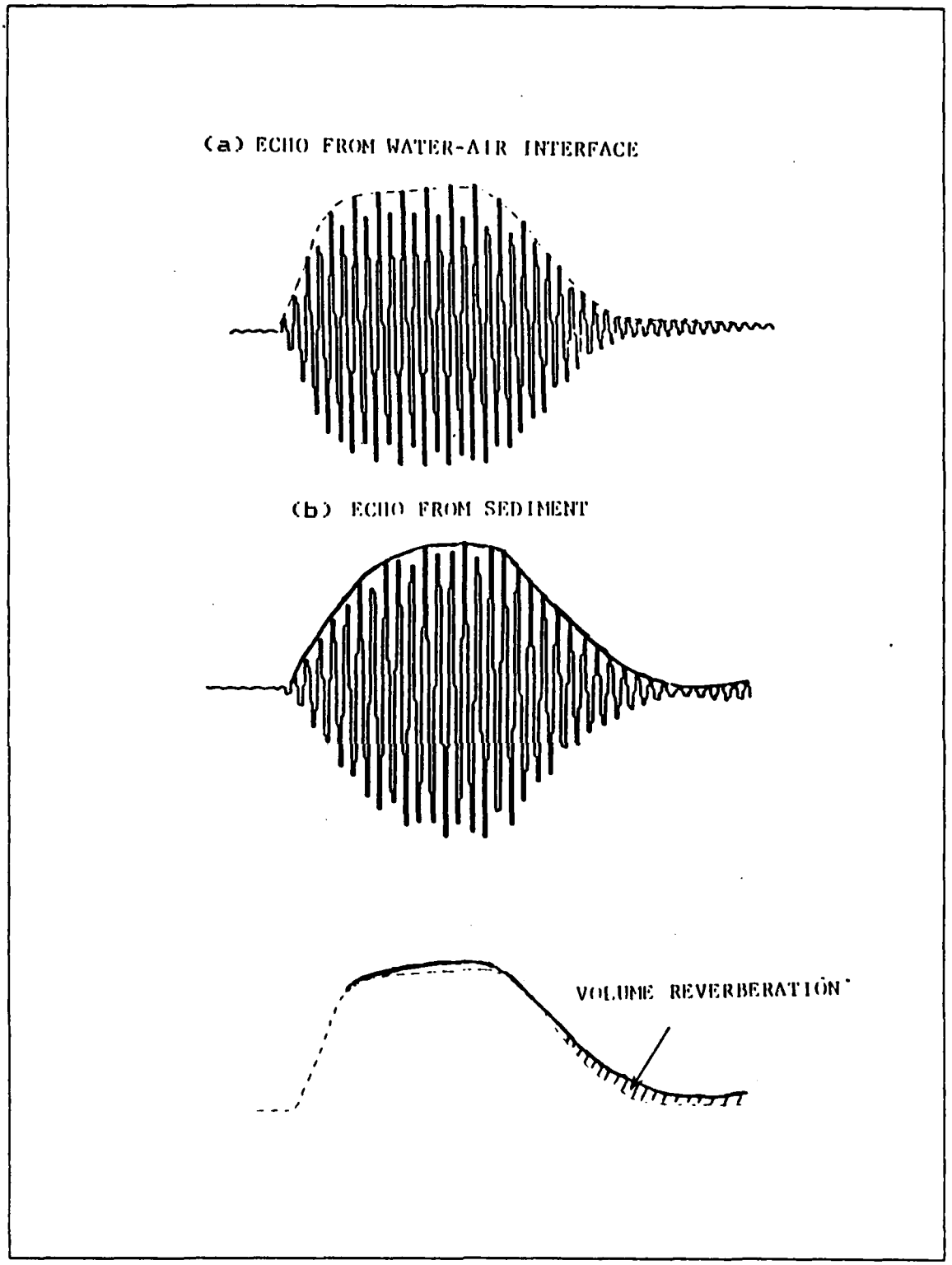

Figure 5.1 The volume reverberation of sediment.

TABLE 2

FINE SAND INDIVIDUAL SLOPES AT 181 KHZ

DATA SET	SLOPE $\times 10^{-2}$ (Np/μs)	CORRELATION COEFFICIENT
DATA10	-3.29	-0.9648
DATA11	-3.38	-0.9548
DATA12	-3.10	-0.9605
DATA13	-3.78	-0.9817
DATA14	-3.11	-0.9814
DATA15	-3.62	-0.9854
DATA16	-3.37	-0.9654
DATA17	-3.57	-0.9545
DATA18	-3.44	-0.9823
DATA19	-3.19	-0.9726

MEAN SLOPE = -3.44×10^{-2} Np/μs

$\sigma = 0.22 \times 10^{-2}$ Np/μs

2. **Aquarium Sand**

Two different frequencies, 62 kHz and 108 kHz, were used for the aquarium sand experiments. Individual and averaged slopes are listed in Tables 3 and 4.

At 62 kHz an 8-cycle of pulse is 129 μs long, and its ka value is about 0.21. At 108 kHz an 8-cycle pulse has a duration of 74 μs and a ka value of about 0.37. Both may be considered within the Rayleigh regime.

The decay slope of this sediment varies from -0.0035 Np μs to -0.0085 Np μs at 62 kHz and have average slope of -0.0059 Np μs. At 108 kHz the slope varies from -0.0152 Np μs to -0.0208 Np μs with the average being -0.0184 Np μs.

As expected, the echo waveforms for aquarium sand are less consistent than for fine sand. This is probably due to the fact that the grain sizes are less homogeneous and the sediment surface is less uniform.

TABLE 3

AQUARIUM SAND INDIVIDUAL SLOPES AT 62 KHZ

DATA SET	SLOPE $\times 10^{-2}$ (Np/μs)	CORRELATION COEFFICIENT
DATA20	-0.62	-0.6961
DATA21	-0.83	-0.8041
DATA22	-0.53	-0.7440
DATA23	-0.60	-0.7728
DATA24	-0.41	-0.6950
DATA25	-0.66	-0.7278
DATA26	-0.35	-0.6817
DATA27	-0.85	-0.6671
DATA28	-0.52	-0.6885
DATA29	-0.50	-0.7338

MEAN SLOPE = -0.59×10^{-2} Np/μs

$\sigma = 0.16 \times 10^{-2}$ Np/μs

3. **Aggregate Sand**

As with aquarium sand, frequencies 62 kHz and 108 kHz were used for the aggregate sand experiment. The individual and average slopes are listed in Tables 5 and 6.

At 62 kHz the decay slopes have a maximum of -0.0070 Np/μs and a minimum of -0.0034 Np/μs; the average is -0.0051 Np/μs. At 108 kHz the maximum is -0.0099 Np μs and the minimum is -0.0032 Np/μs, and the average value is -0.0069 Np μs.

TABLE 4

AQUARIUM SAND INDIVIDUAL SLOPES AT 108 KHZ

DATA SET	SLOPE $\times 10^{-2}$ (Np/μs)	CORRELATION COEFFICIENT
DATA30	-1.52	-0.8949
DATA31	-2.01	-0.8921
DATA32	-2.08	-0.7076
DATA33	-1.70	-0.8774
DATA34	-1.76	-0.8023
DATA35	-1.58	-0.6813
DATA36	-1.96	-0.8148
DATA37	-2.07	-0.9072
DATA38	-1.73	-0.8396
DATA39	-1.98	-0.8741

MEAN SLOPE = -1.84×10^{-2} Np/μs

$\sigma = 0.20 \times 10^{-2}$ Np/μs

4. **Glass Beads**

Two types of glass beads were chosen for this experiment. Their homogeneity in size and shape are the reason why they were used.

The average grain sizes of the beads were 1.7 mm and 0.16 mm. Because only limited amounts of these glass beads were available, they were put into a plastic bucket inside the experimental tank. 181 kHz was used with a pulse length about 88 μs for a 16-cycle pulse. The ka value for coarse glass beads was about 0.60 and for fine glass beads about 0.06. Even though the glass beads were homogeneous in size and shape, the individual slopes still varied considerably. Thus, the standard deviation for a total of 10 sets of measurements was 0.0023 Np/μs for coarse glass beads and 0.0021 Np/μs for fine glass beads. Compared with the value for fine sand of 0.0022 Np/μs there is little difference.

The echo decay slope for coarse glass beads has a maximum of -0.0358 Np/μs and a minimum of -0.0285 Np/μs, and its average is -0.0338 Np/μs. For fine glass beads the maximum is -0.0415 Np/μs, the minimum is -0.0342 Np/μs, and the average is -0.0363 Np/μs. All these individual slopes are listed in Tables 7 and 8

TABLE 5

AGGREGATE SAND INDIVIDUAL SLOPES AT 62 KHZ

DATA SET	SLOPE $\times 10^{-2}$ (Np/μs)	CORRELATION COEFFICIENT
DATA40	-0.64	-0.8739
DATA41	-0.51	-0.7876
DATA42	-0.56	-0.7409
DATA43	-0.70	-0.6146
DATA44	-0.54	-0.7687
DATA45	-0.38	-0.2952
DATA46	-0.38	-0.7413
DATA47	-0.34	-0.3158

MEAN SLOPE = -0.51×10^{-2} Np/μs

$\sigma = 0.11 \times 10^{-2}$ Np/μs

TABLE 6

AGGREGATE SAND INDIVIDUAL SLOPES AT 108 KHZ

DATA SET	SLOPE $\times 10^{-2}$ (Np/μs)	CORRELATION COEFFICIENT
DATA50	-0.32	-0.3014
DATA51	-0.72	-0.6927
DATA52	-0.73	-0.7628
DATA53	-0.99	-0.5083
DATA54	-0.45	-0.1711
DATA55	-0.89	-0.4688
DATA56	-0.65	-0.3098
DATA57	-0.74	-0.6292

MEAN SLOPE = -0.69×10^{-2} Np/μs

$\sigma = 0.21 \times 10^{-2}$ Np/μs

B. RELATIONSHIP OF DECAYING SLOPE TO GRAIN SIZE

TABLE 7
COARSE GLASS BEADS INDIVIDUAL SLOPES AT 181 KHZ

DATA SET	SLOPE $\times 10^{-2}$ (Np/μs)	CORRELATION COEFFICIENT
DATA60	-3.54	-0.8174
DATA61	-3.26	-0.9159
DATA62	-3.56	-0.9800
DATA63	-3.40	-0.9417
DATA64	-2.85	-0.9639
DATA65	-3.51	-0.9705
DATA66	-3.38	-0.9610
DATA67	-3.53	-0.9451
DATA68	-3.14	-0.9800
DATA69	-3.58	-0.9869

MEAN SLOPE = -3.38×10^{-2} Np/μs
$\sigma = 0.23 \times 10^{-2}$ Np/μs

Materials of different grain sizes, (fine sand, aquarium sand, aggregate sand, fine glass beads and coarse glass beads) were used in this experiment. The grain size and average decay slopes are shown in the individual tables. From these results an important relationship between volume reverberation and sediment grain size can be drawn; that is, for a given frequency the amount of volume reverberation increases as the sediment grain size increases (Figures 5, 6, and 7). This was expected from the suggestion of Clark, Proni, Seem and Tsai (1984).

TABLE 8

FINE GLASS BEADS INDIVIDUAL SLOPES AT 181 KHZ

DATA SET	SLOPE $\times 10^{-2}$ (Np/μs)	CORRELATION COEFFICIENT
DATA70	-3.47	-0.9417
DATA71	-3.62	-0.9554
DATA72	-3.83	-0.9042
DATA73	-3.78	-0.9209
DATA74	-4.15	-0.9904
DATA75	-3.82	-0.9663
DATA76	-3.53	-0.9911
DATA77	-3.66	-0.9768
DATA78	-3.42	-0.9658
DATA79	-3.77	-0.9580

MEAN SLOPE = -3.63×10^{-2} Np/μs

$\sigma = 0.21 \times 10^{-2}$ Np/μs

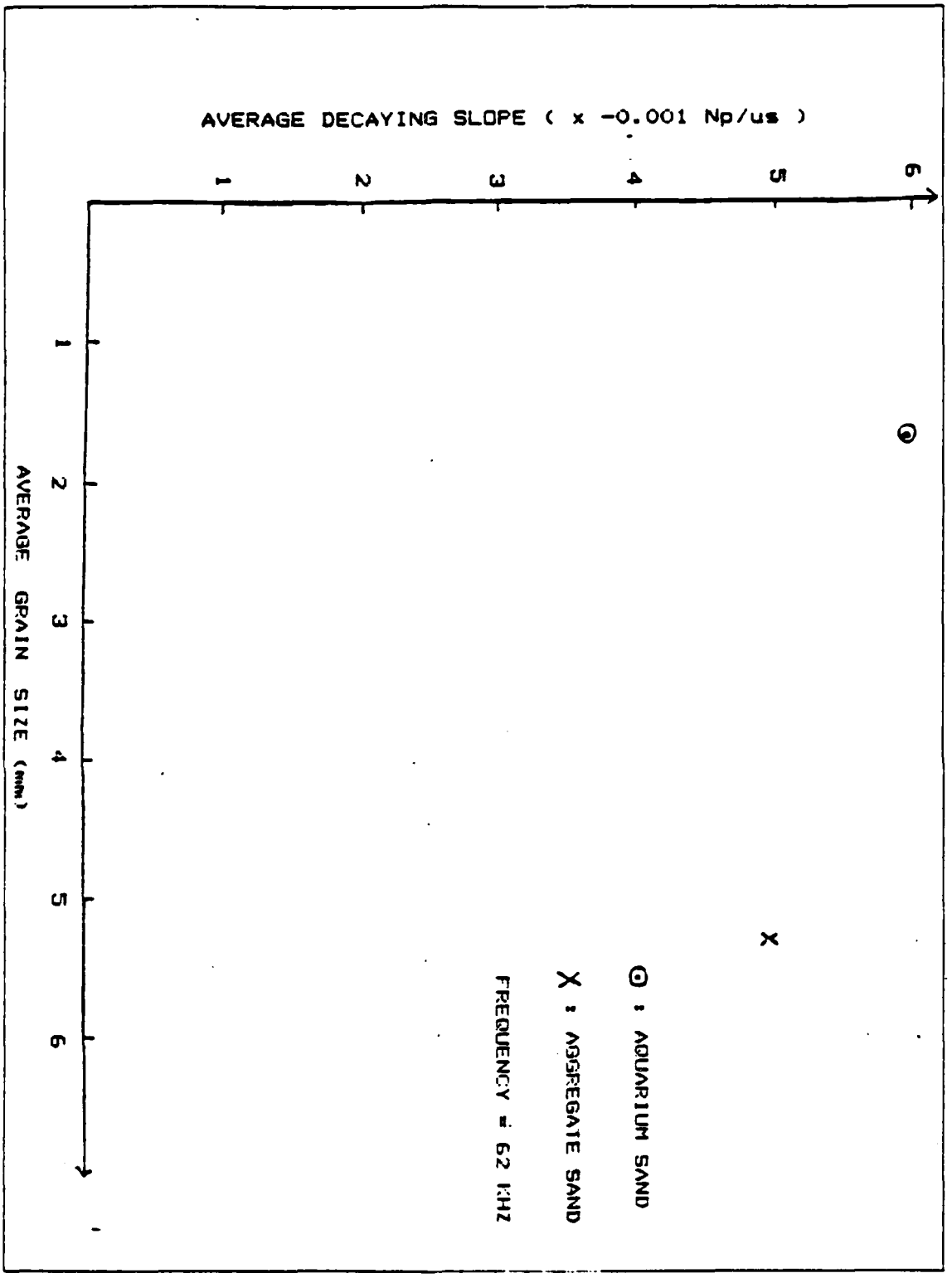

Figure 5.2 Average decaying slope vs. sediment grain size at 62 kHz.

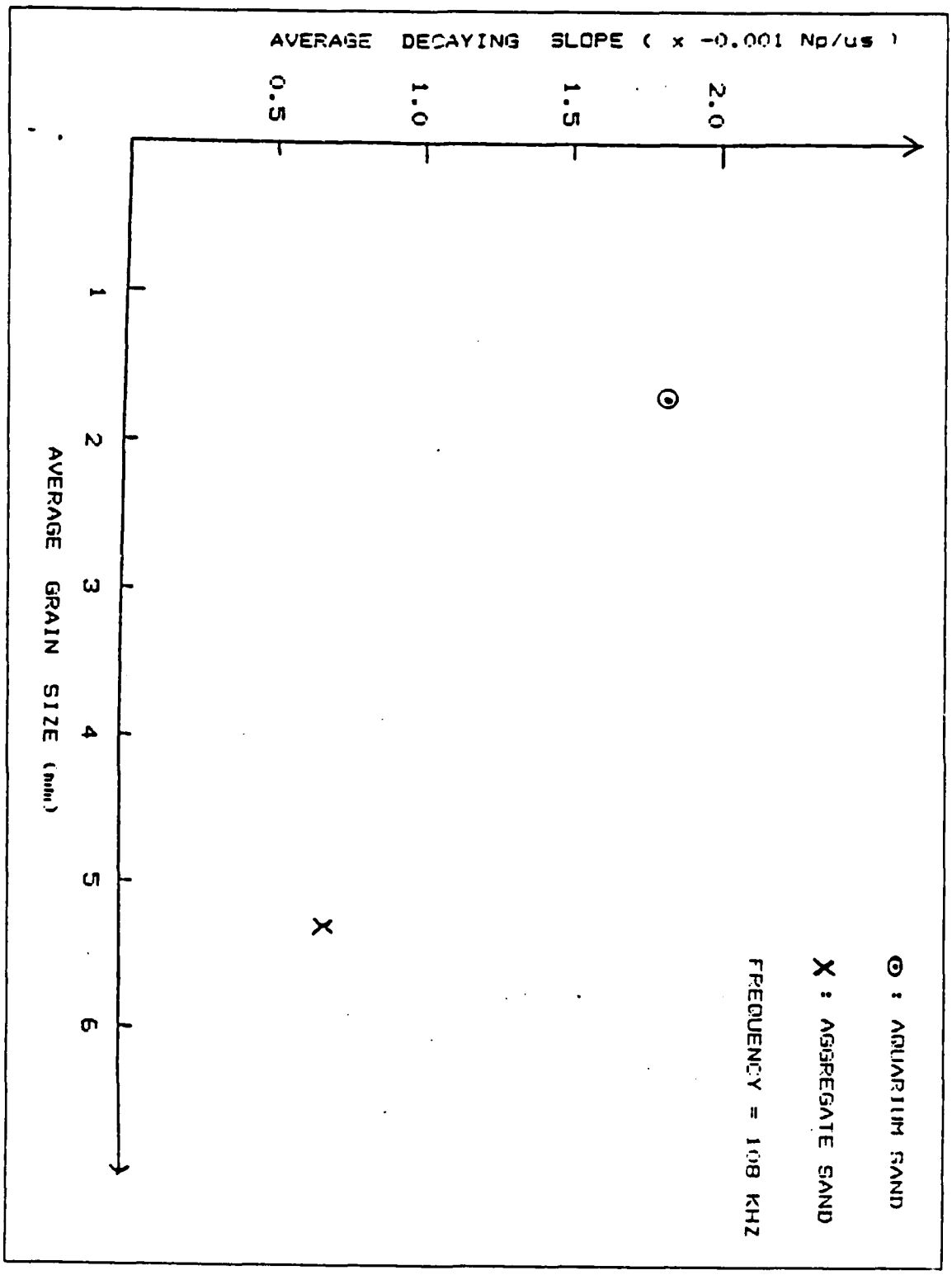

Figure 5.3 Average decaying slope vs. sediment grain size at 108 kHz.

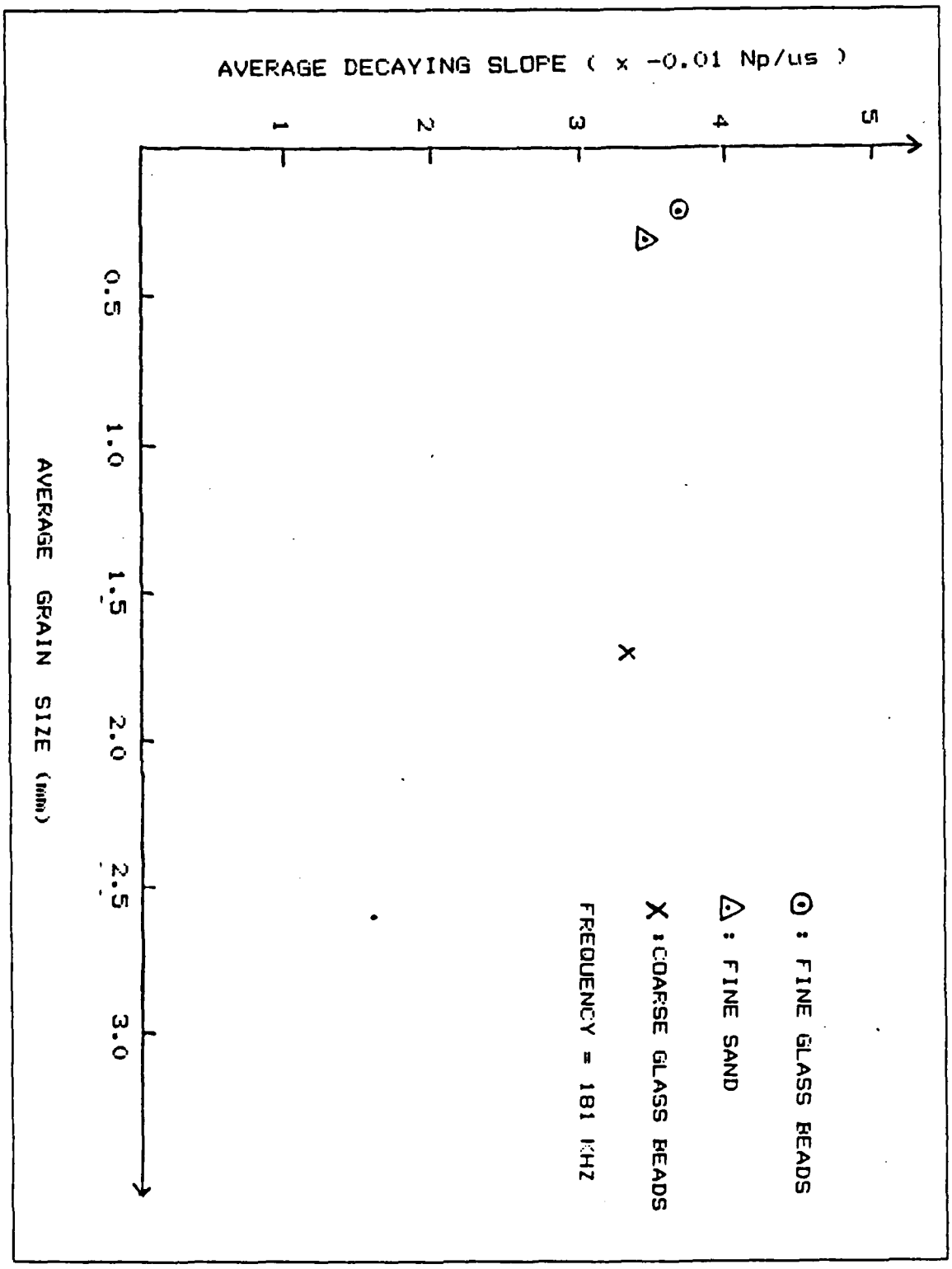

Figure 5.4 Average decaying slope vs. sediment grain size at 181 kHz.

C. RESULTS OF SCATTERING MODEL

In the model used for this experiment, the total intensity received by the transducer is

$$I = N\{T_i^2 s_v/\beta[e^{-c\beta t/2}(e^{c\beta\tau/2}-1)] + T_i^2 s_v/(-\beta+2\alpha/c) \qquad (5.1)$$

$$[e^{-c\beta t/2}(e^{c\beta\tau/2}-1) + e^{-\alpha t}(1-e^{\alpha\tau})] + R_i(e^{\alpha\tau}-1)e^{-\alpha t}\}$$

where $N = I_{o/r}4$

All variables are known in this formula except s_v. If the part included inside braces is called M, then

$$I = (I_{o/r}4)M$$

The different sediments have different M values; by assuming a series of scattering coefficients and computing $Log(M)^{1/2}$ for each and normalizing it, the model envelopes may be determined. A simple basic program was used, and different s_v value are used to find the one for which the slope of the model envelope is equal to the average slope of experimental data. (Figure 5.5, 5.6, 5.7 and 5.8). Figure 5.9 showed the relationship between the scattering coefficient and the ka value.

In this model, at the beginning of decay the reflection term is dominant and is independent of s_v, while the scattering term is negligible. This means the model value will not change in the beginning of decay as the scattering coefficient changes. At the tail end of the decay the scattering term is dominant and the decay tails change when different scattering coefficients are used.

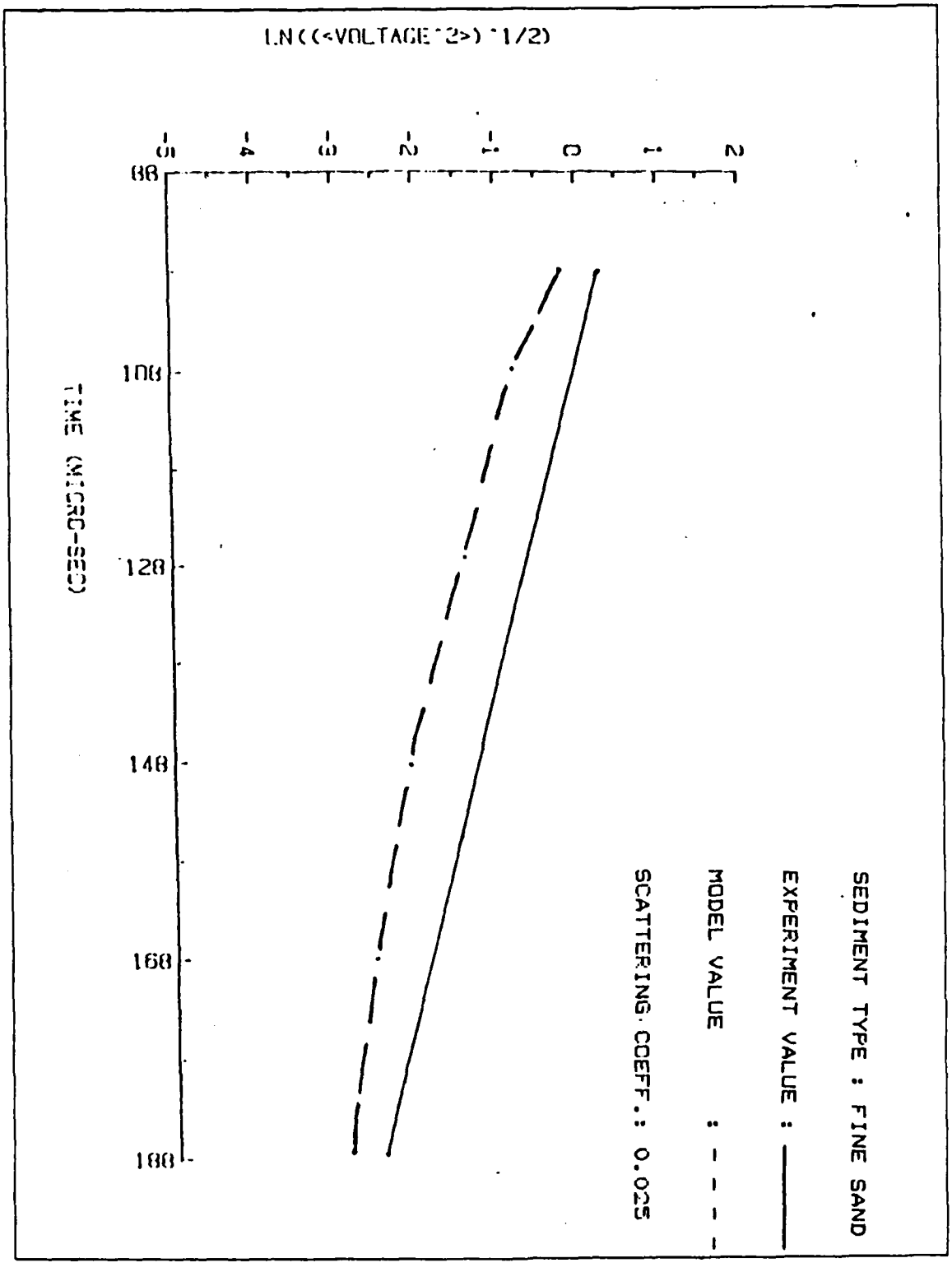

Figure 5.5 Decay slopes of the experiment vs. model for the fine sand.

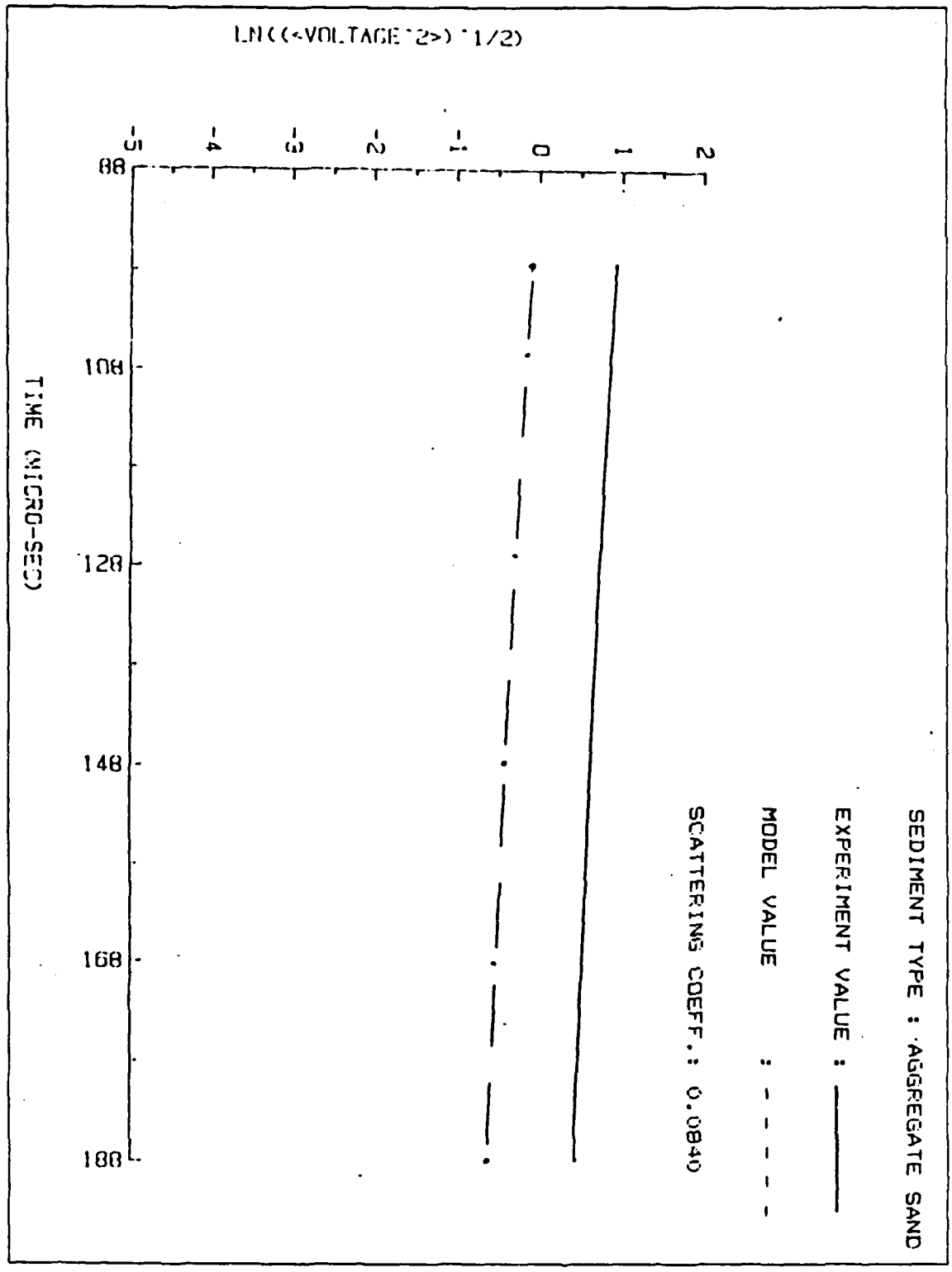

Figure 5.6 Decay slope of experiment vs. model for the aggregate sand.

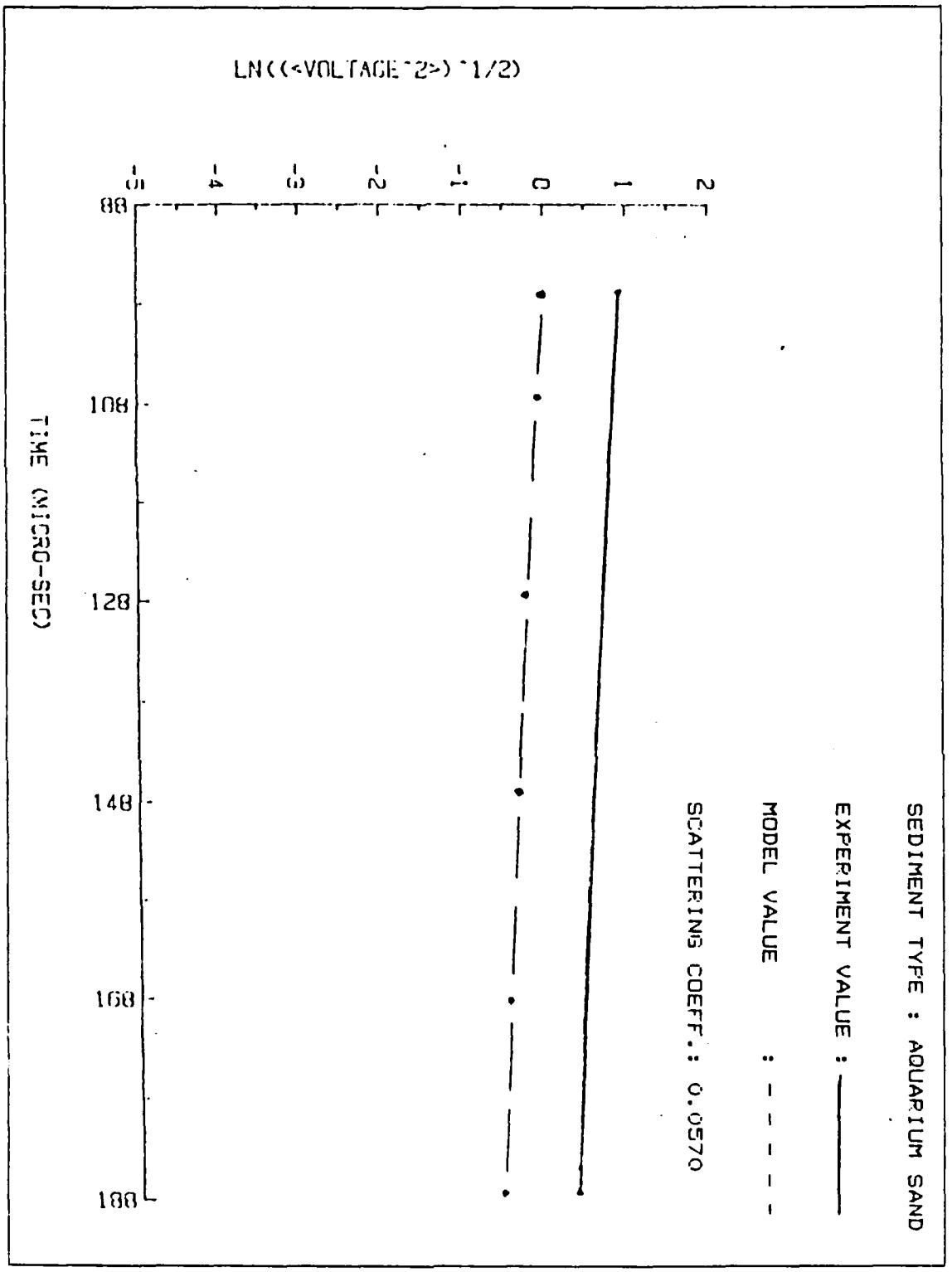

Figure 5.7 Decay slopes of experiment vs. model for the aquarium sand.

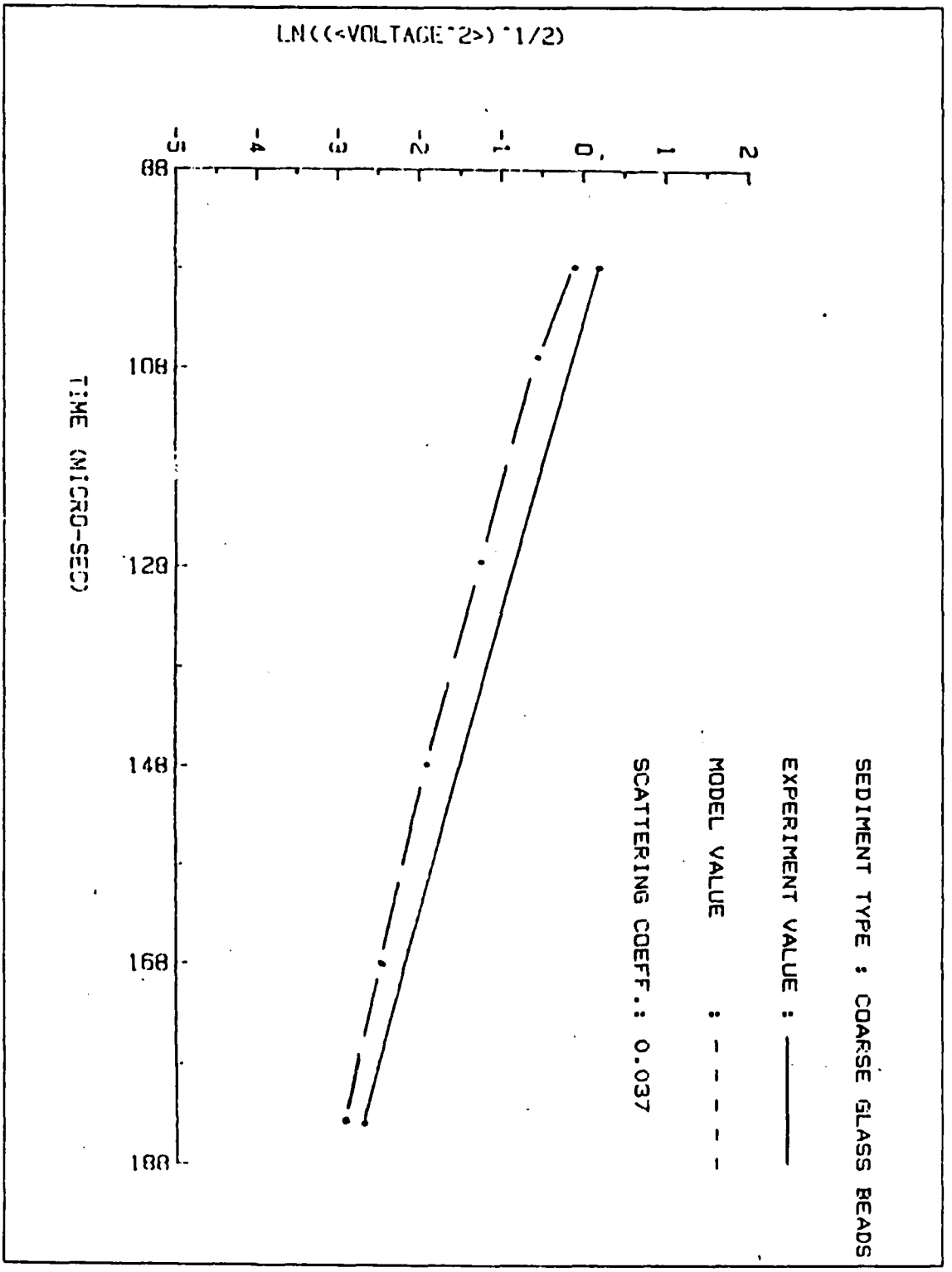

Figure 5.8 Decay slopes of experiment vs. model for the glass beads.

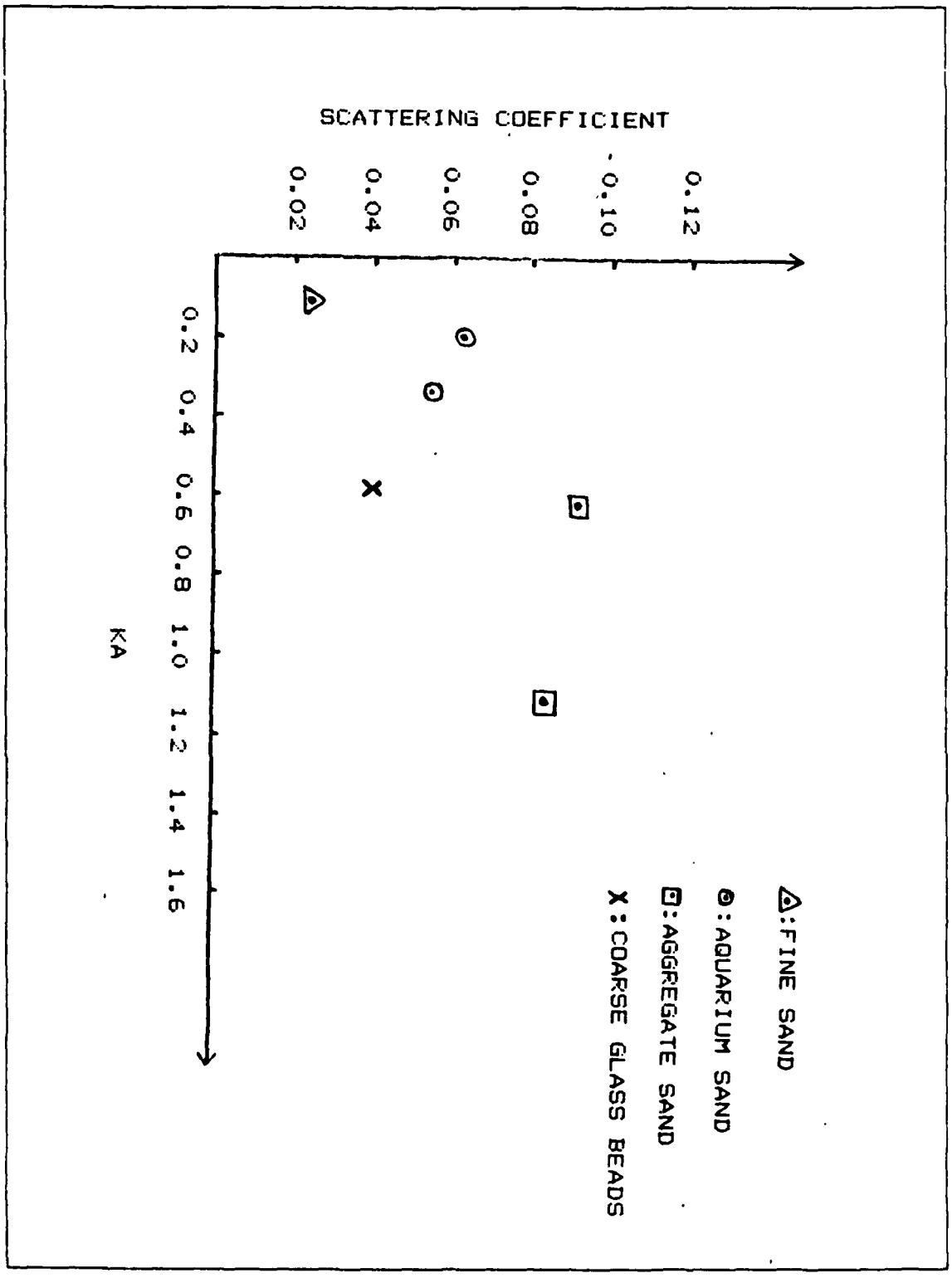

Figure 5.9 Sediments scattering coefficient vs. ka value.

I. CONCLUSIONS AND RECOMMENDATION

The following conclusions can be drawn:

1. For a fixed frequency, with increase in sediment grain size there is an increase in the volume reverberation of the sediment.
2. For a fixed grain size, if frequency is increased, the volume reverberation of the sediment decreases.
3. Scattering coefficients are roughly proportional to ka; that is, if ka increases, the scattering coefficient of the sediment is larger.
4. In theory the sediment volume reverberation can be used to classify sediment types using of the model to find the best-fitting value of scattering coefficient for different kinds of sediment.
5. In the real world the ocean environment is so complicated and unpredictable that the method suggested may not be practicable.

APPENDIX A
DECAY ENVELOPE GRAPHS FOR FINE SAND SEDIMENT AT 181 KHZ

The decay envelopes for fine sand sediment at 181 kHz (DATA 10 to DATA 19) were showed in this appendix.

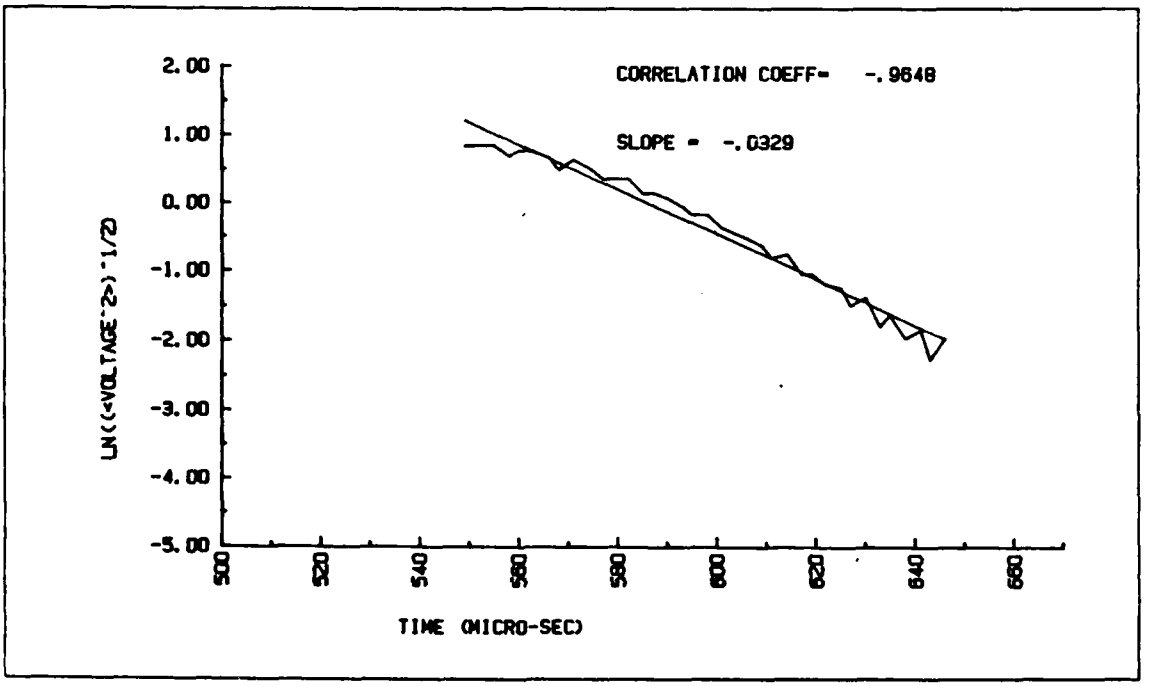

Figure A.1 DATA 10.

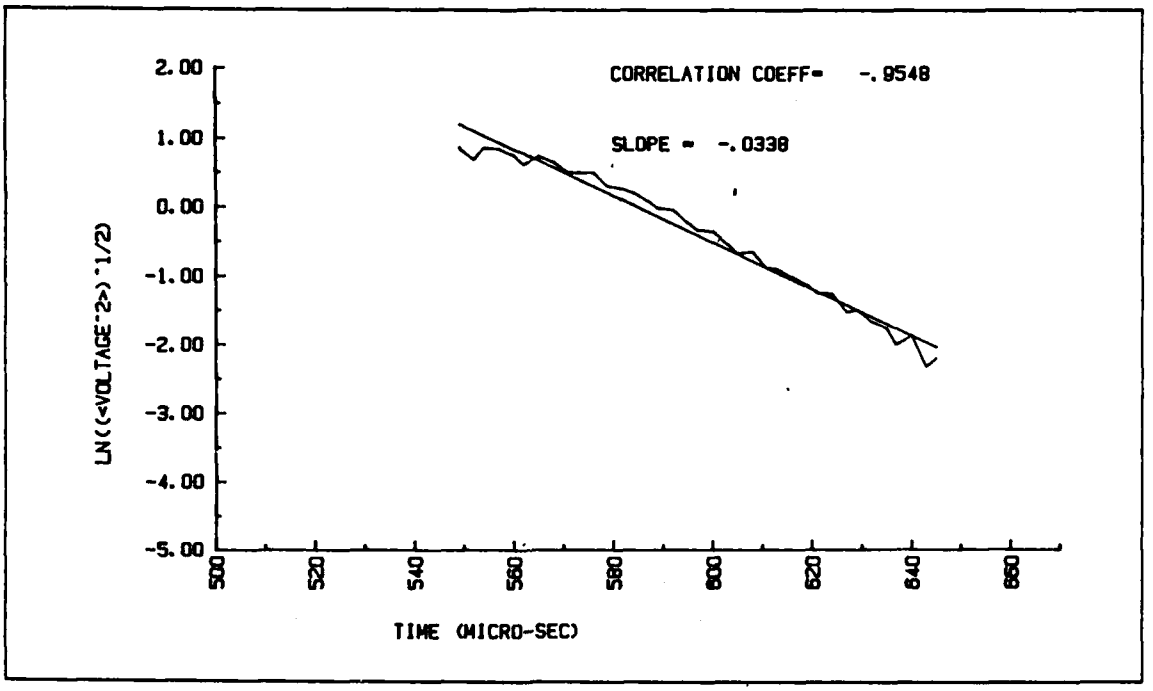

Figure A.2 DATA 11.

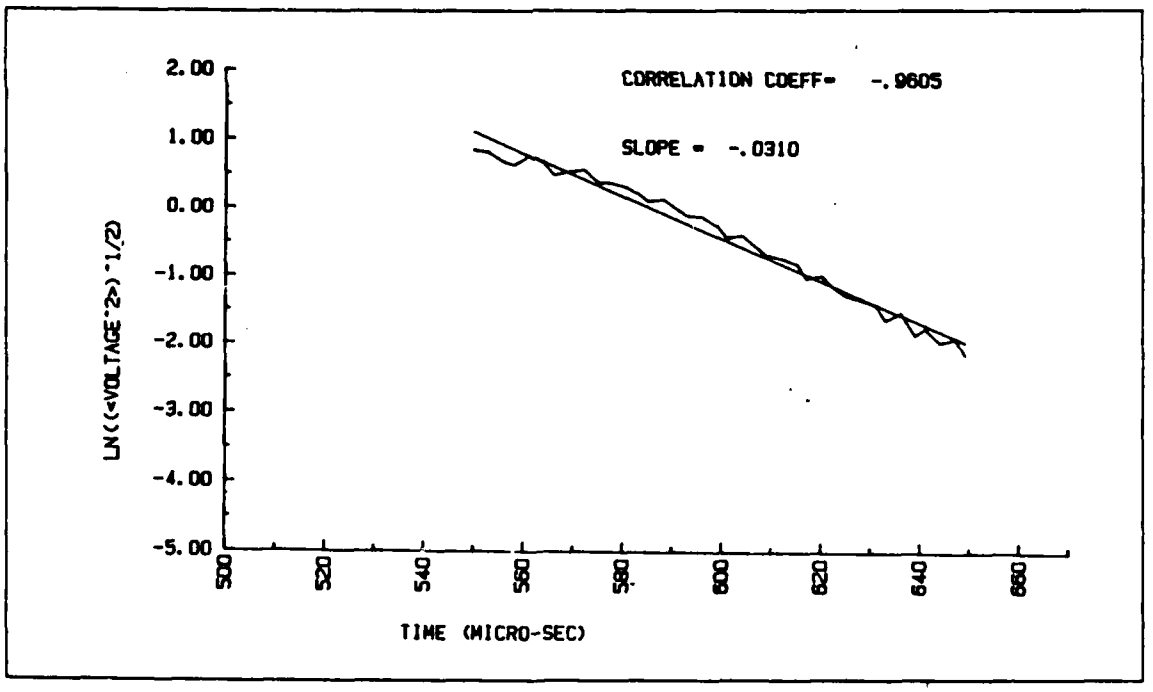

Figure A.3 DATA 12.

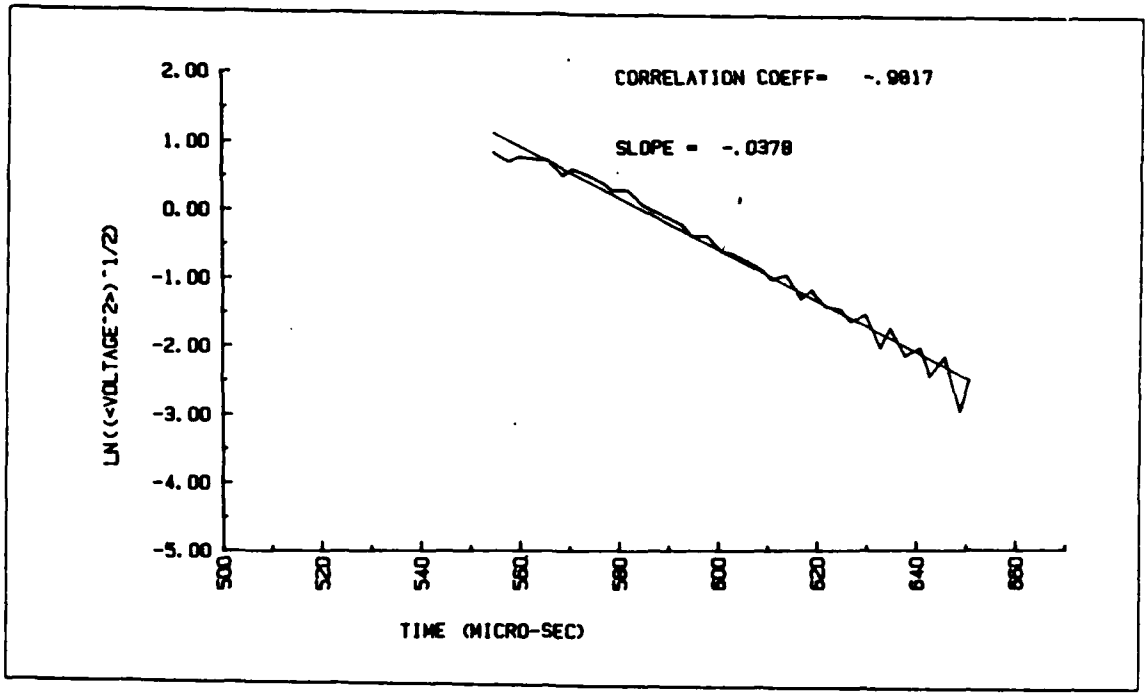

Figure A.4 DATA 13.

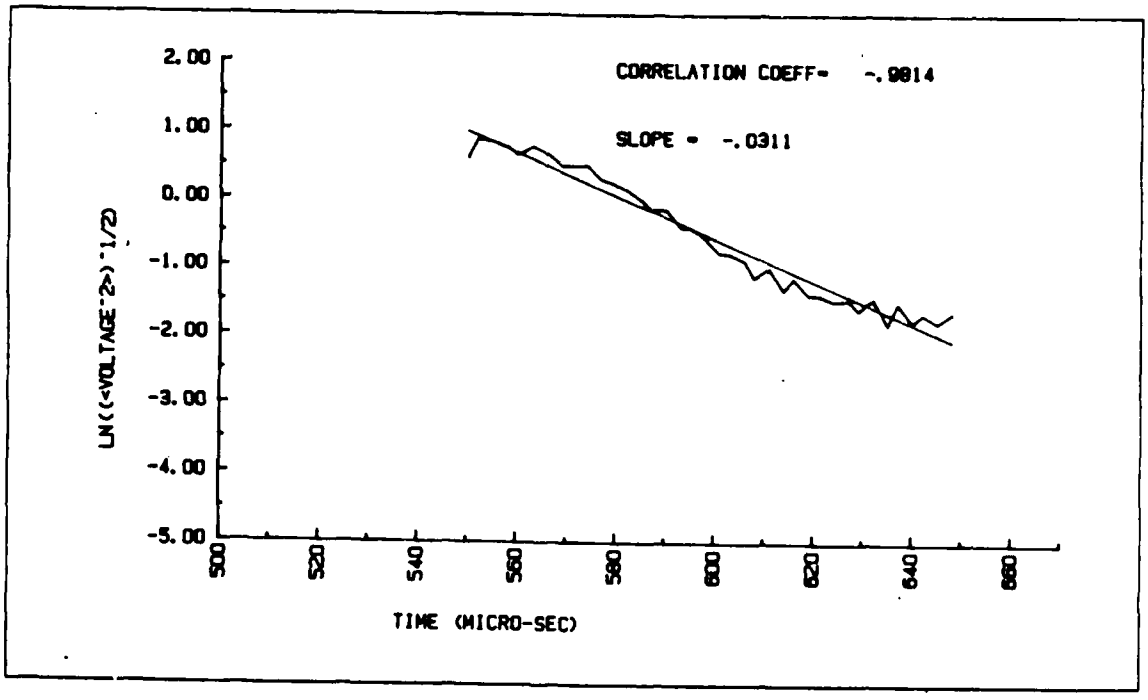

Figure A.5 DATA 14.

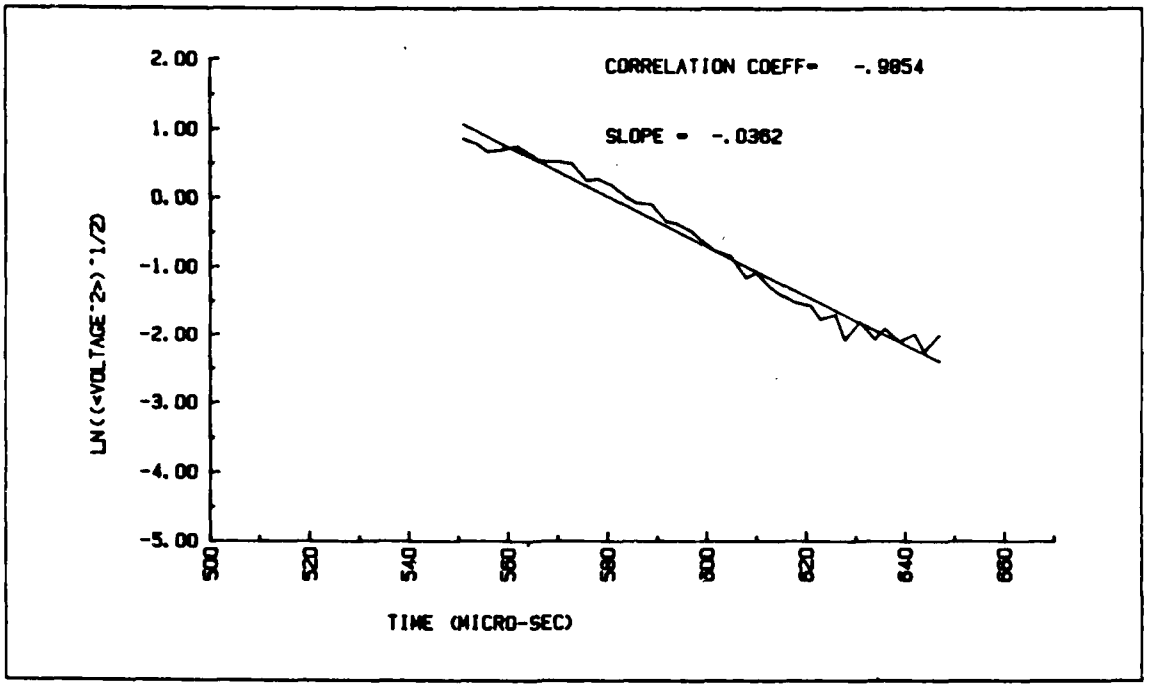

Figure A.6 DATA 15.

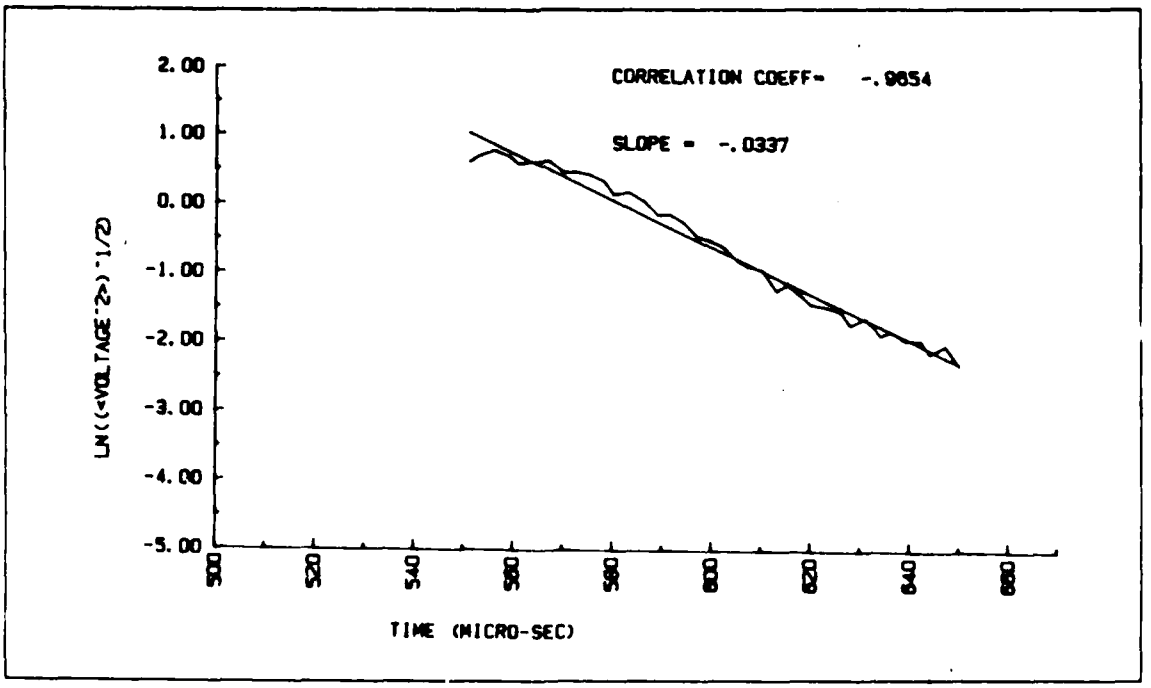

Figure A.7 DATA 16.

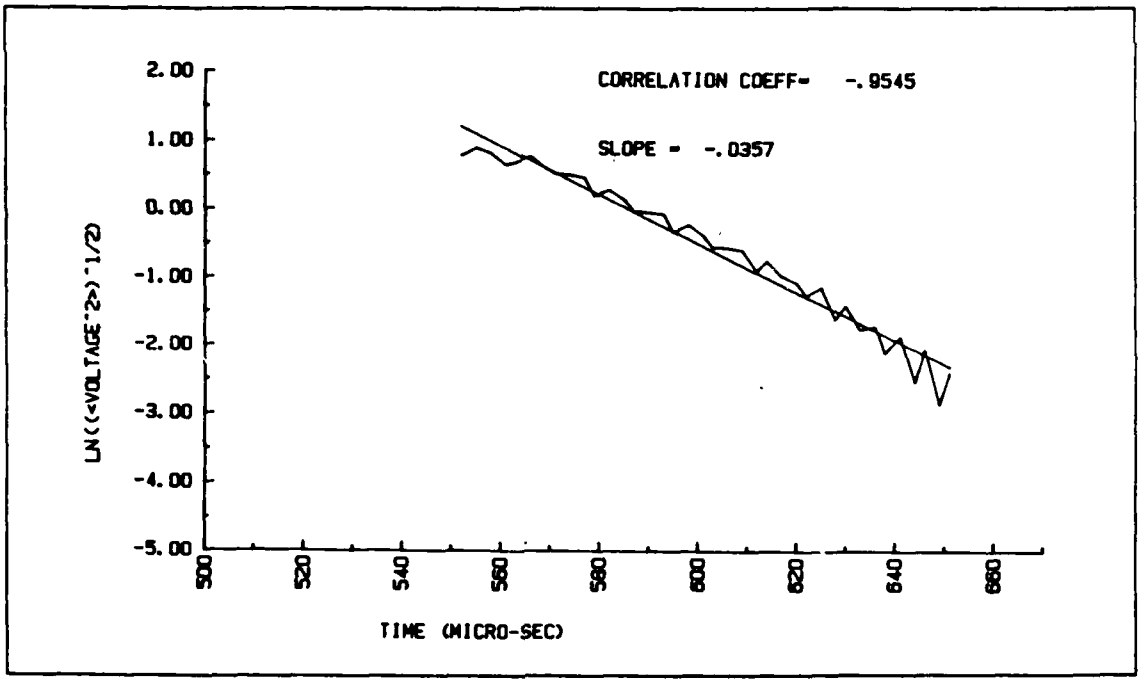

Figure A.8 DATA 17.

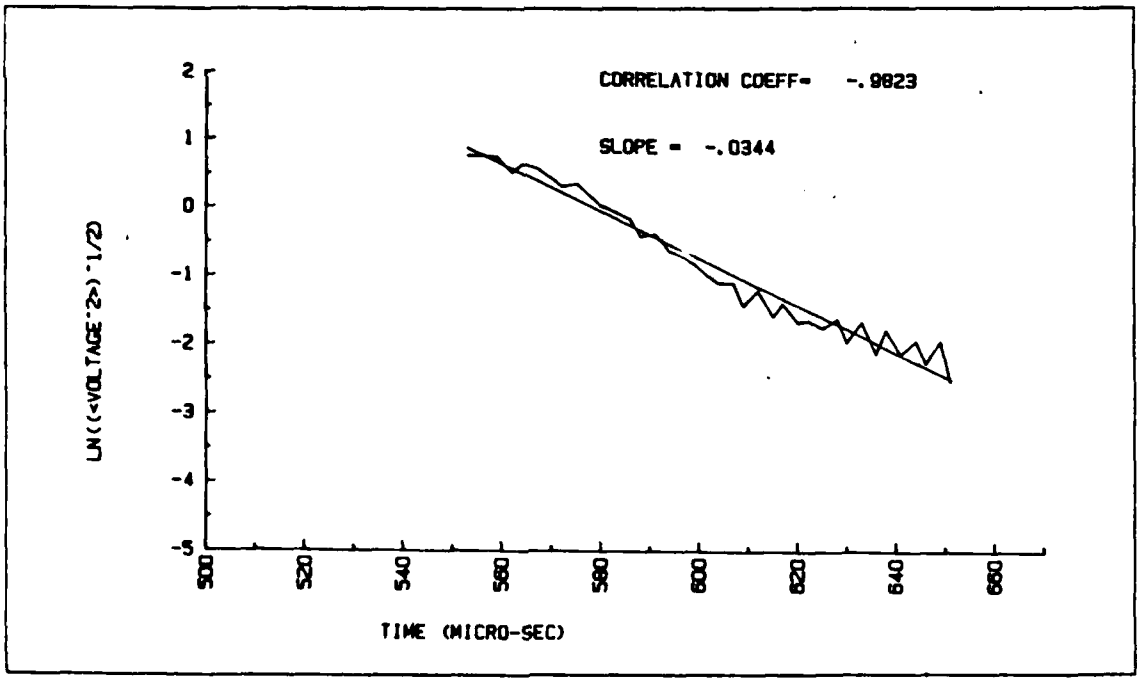

Figure A.9 DATA 18.

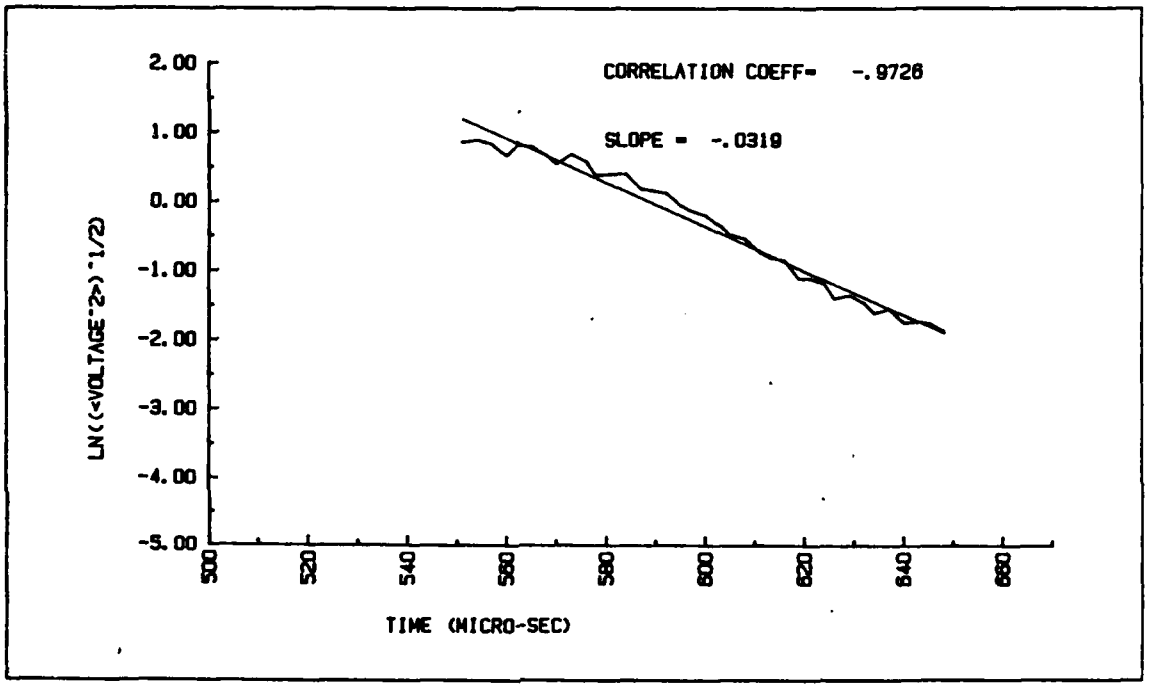

Figure A.10 DATA 19.

APPENDIX B
DECAY ENVELOPE GRAPHS FOR AQUARIUM SAND SEDIMENT AT 62 KHZ

The decay envelopes for aquarium send sediment at 62 kHz (DATA 20 to DATA 29) were showed in this appendix.

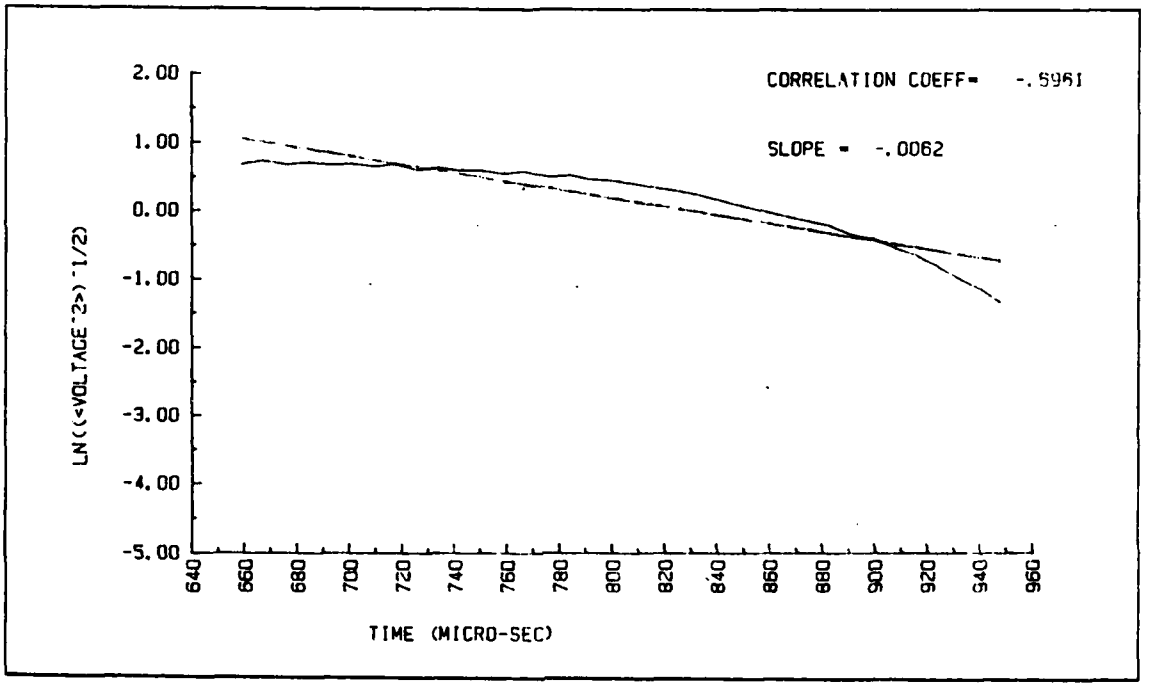

Figure B.1 DATA 20.

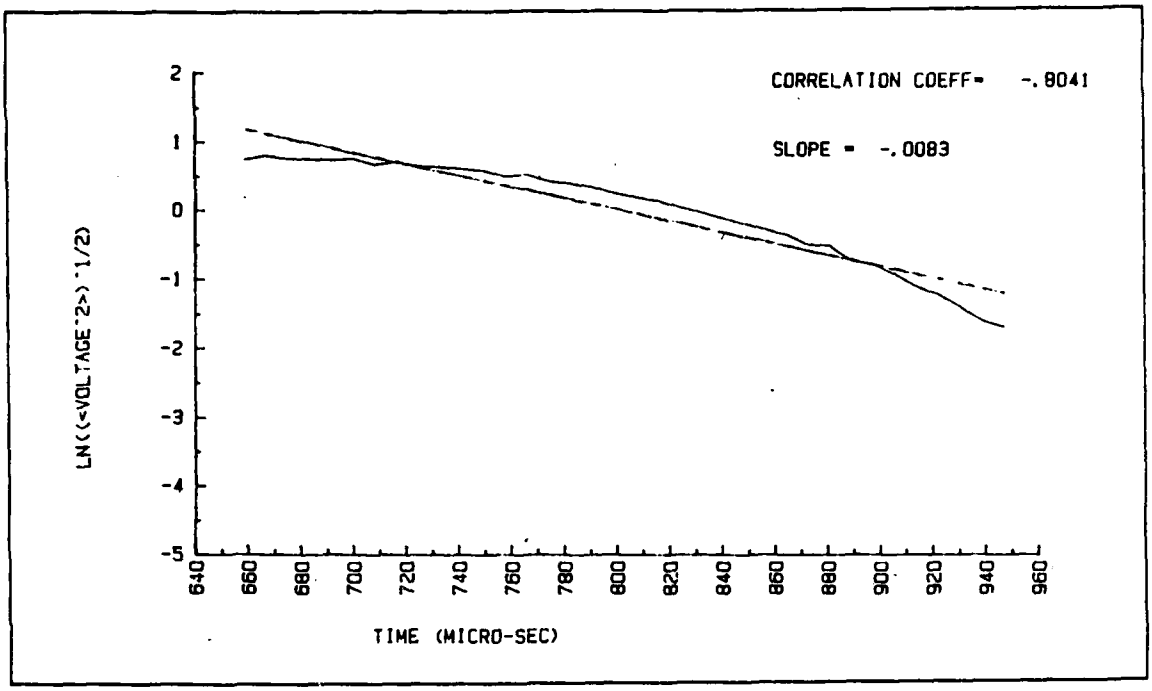

Figure B.2 DATA 21.

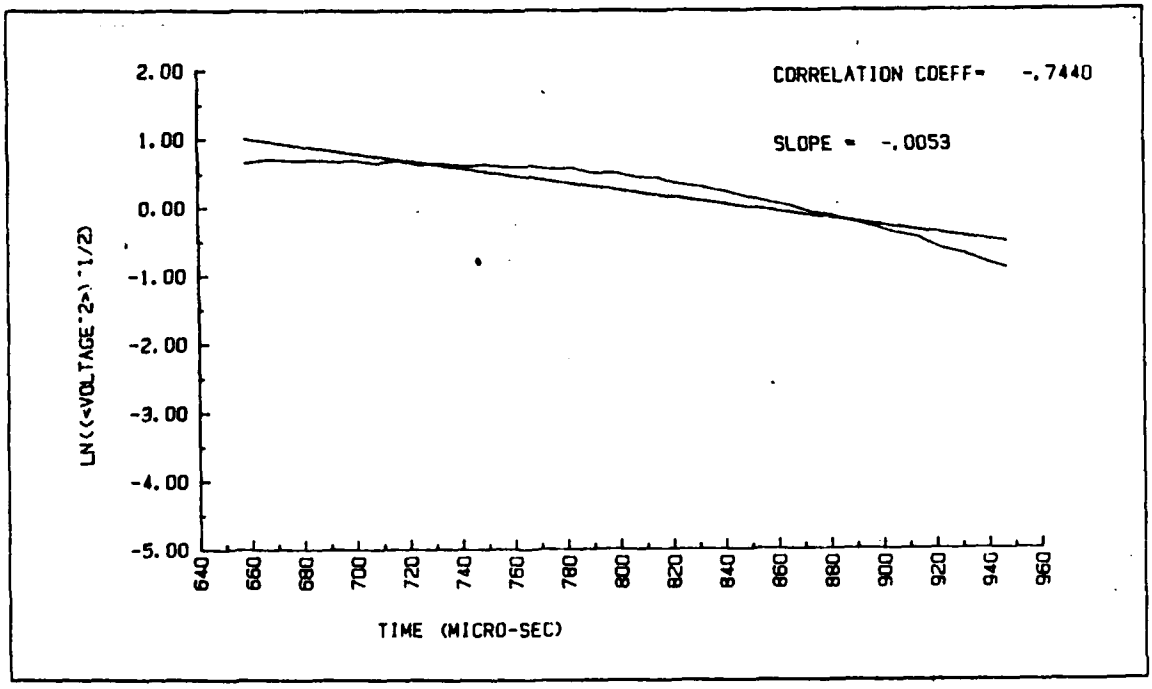

Figure B.3 DATA 22.

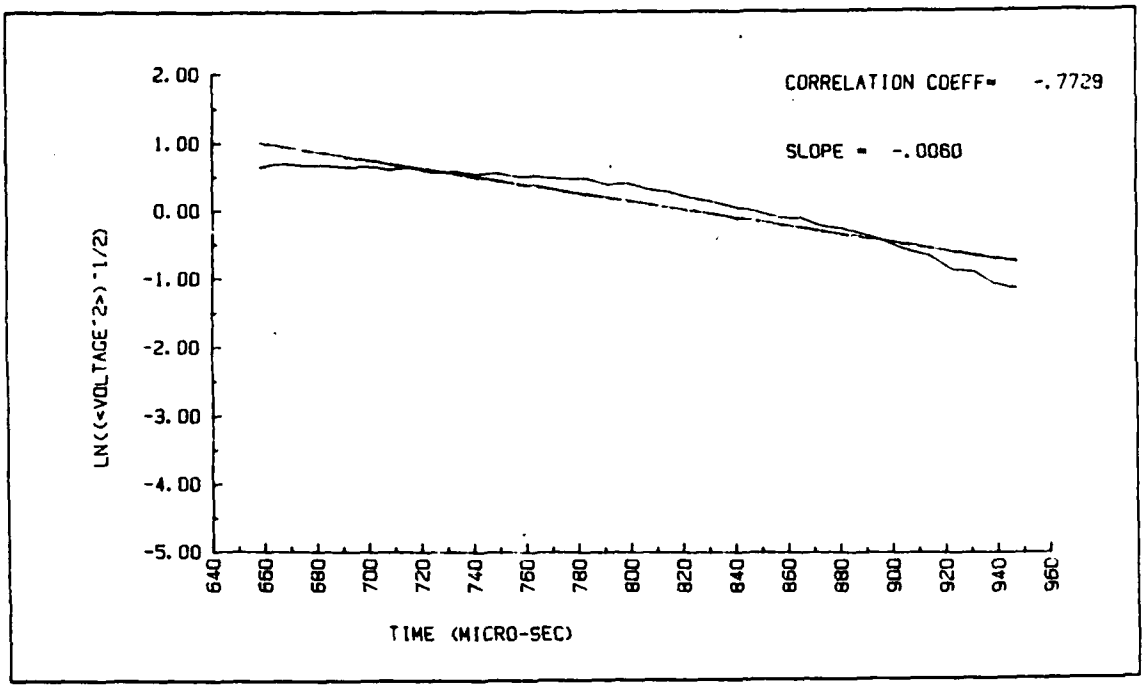

Figure B.4 DATA 23.

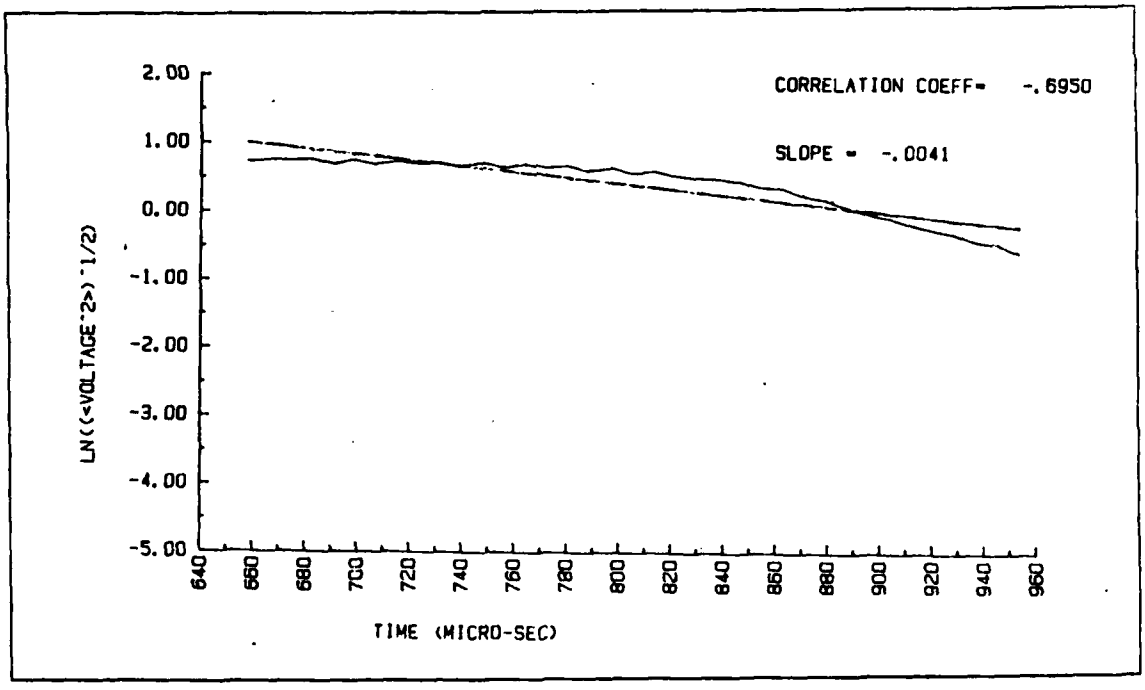

Figure B.5 DATA 24.

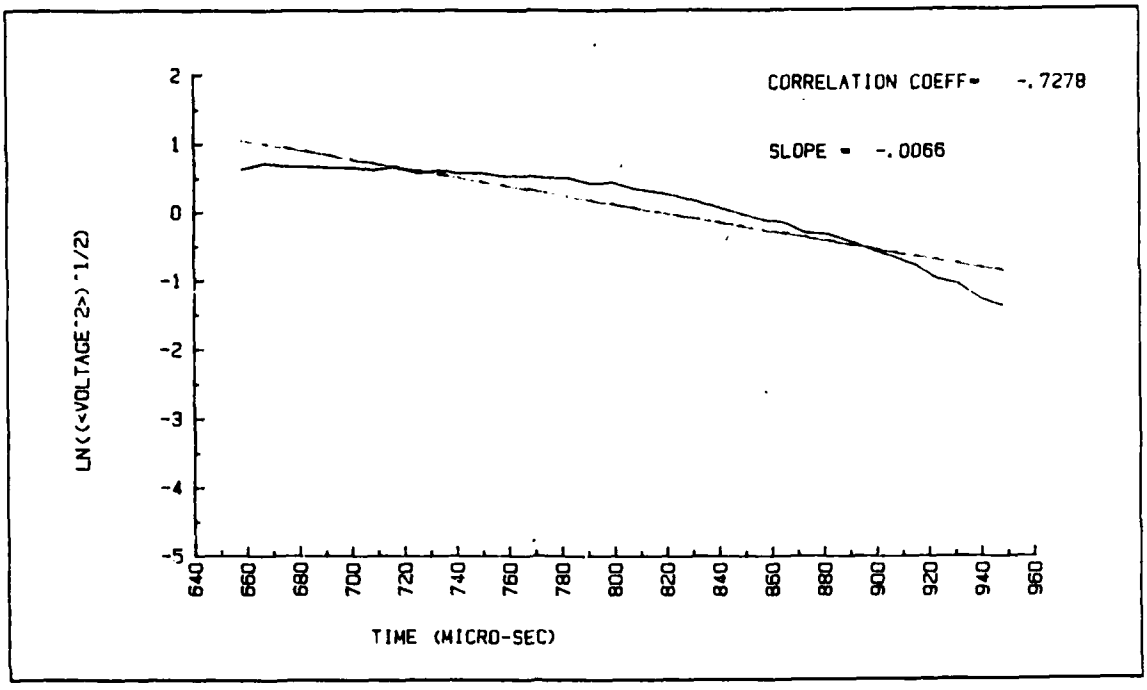

Figure B.6 DATA 25.

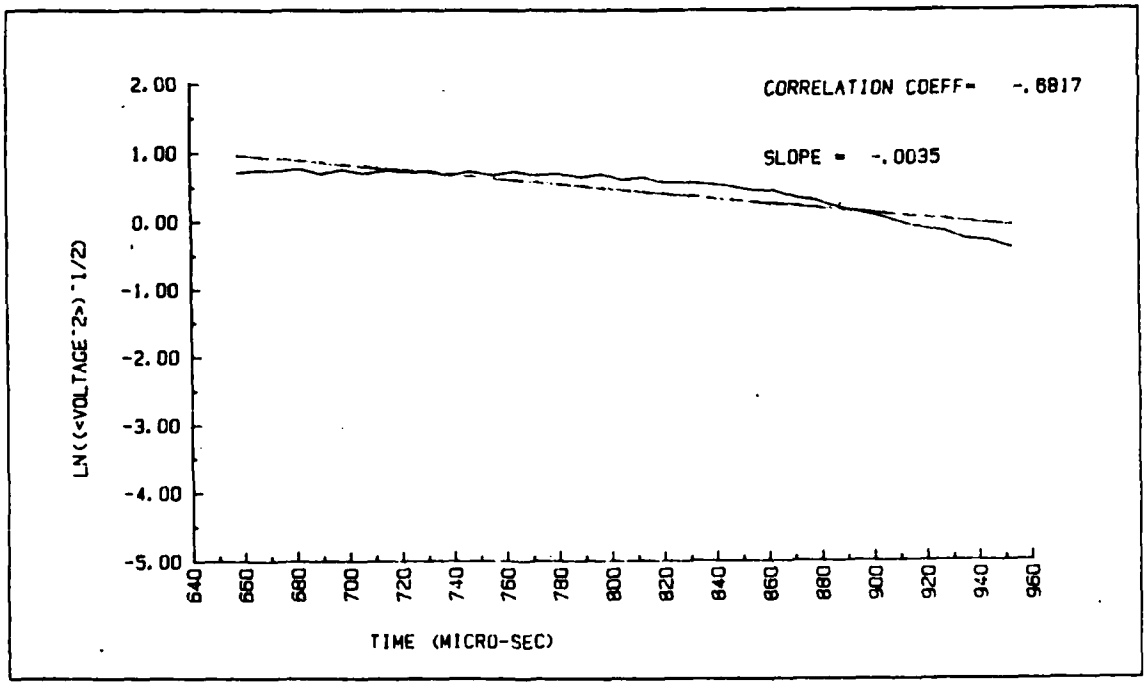

Figure B.7 DATA 26.

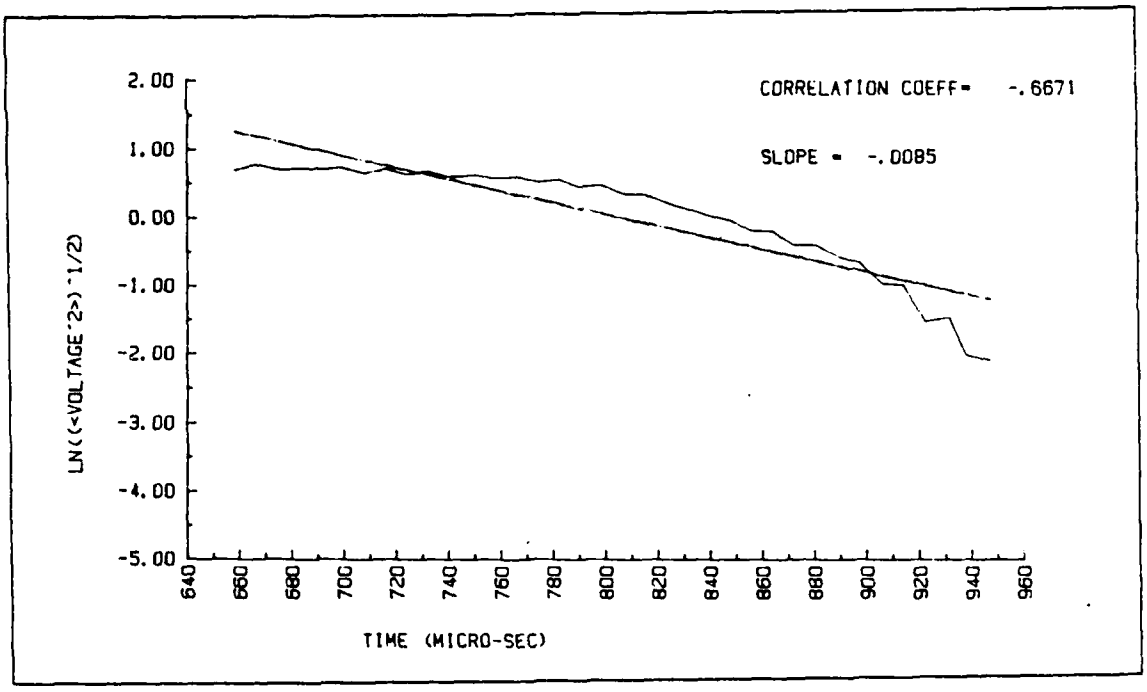

Figure B.8 DATA 27.

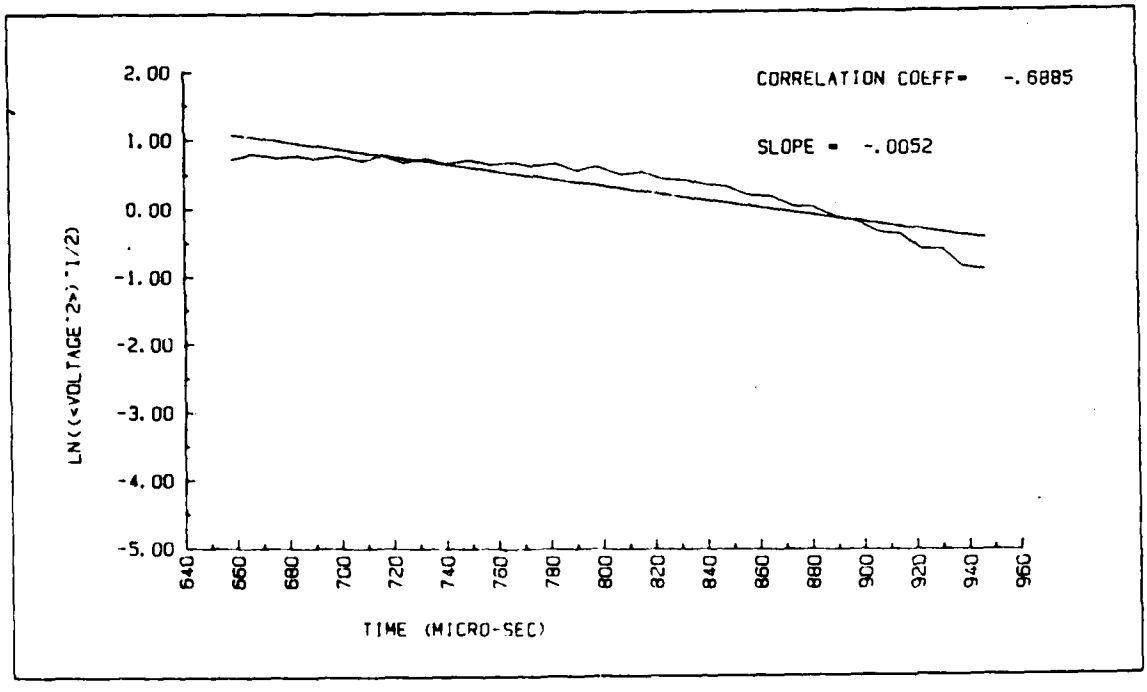

Figure B.9 DATA 28.

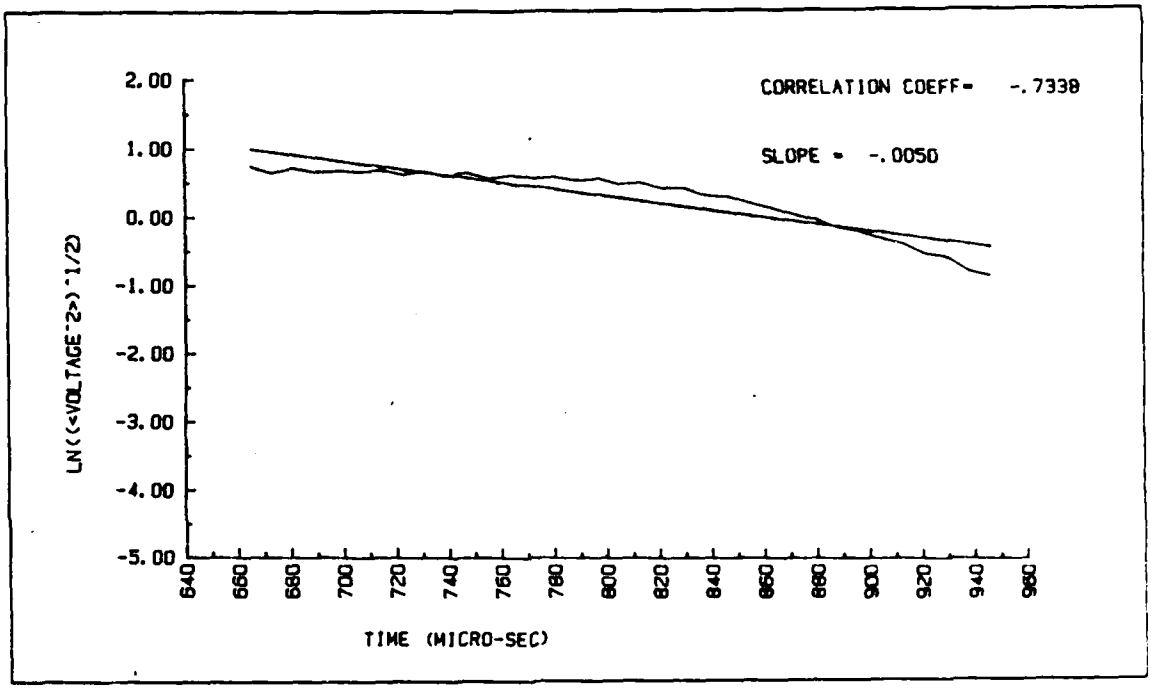

Figure B.10 DATA 29.

APPENDIX C
DECAY ENVELOPE GRAPHS FOR AQUARIUM SAND SEDIMENT AT 108 KHZ

The decay envelopes for aquarium sand sediment at 108 kHz (DATA 30 to DATA 39) were showed in this appendix.

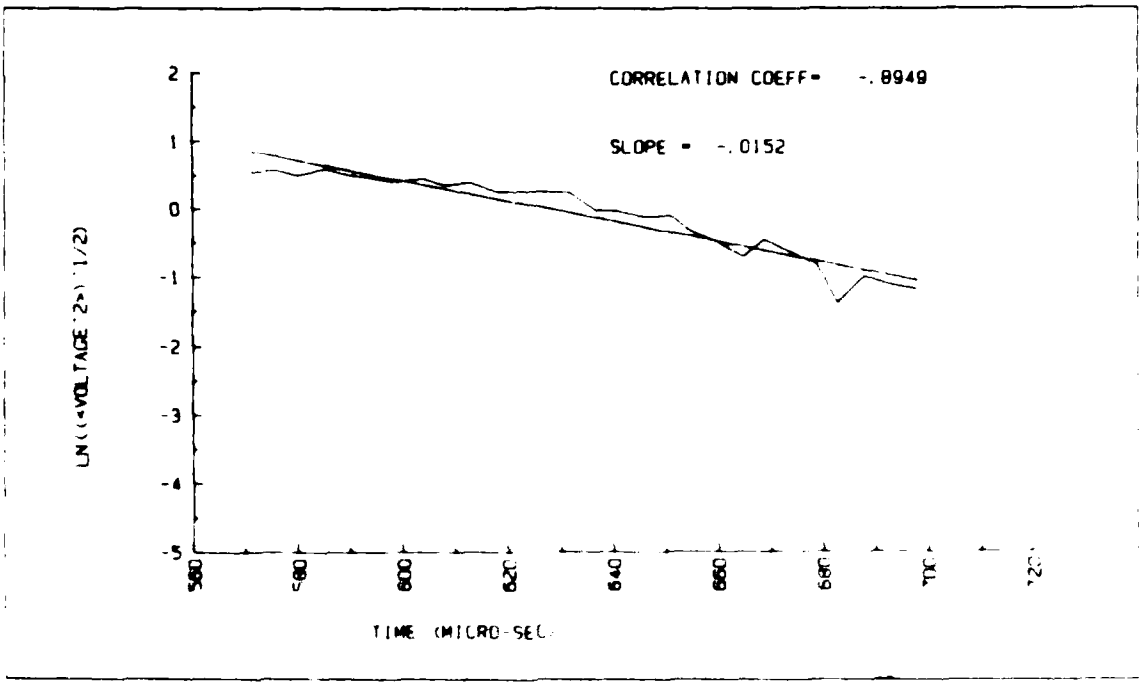

Figure C.1 DATA 30

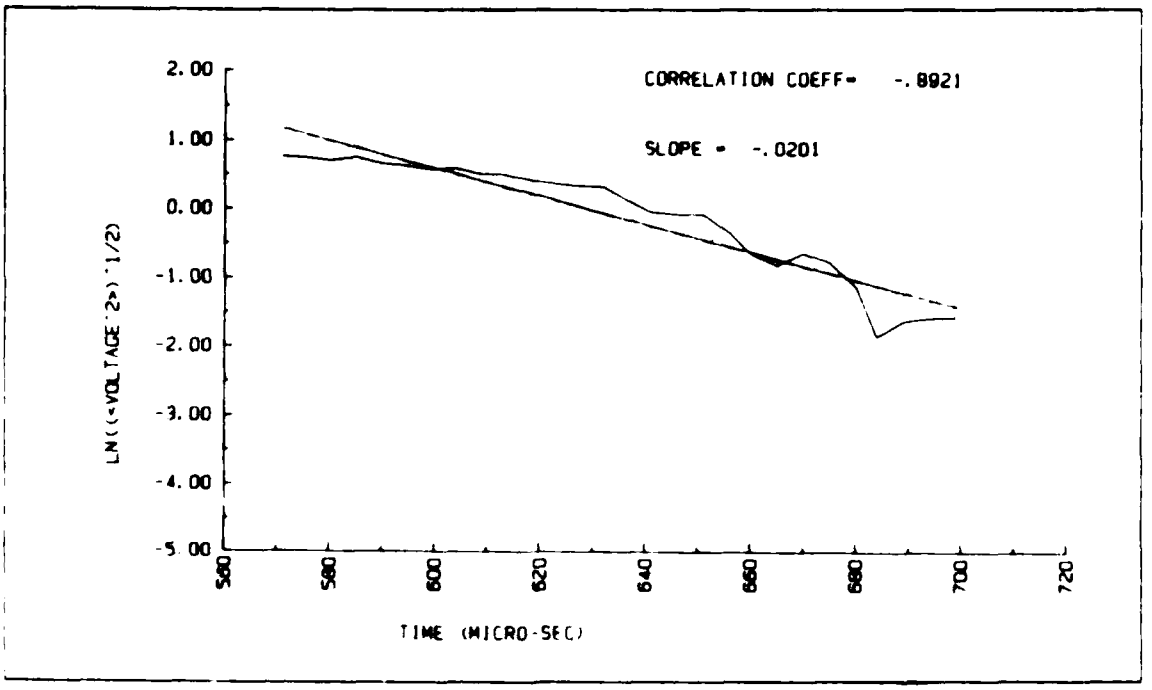

Figure C 2 DATA 31.

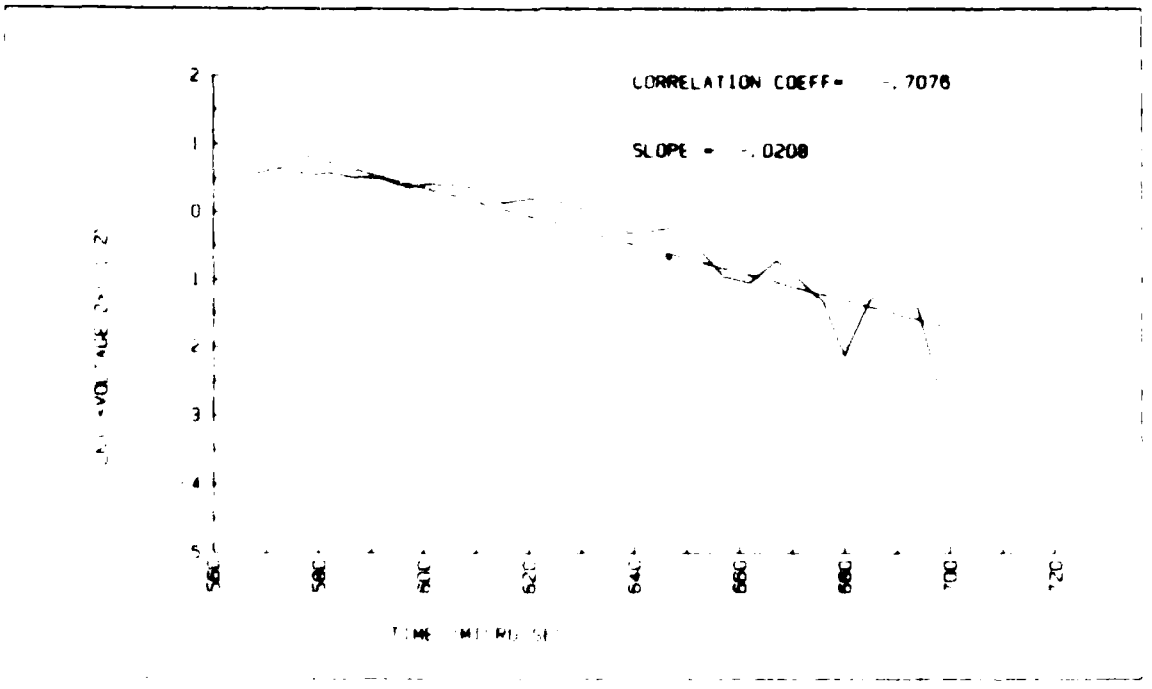

Figure C DATA 32

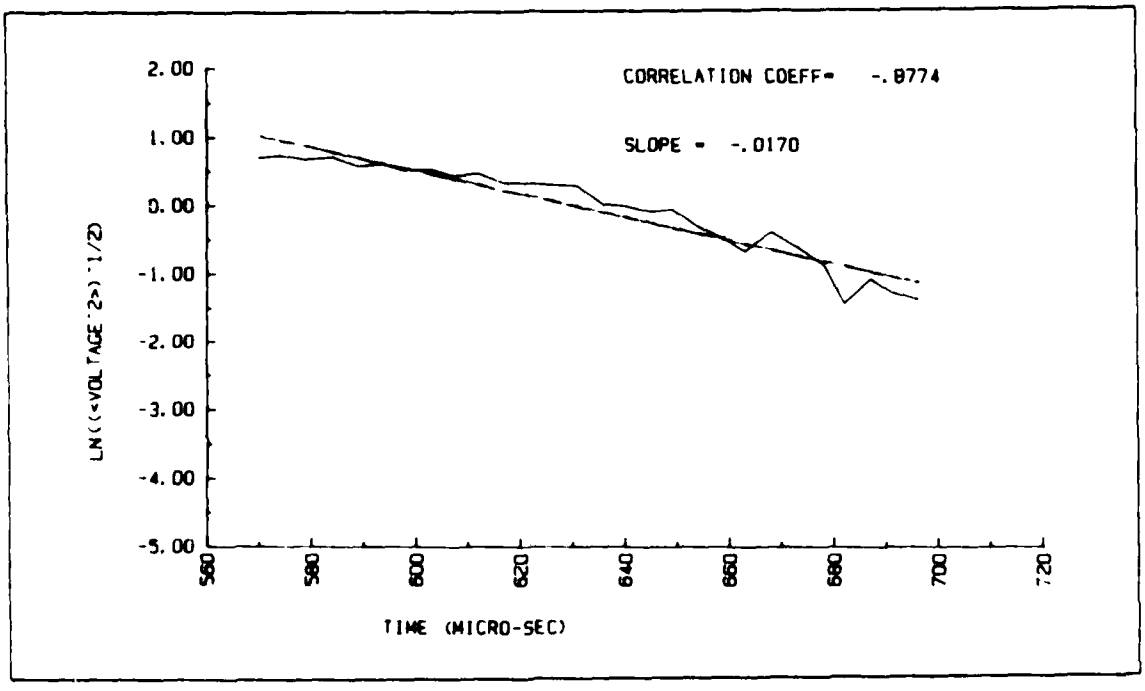

Figure C.4 DATA 33.

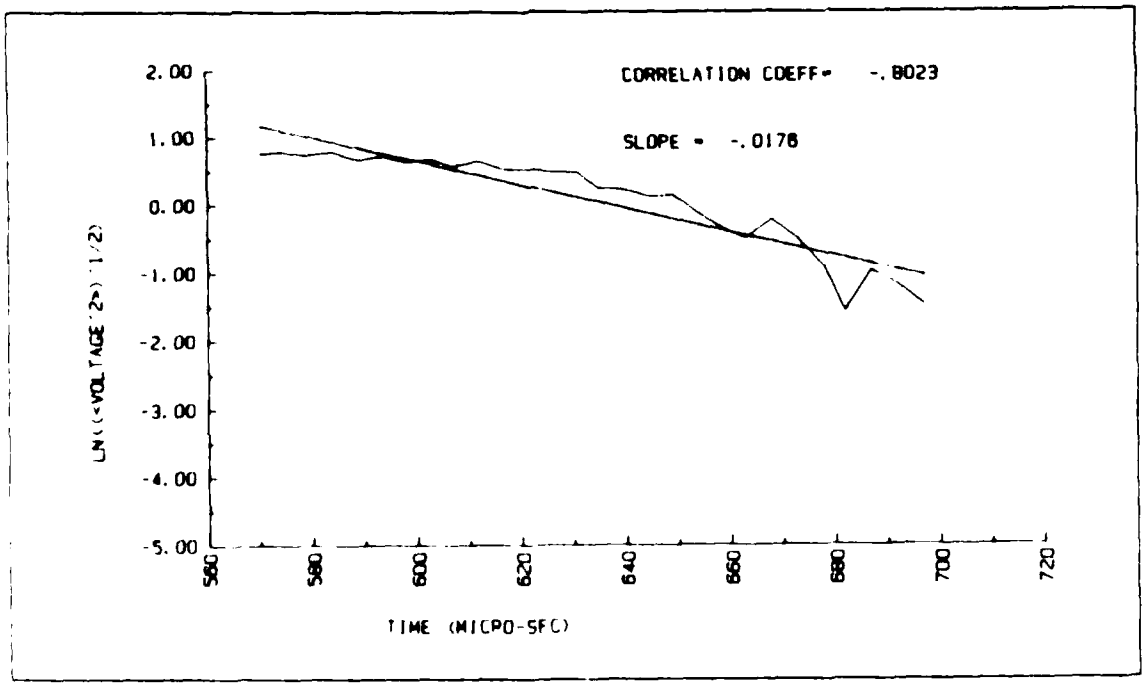

Figure C.5 DATA 34.

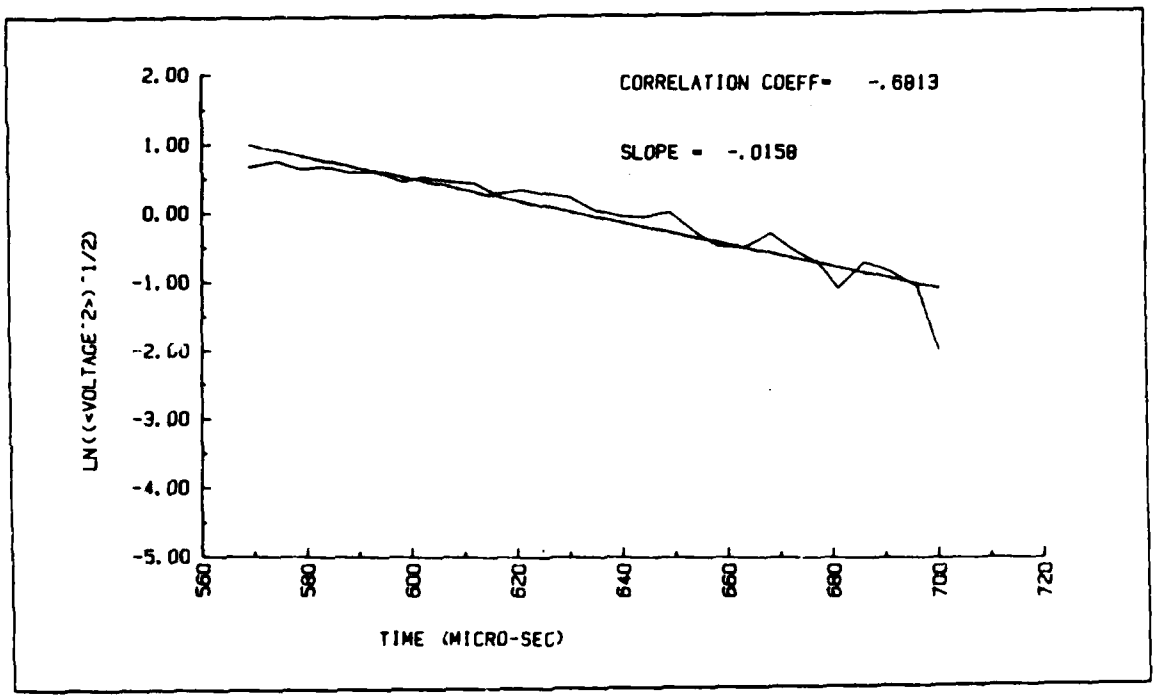

Figure C.6 DATA 35.

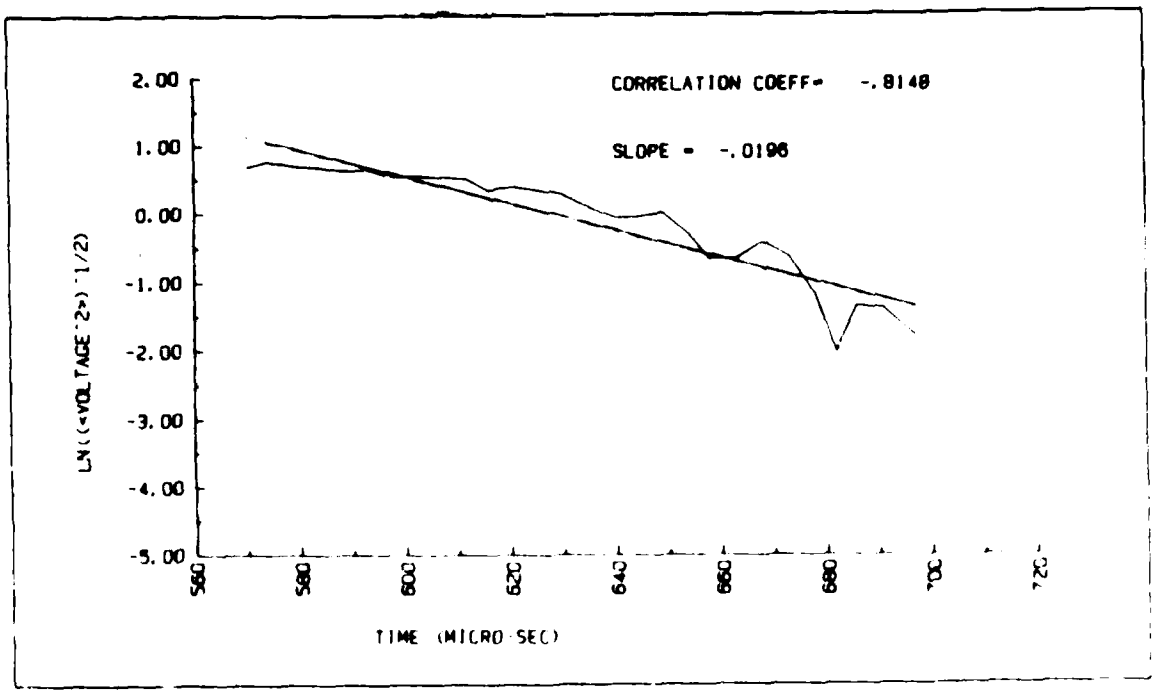

Figure C.7 DATA 36

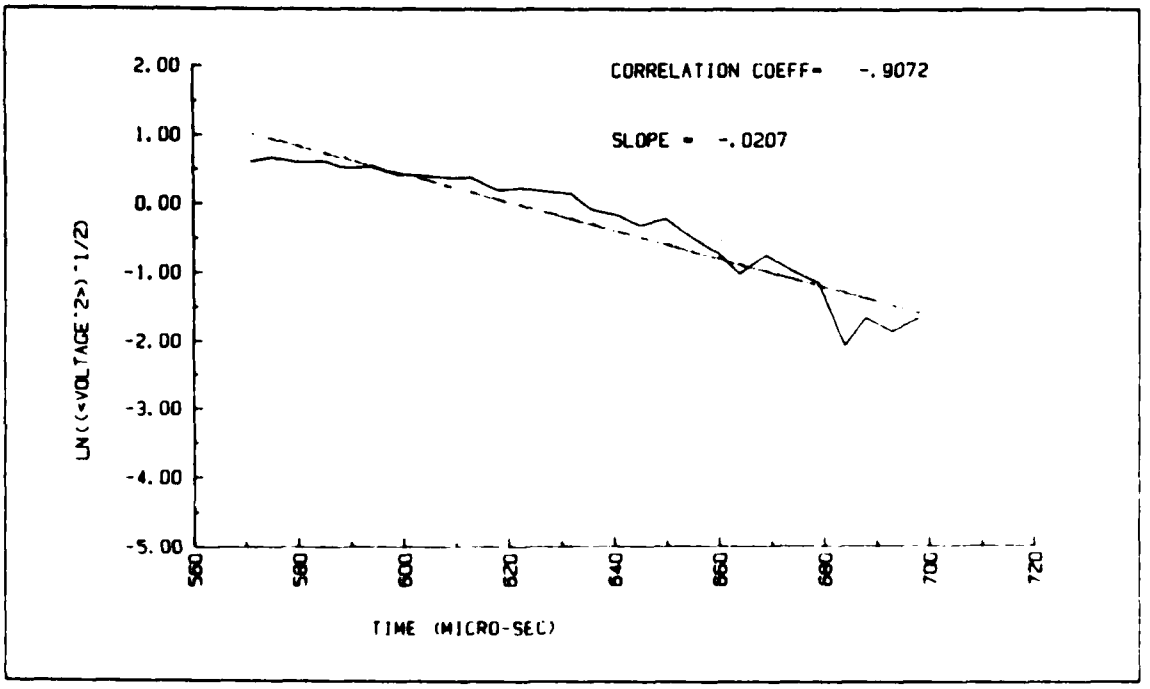

Figure C.8 DATA 37.

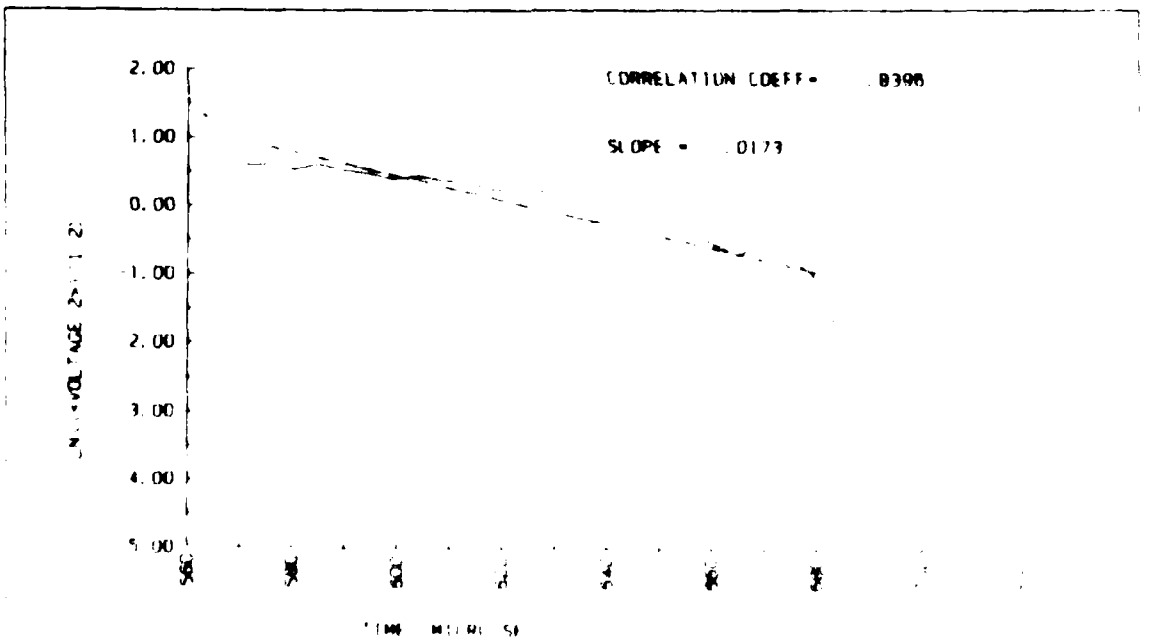

Figure C.9 DATA 38

APPENDIX D
DECAY ENVELOPE GRAPHS FOR AGGREGATE SAND AT 62 KHZ

The decay envelopes for aggregate sand sediment at 62 kHz (DATA 40 to DATA 47) were showed in this appendix.

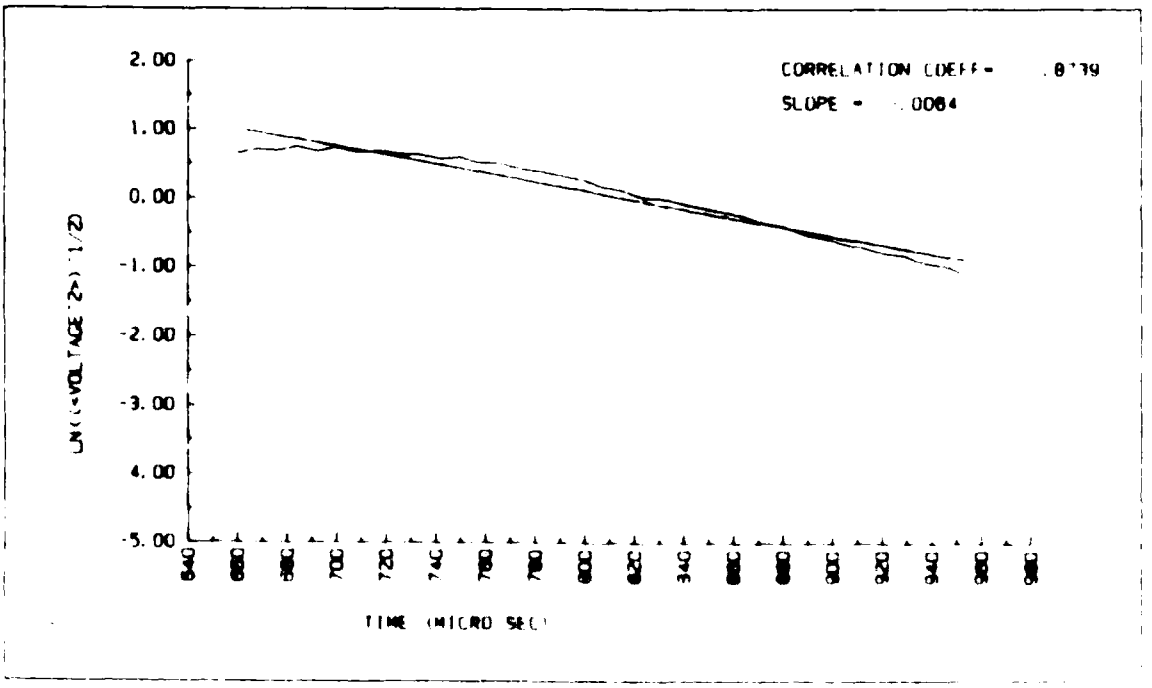

Figure D.1 DATA 40

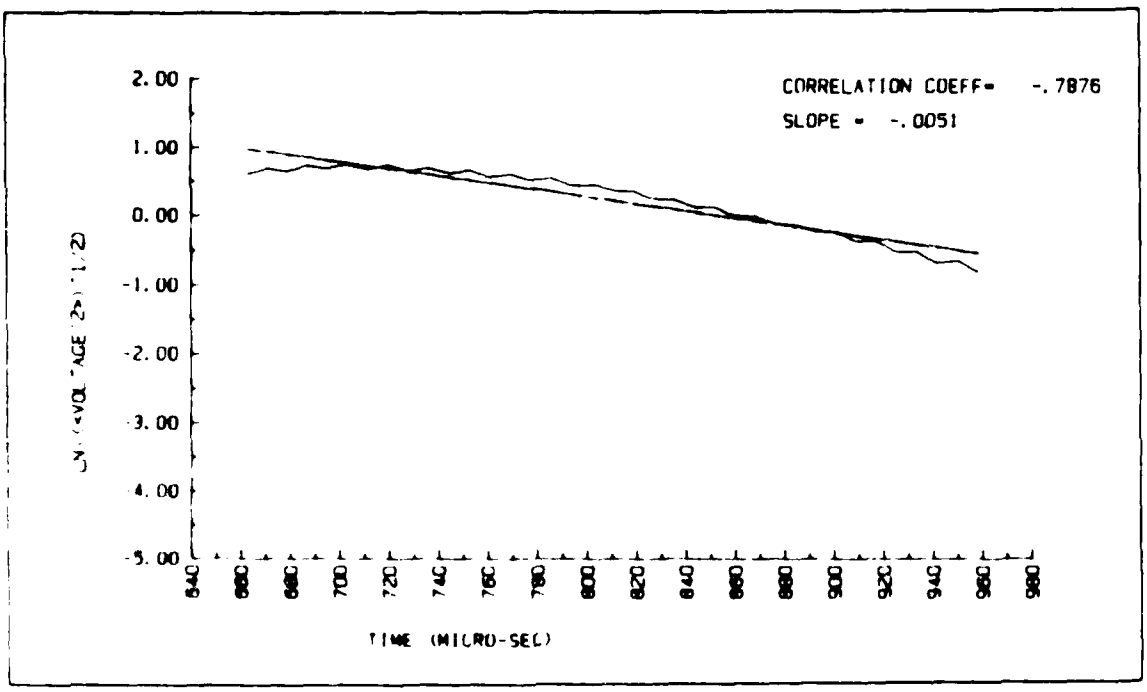

Figure D.2 DATA 41.

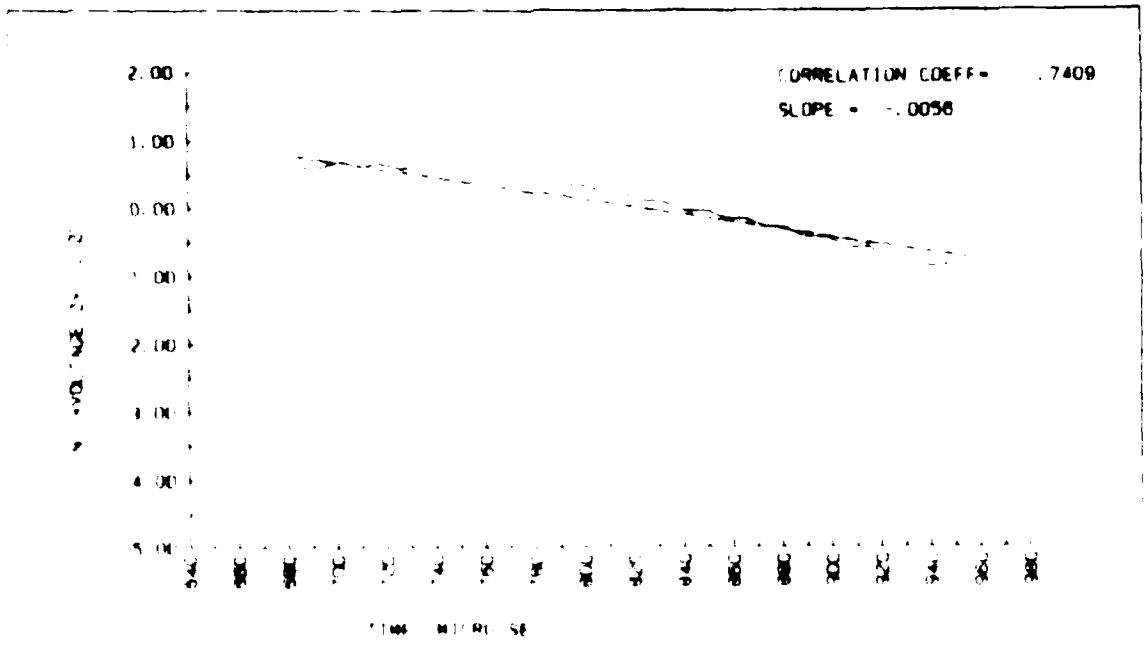

Figure D.3 DATA 42.

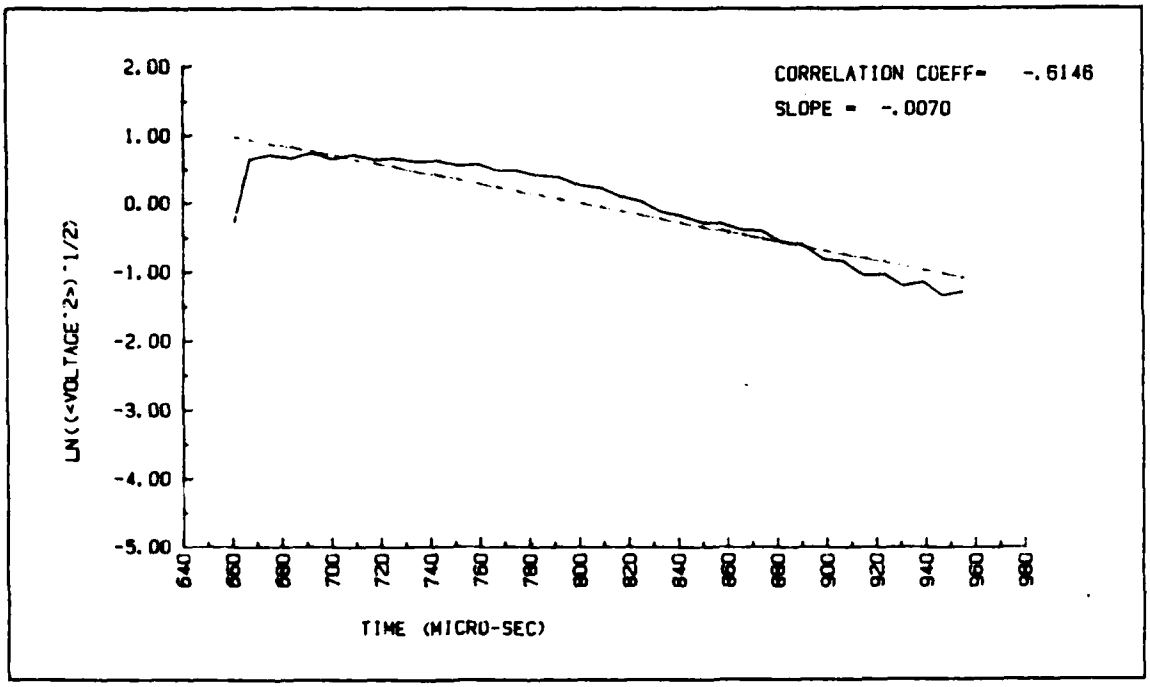

Figure D.4 DATA 43.

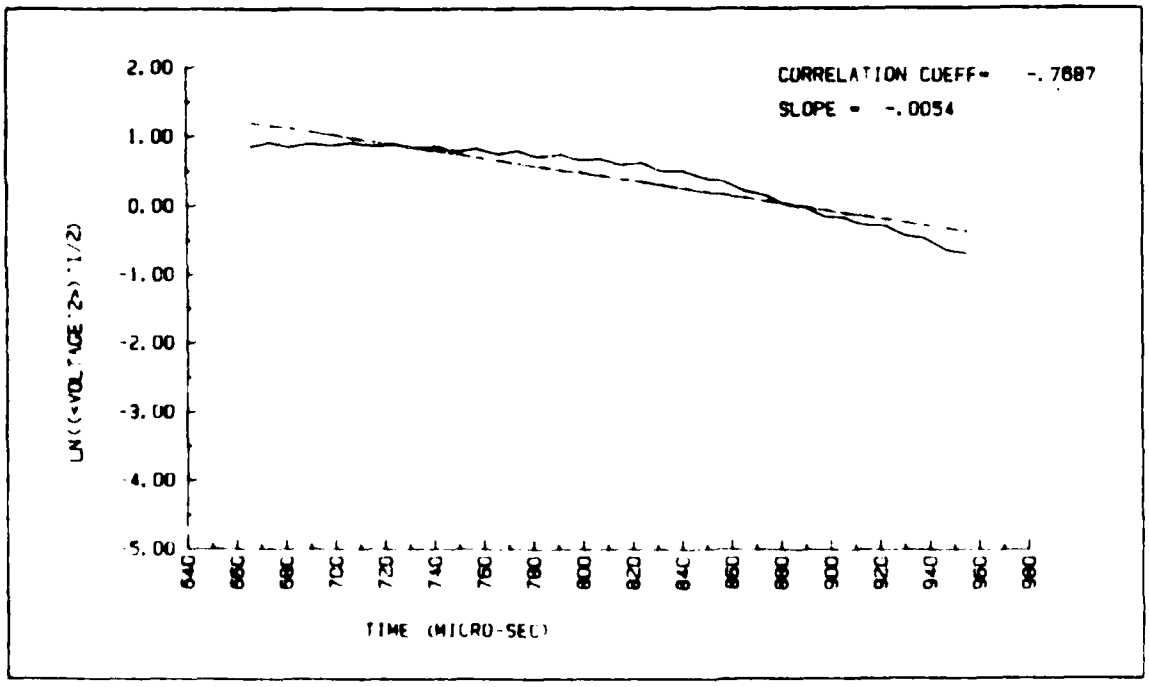

Figure D.5 DATA 44.

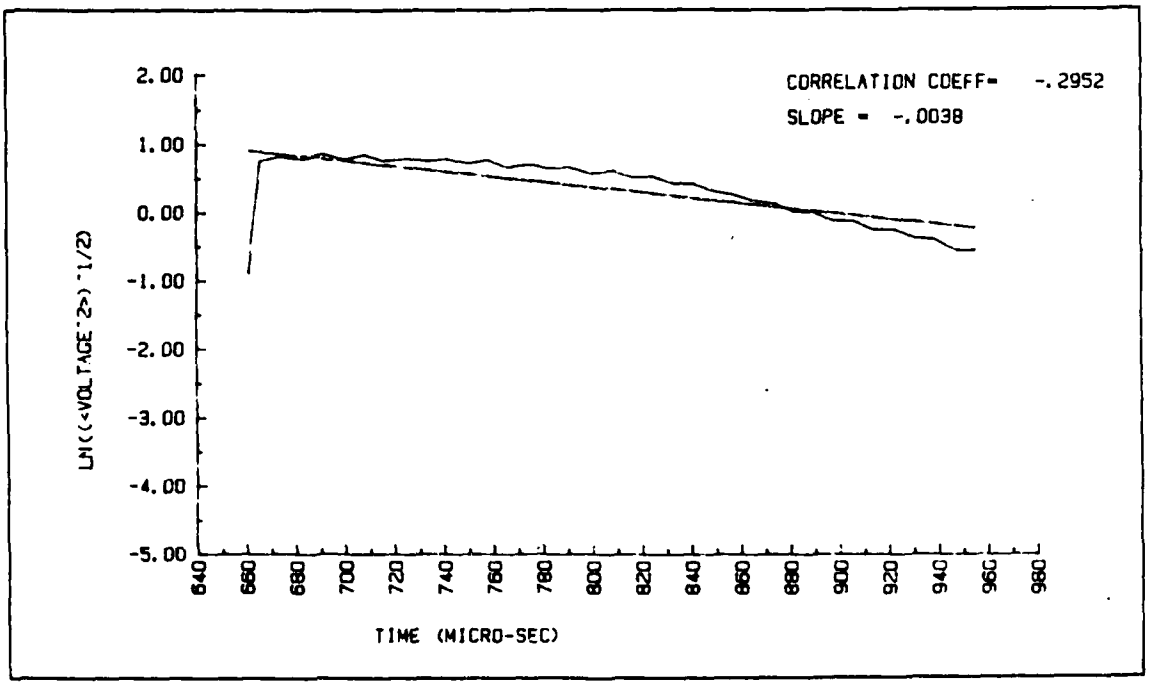

Figure D.6 DATA 45.

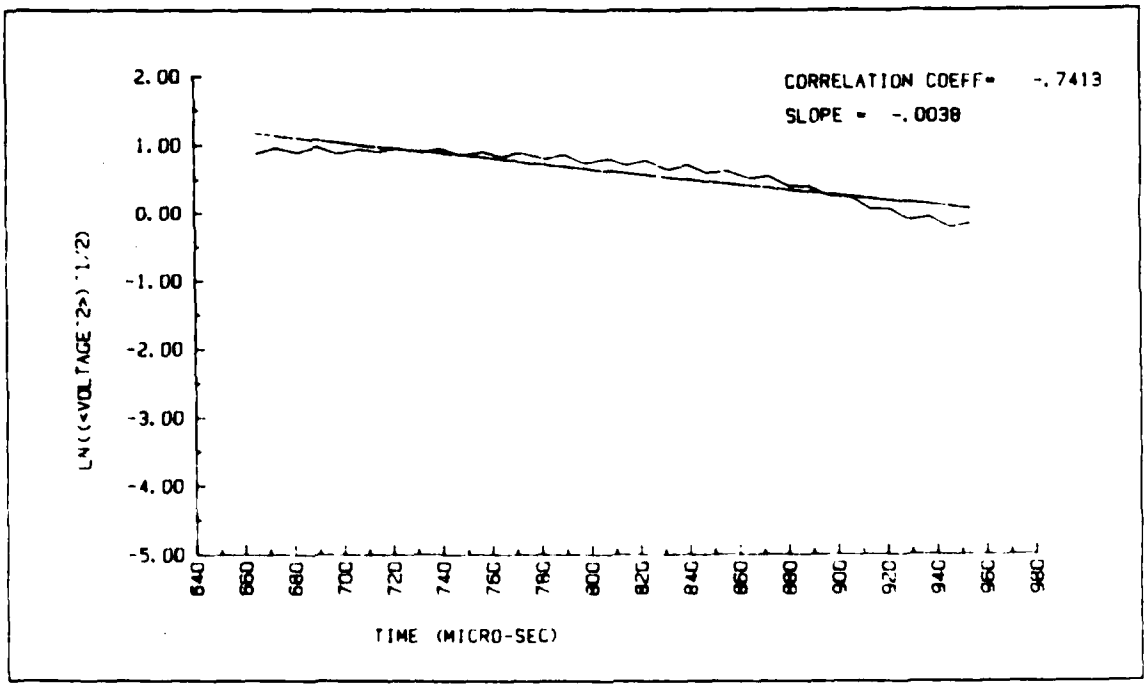

Figure D.7 DATA 46.

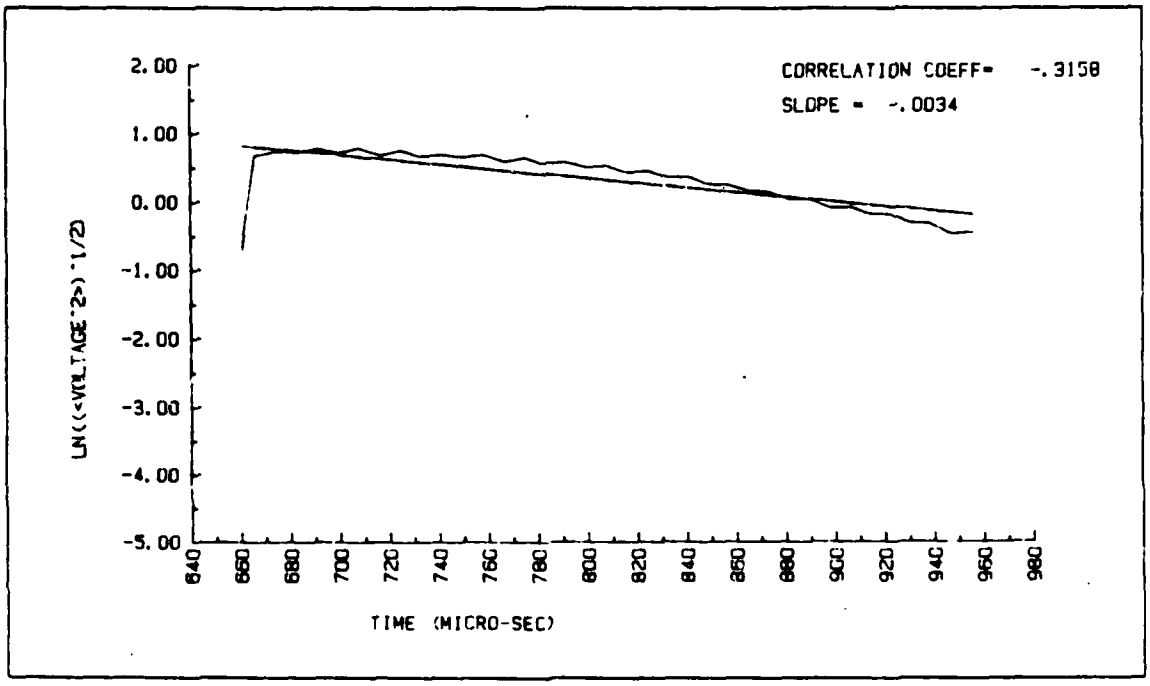

Figure D.8 DATA 47.

APPENDIX E
DECAY ENVELOPE FOR AGGREGATE SAND SEDIMENT AT 108 KHZ

The decay envelopes for aggregate sand sediment at 108 kHz (DATA 50 to DATA 57) were showed in this appendix.

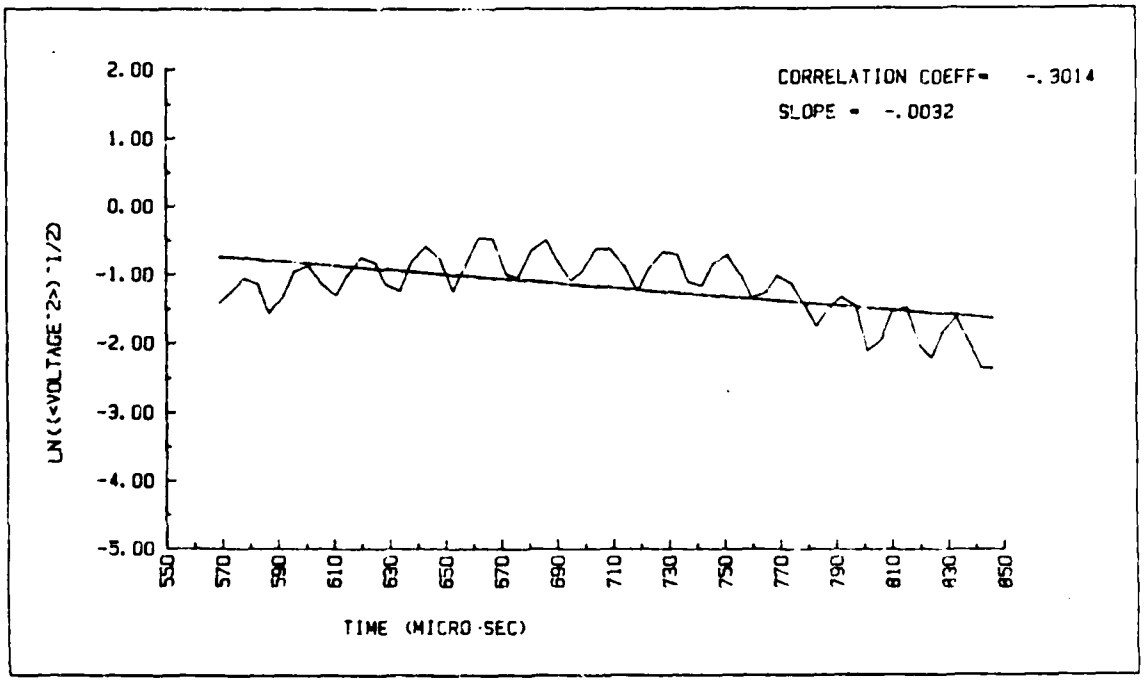

Figure E.1 DATA 50.

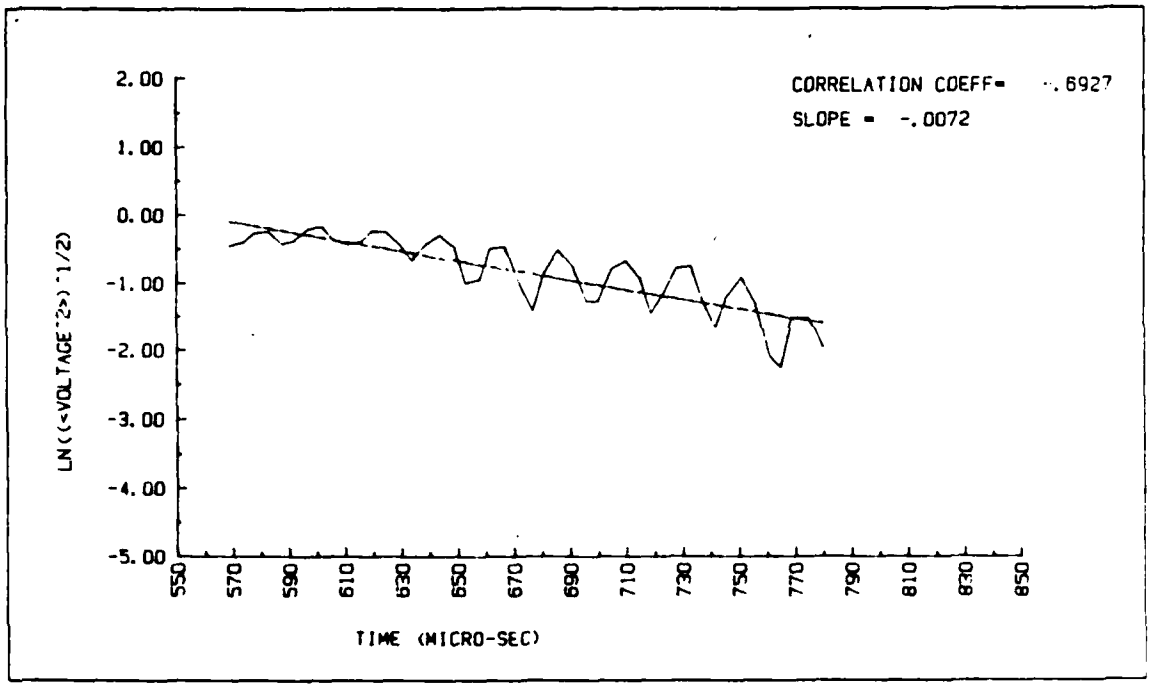

Figure E.2 DATA 51.

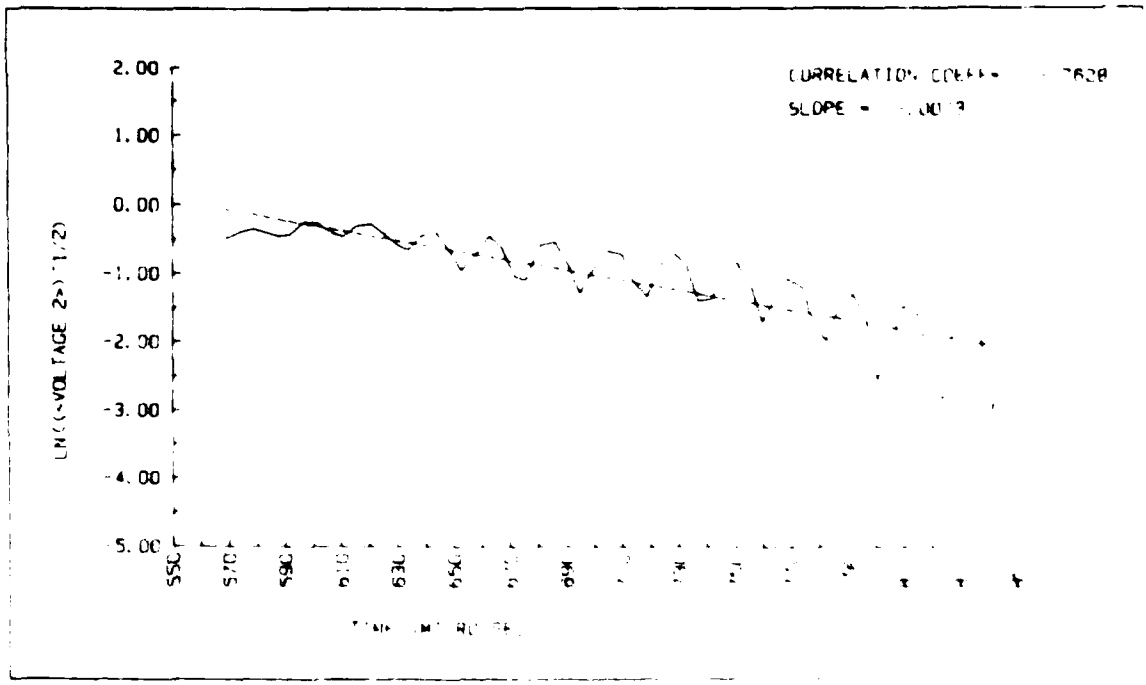

Figure E.3 DATA 52.

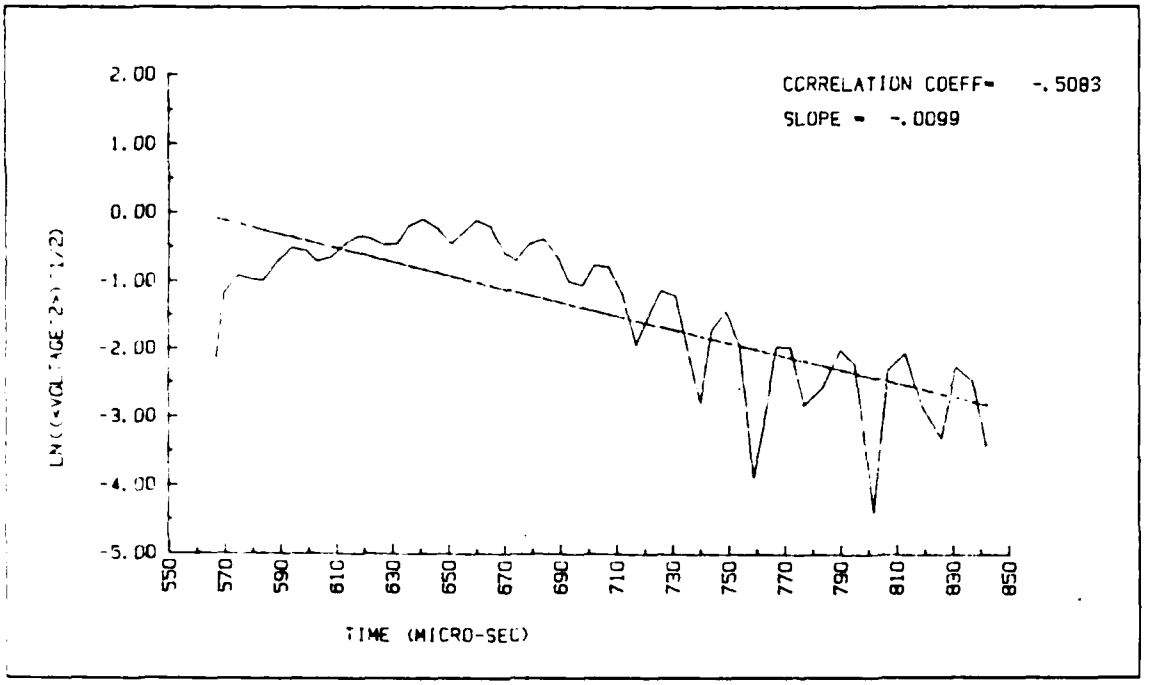

Figure E.4 DATA 53.

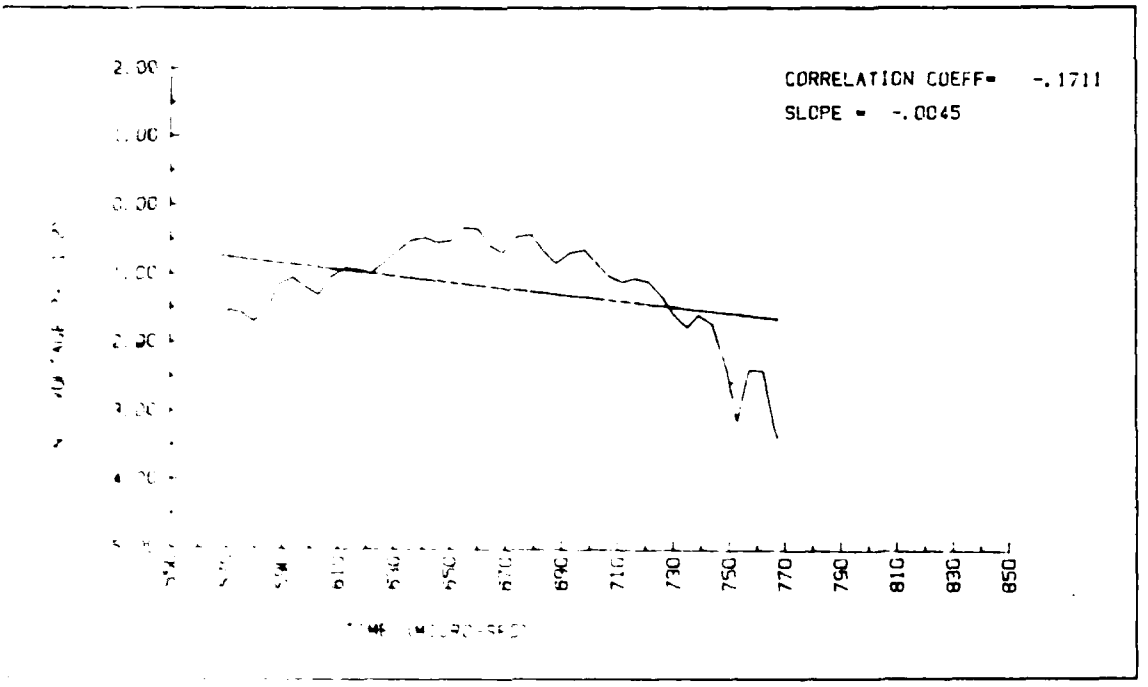

Figure E.5 DATA 54.

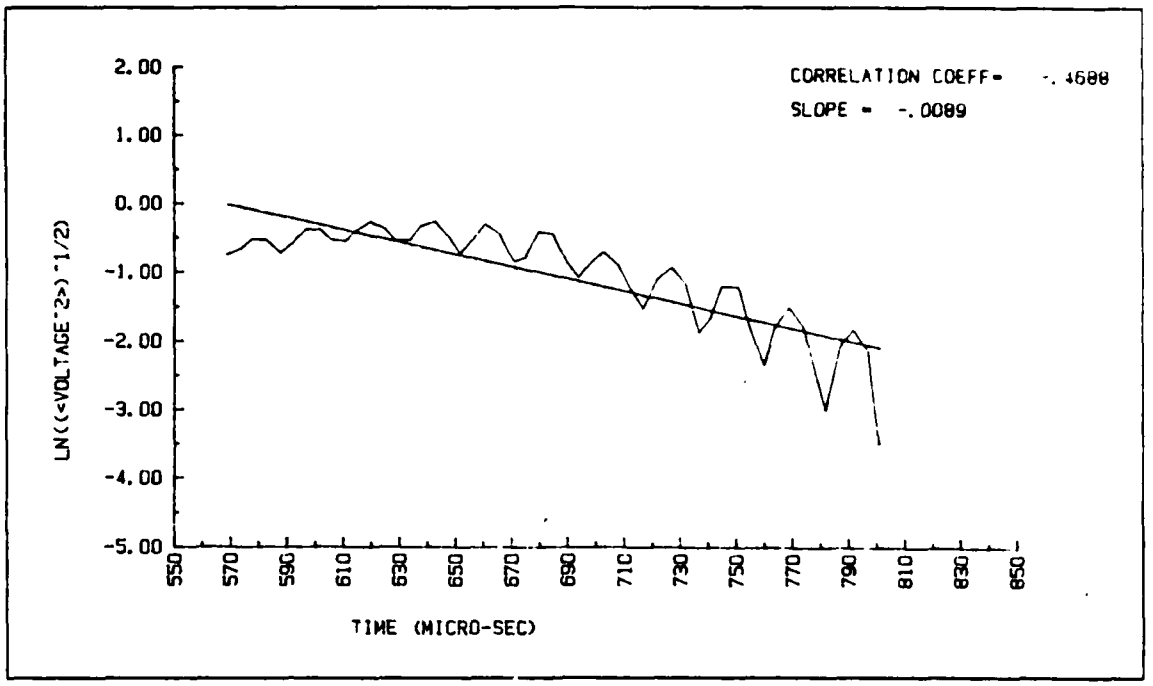

Figure E.6 DATA 55.

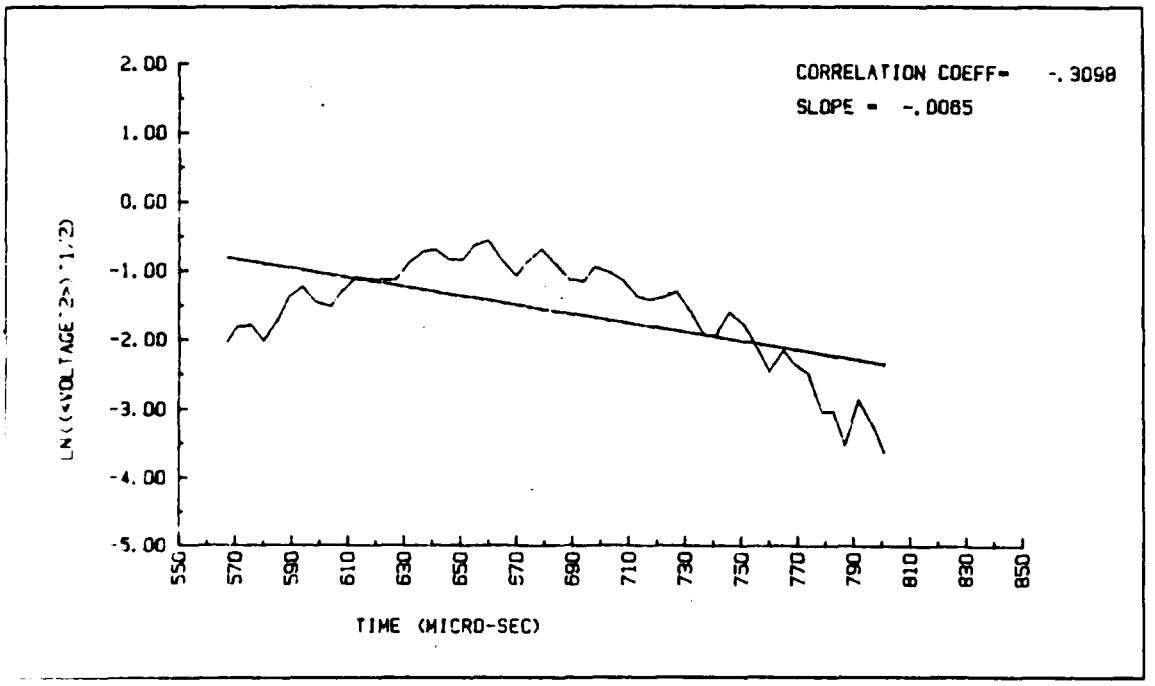

Figure E.7 DATA 56.

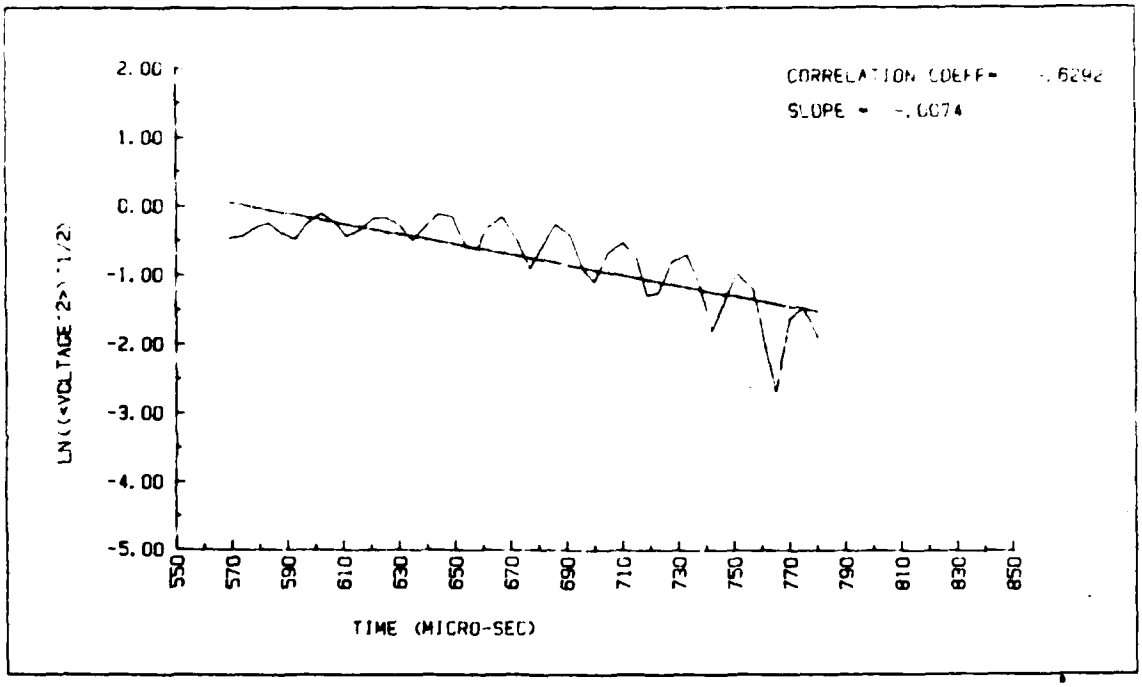

Figure E.8 DATA 57.

APPENDIX F
DECAY ENVELOPE GRAPHS FOR COARSE GLASS BEADS SEDIMENT AT 181 KHZ

The decay envelopes for coarse glass beads (DATA 60 to DATA 69) were showed in this appendix.

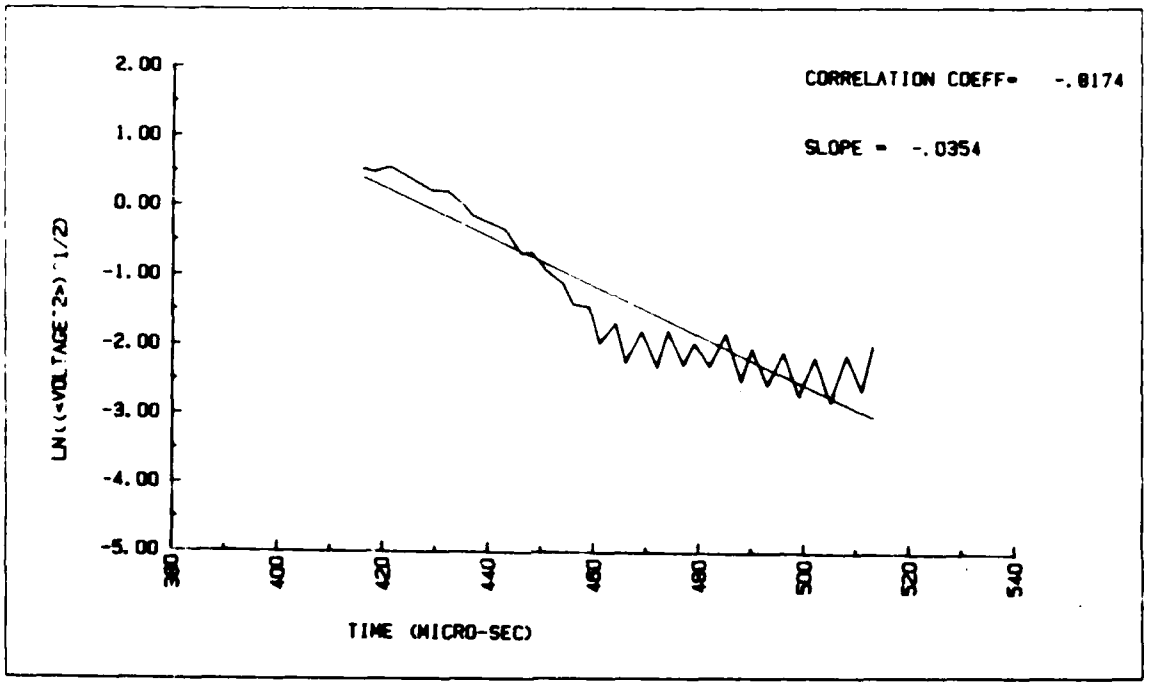

Figure F.1 DATA 60.

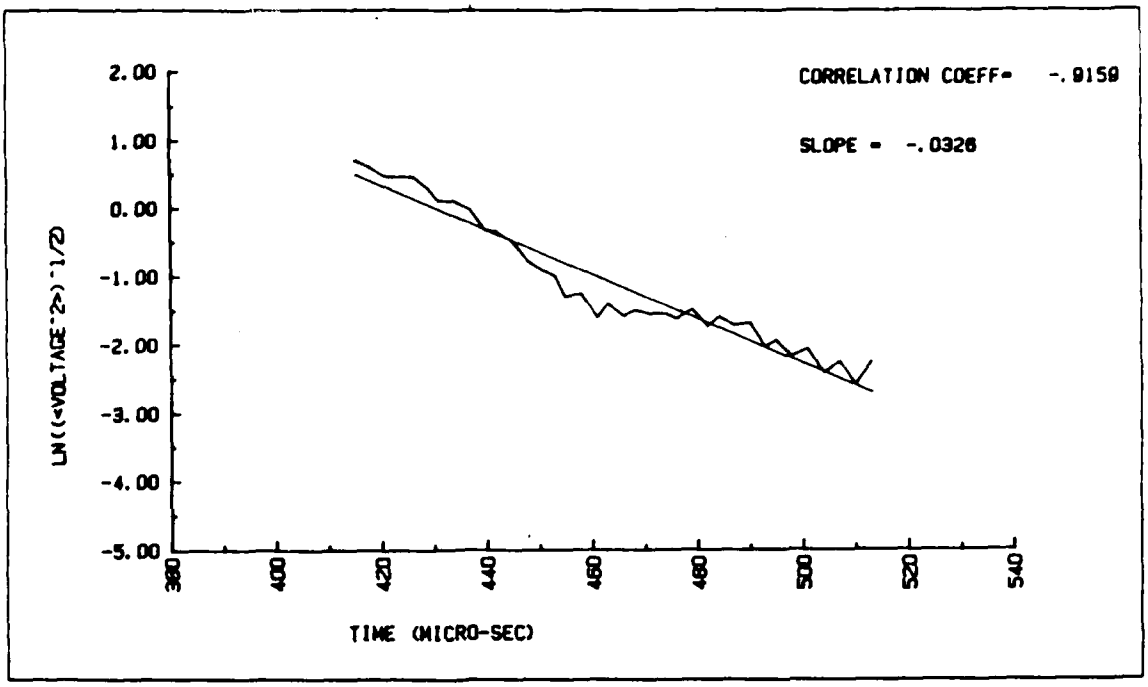

Figure F.2 DATA 61.

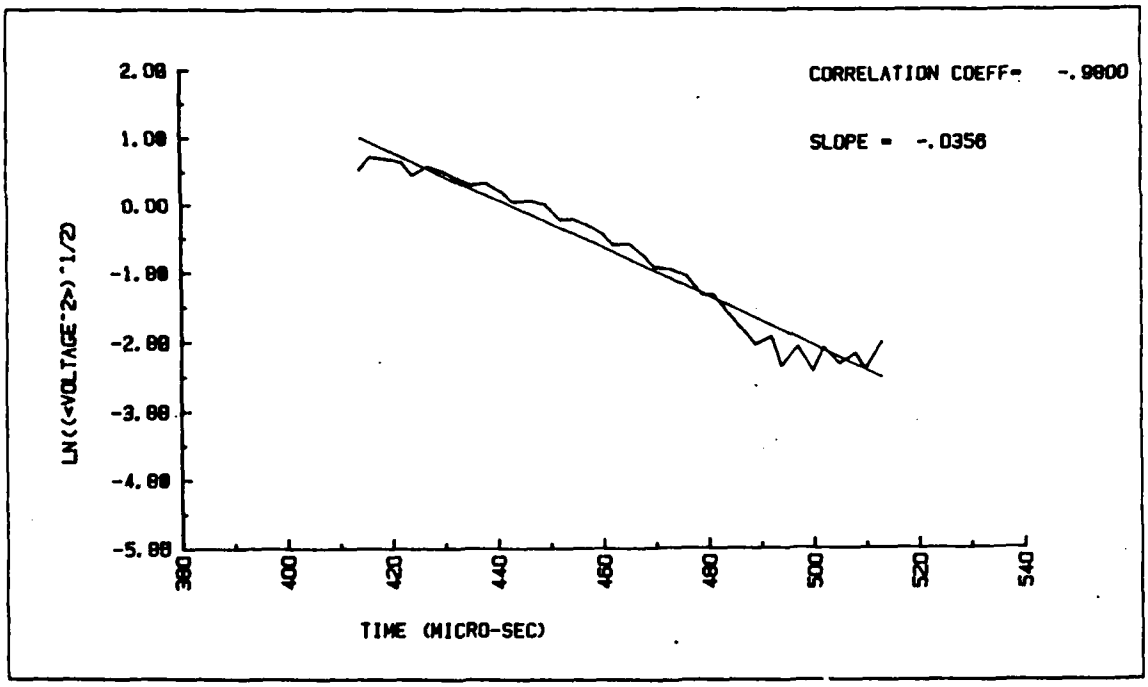

Figure F.3 DATA 62.

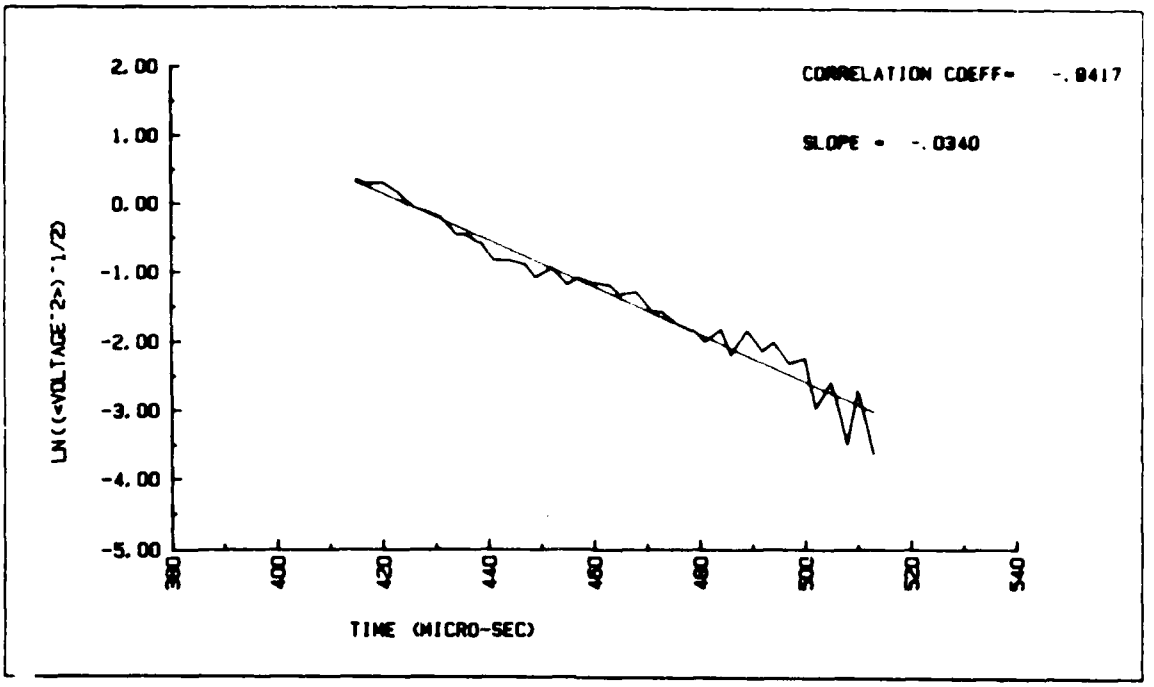

Figure F.4 DATA 63.

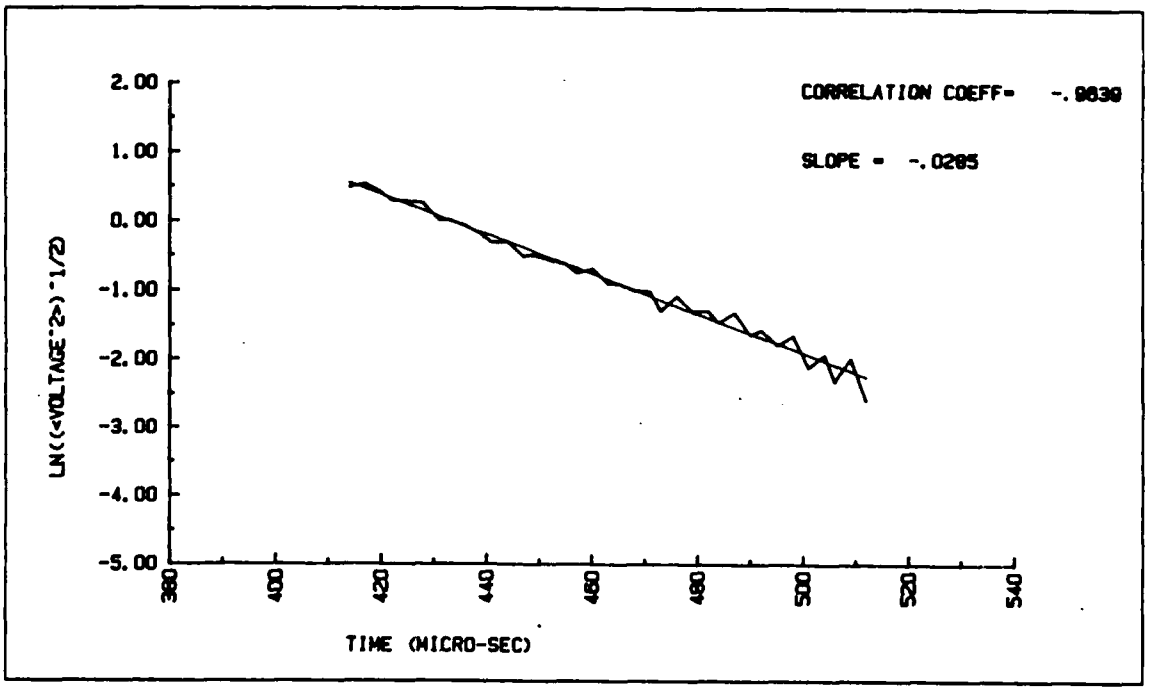

Figure F.5 DATA 64.

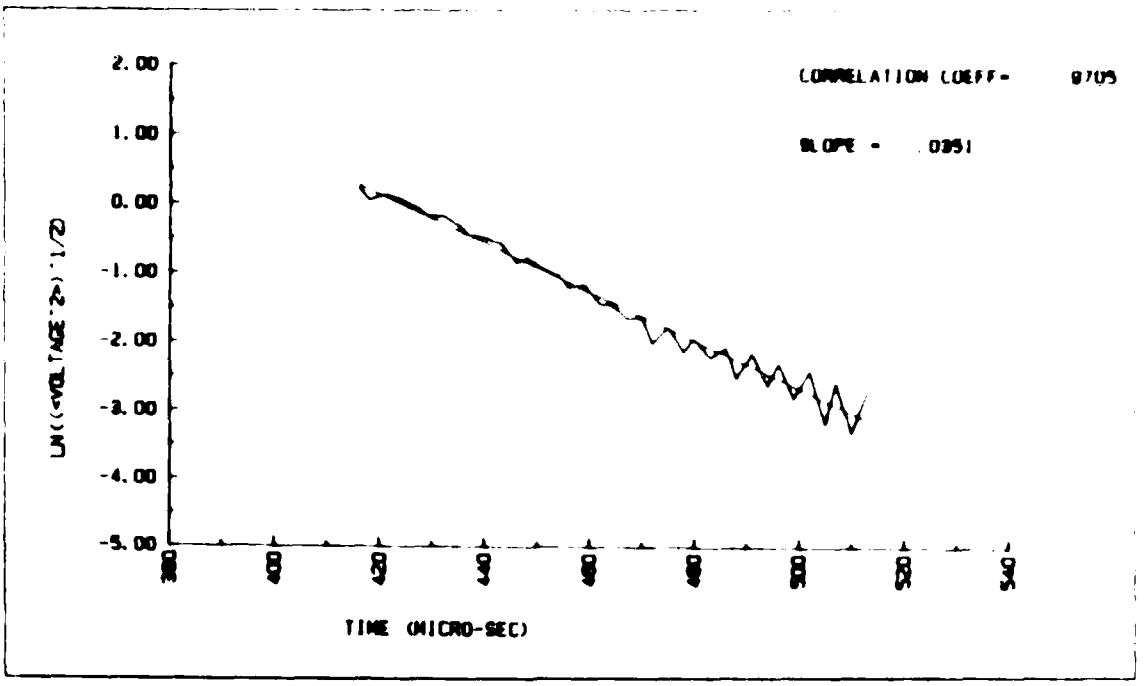

Figure F.6 DATA 65.

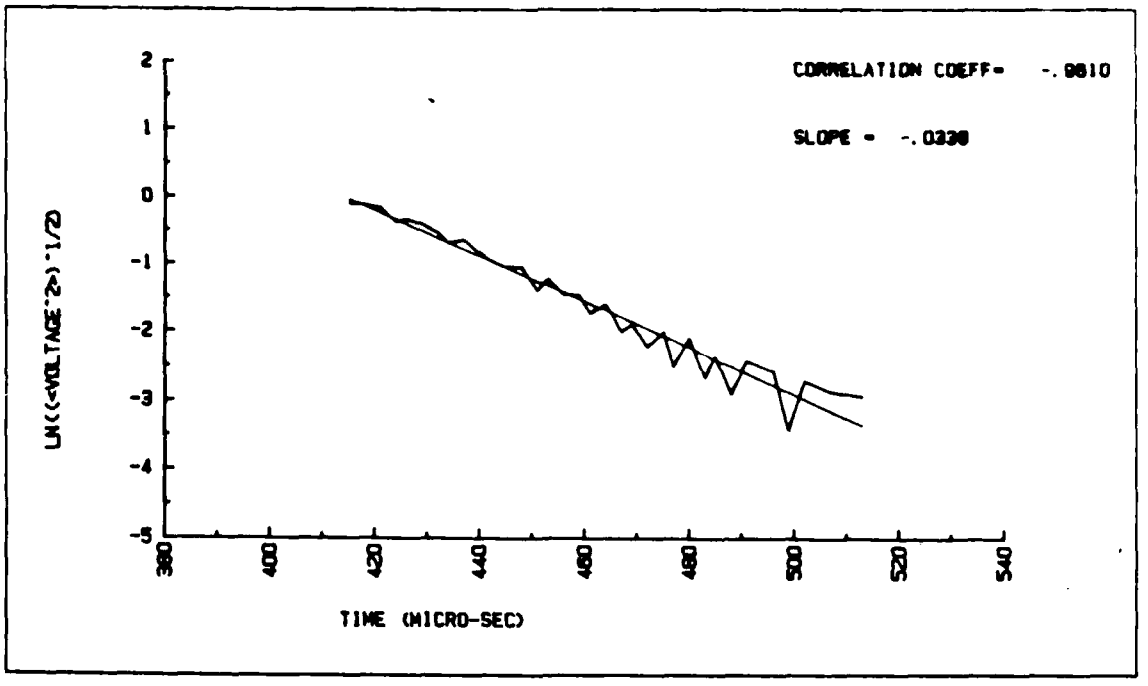

Figure F.7 DATA 66.

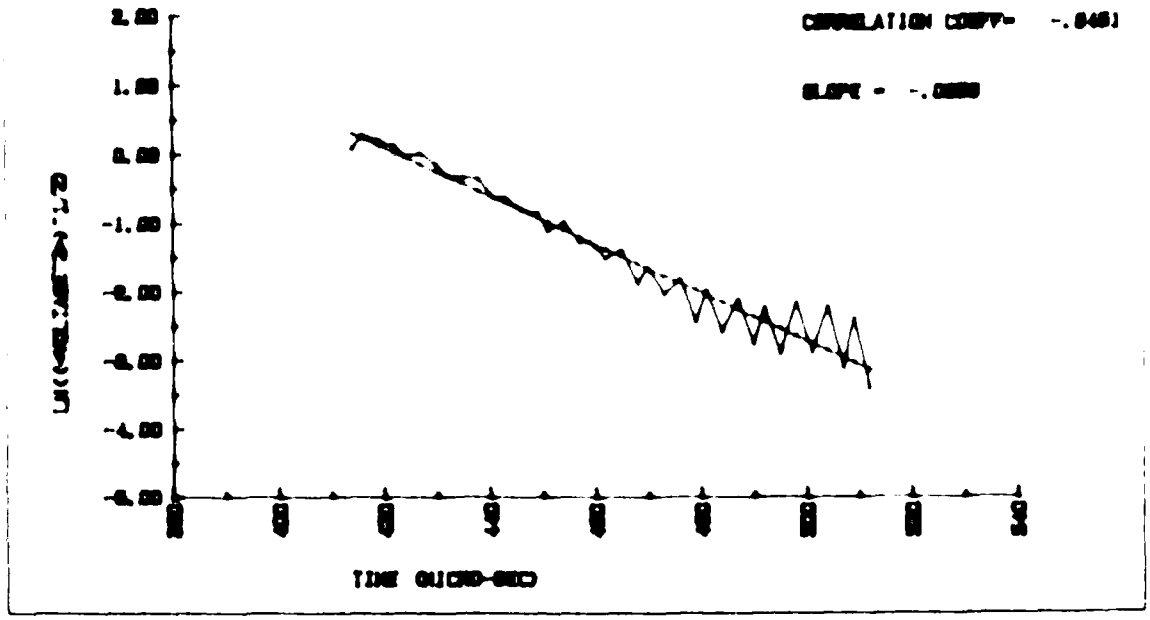

Figure F.8 DATA 67.

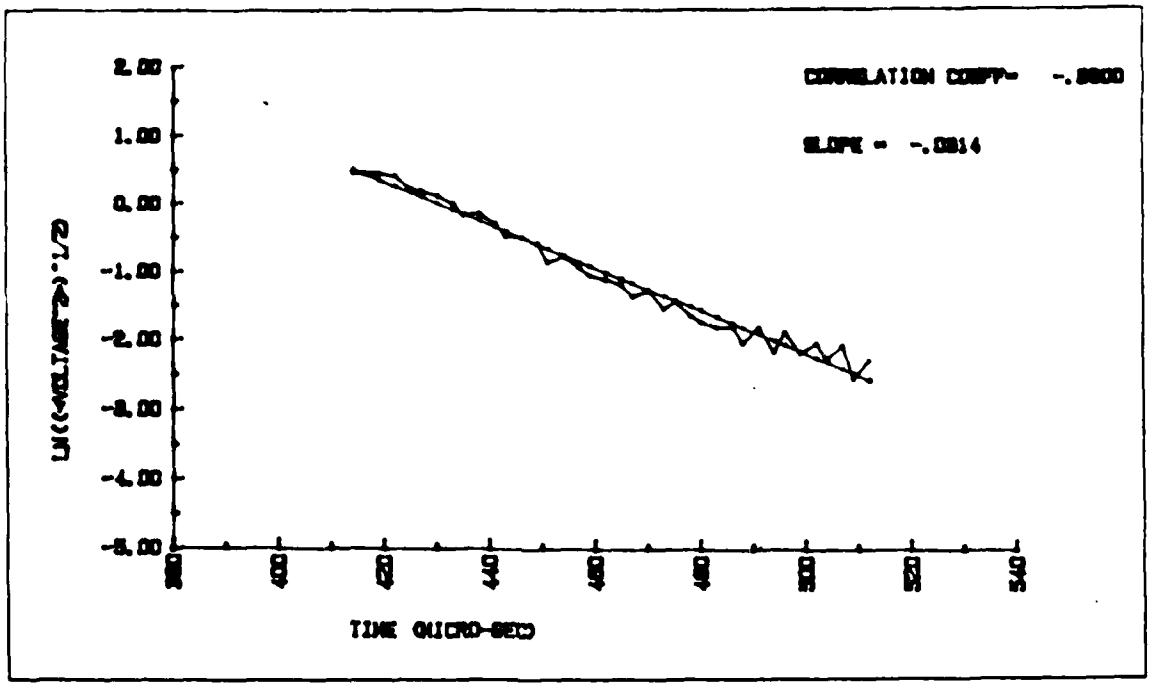

Figure F.9 DATA 68.

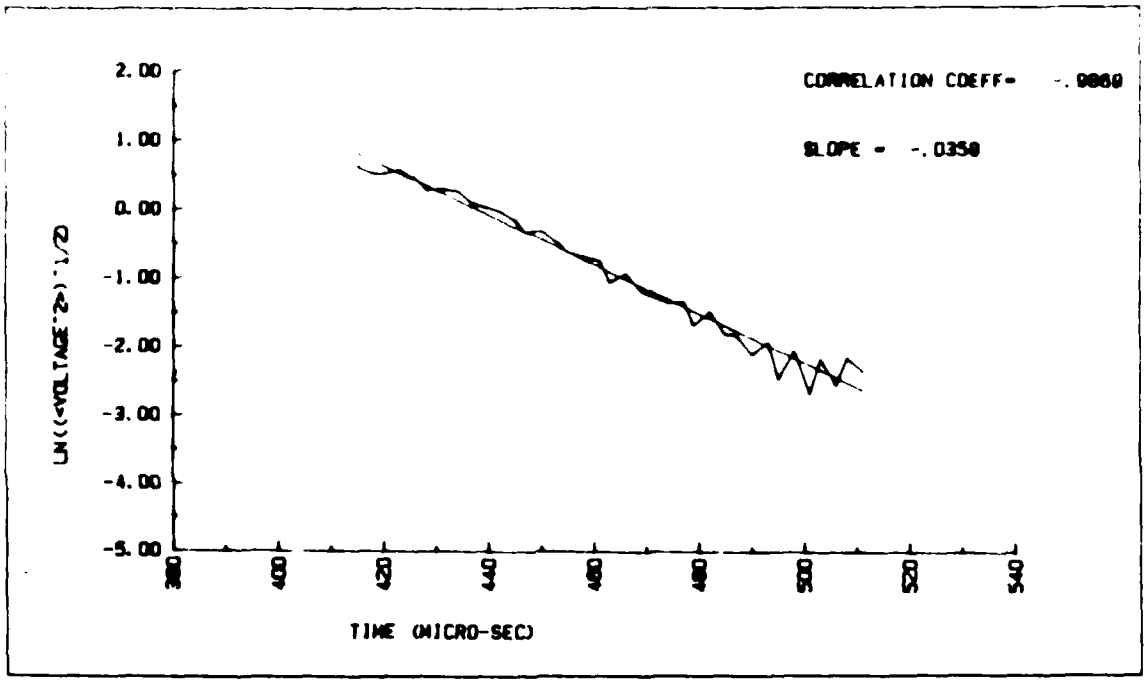

Figure F.10 DATA 69.

APPENDIX G
DECAY ENVELOPE GRAPHS FOR FINE GLASS BEADS AT 181 KHZ

The decay envelopes for fine glass beads sediment (DATA 70 to DATA 79) were showed in this appendix.

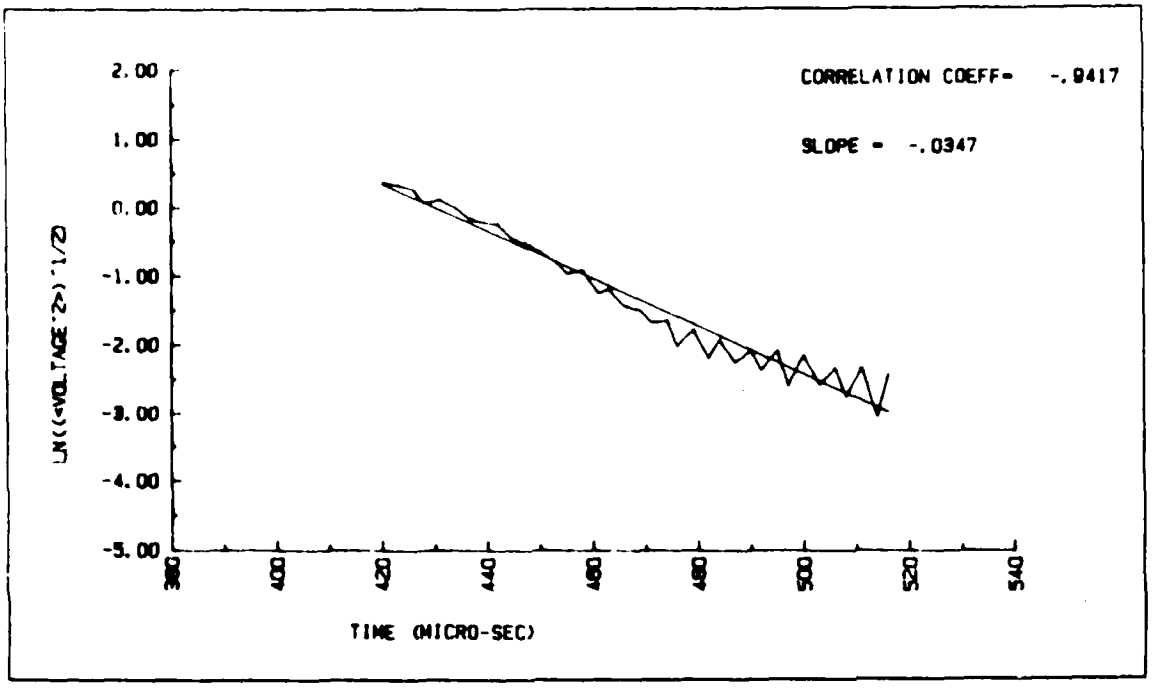

Figure G.1 DATA 70.

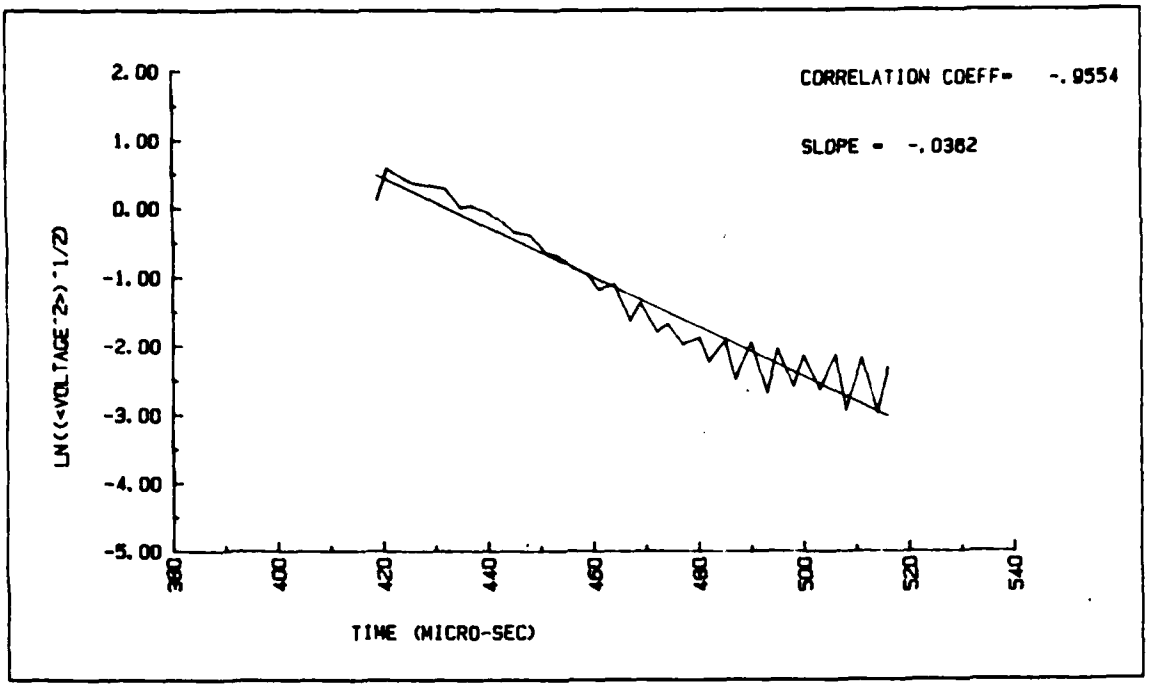

Figure G.2 DATA 71.

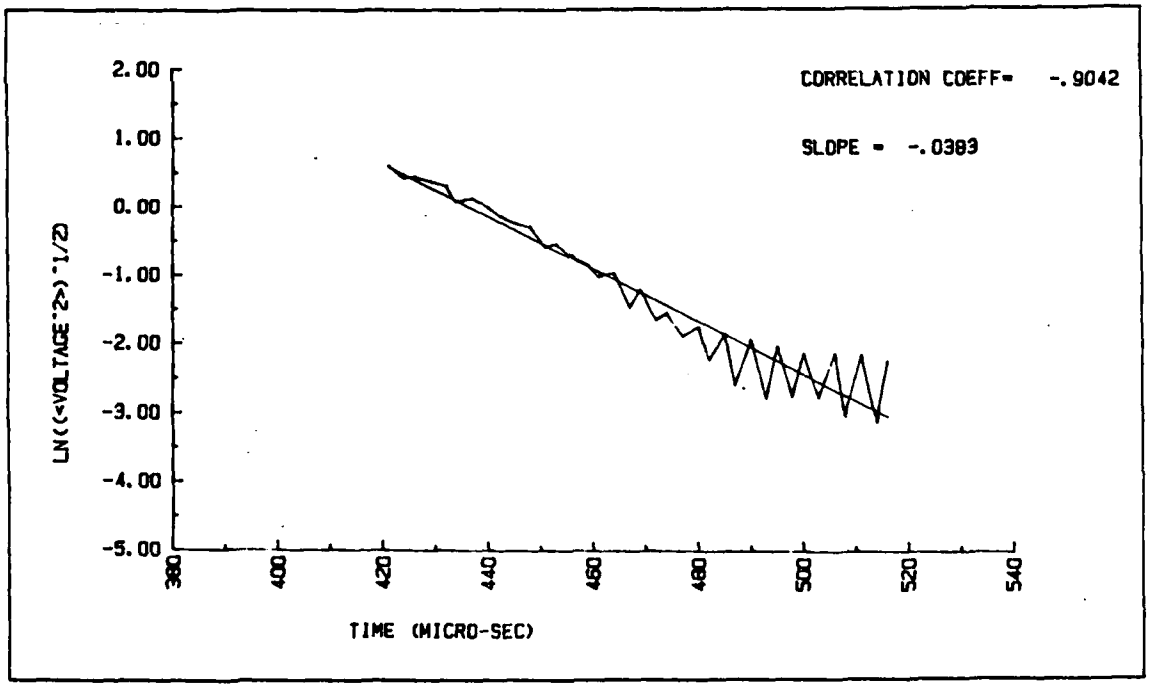

Figure G.3 DATA 72.

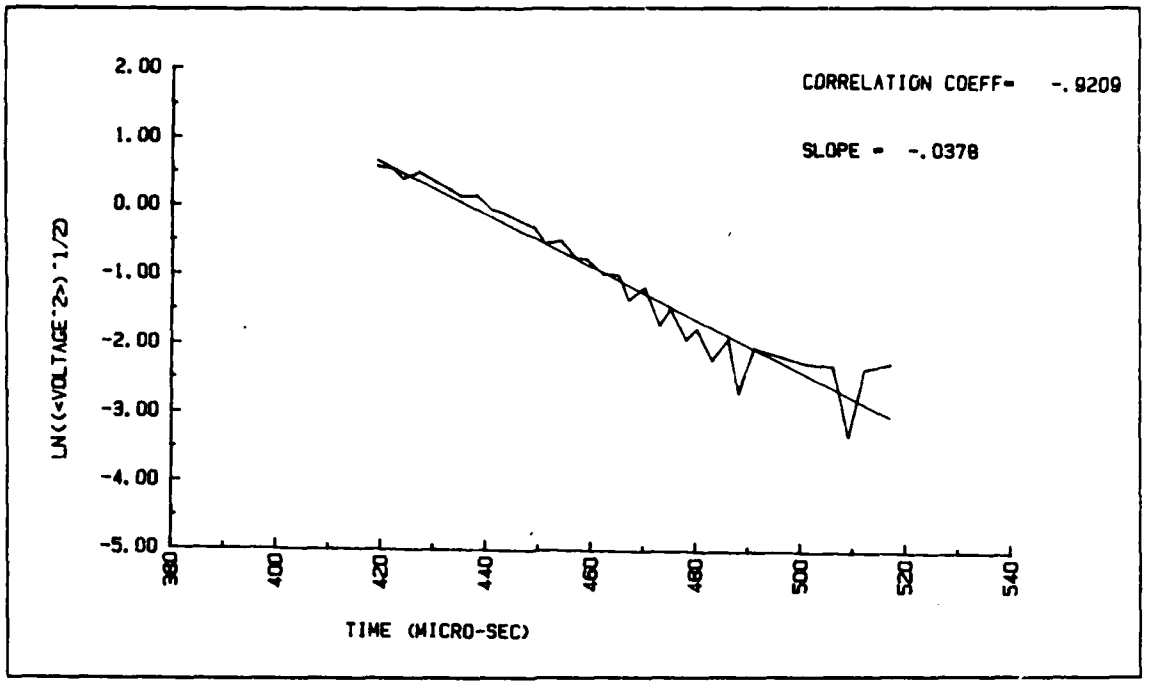

Figure G.4 DATA 73.

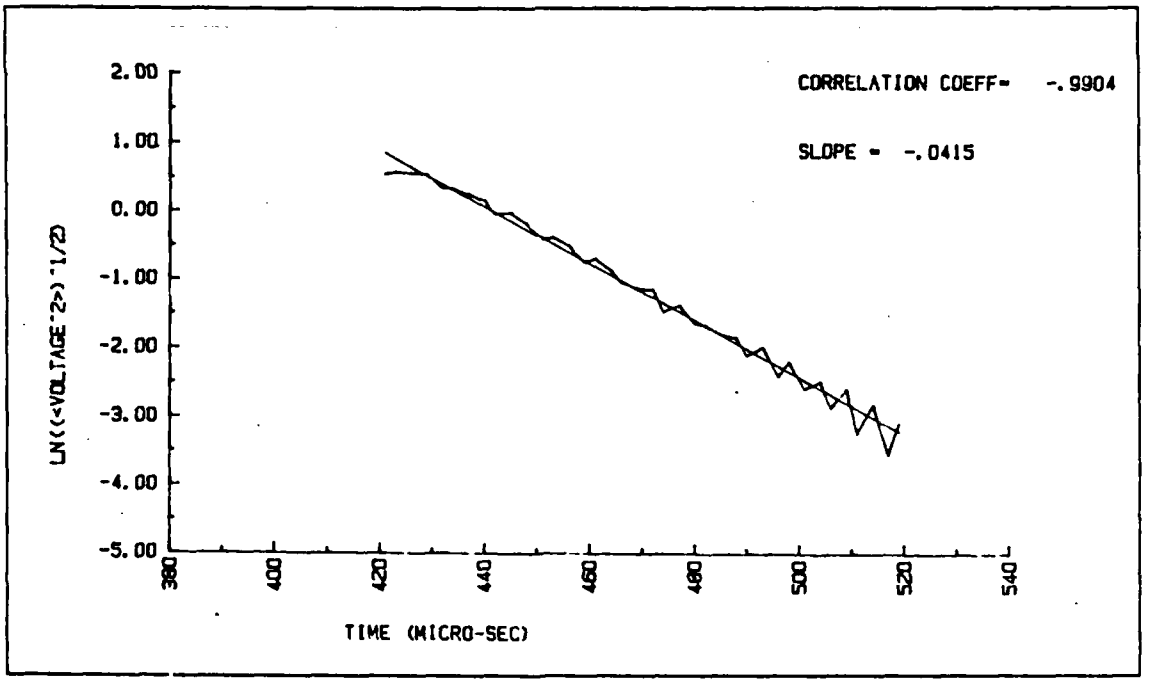

Figure G.5 DATA 74.

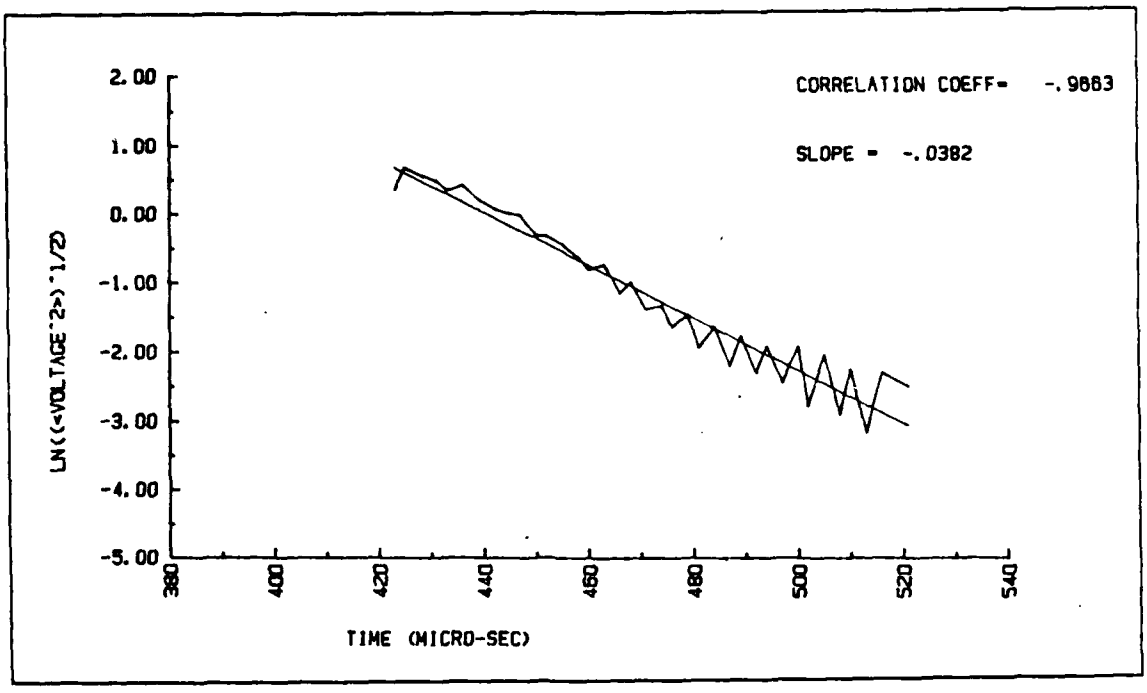

Figure G.6 DATA 75.

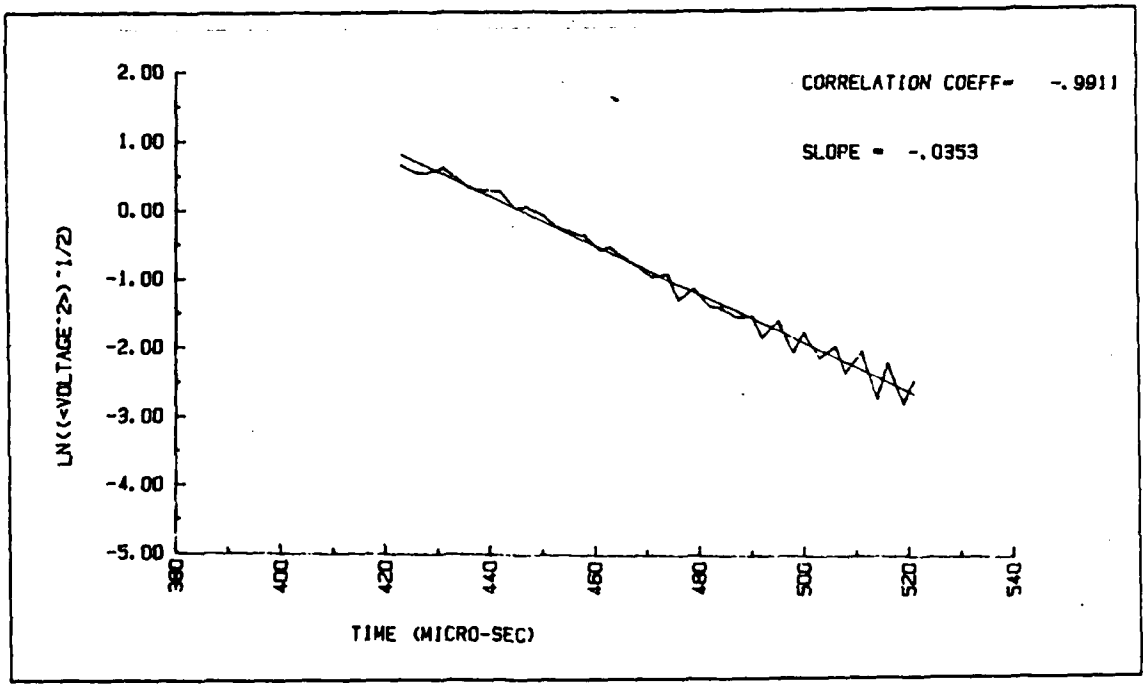

Figure G.7 DATA 76.

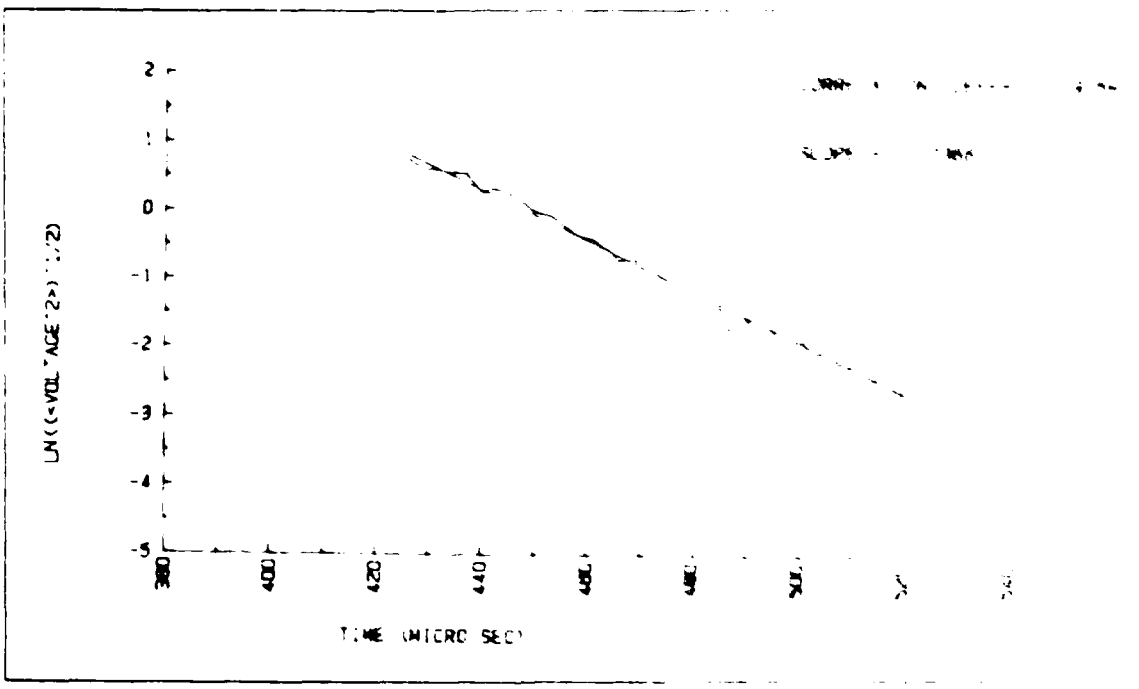

Figure G.8 DATA 77.

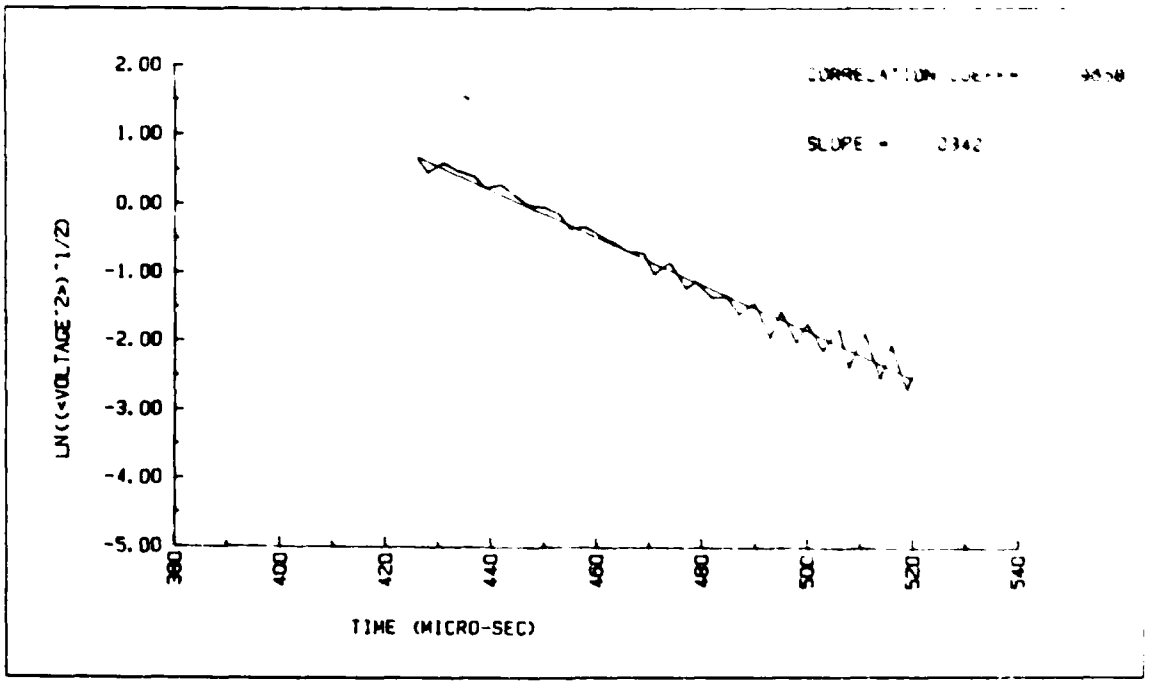

Figure G.9 DATA 78.

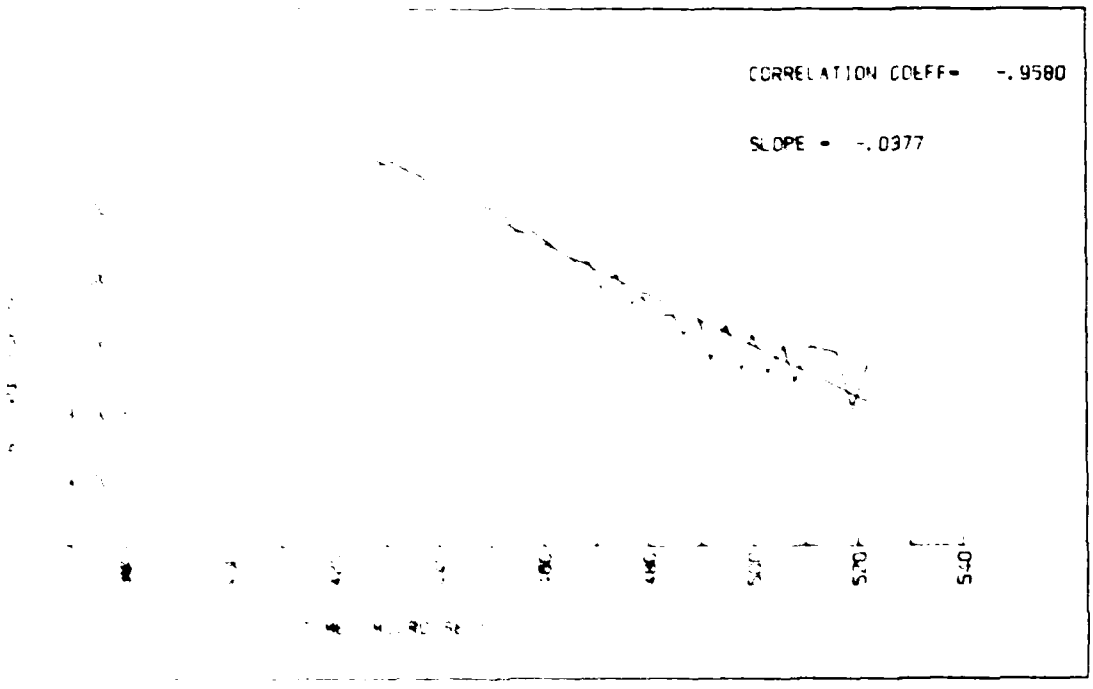

Figure C-10. DATA 79

AD-A186 905 ACOUSTIC BACKSCATTERING FROM BOTTOM SEDIMENT AT NORMAL INCIDENCE IN THE LABORATORY(U) NAVAL POSTGRADUATE SCHOOL MONTEREY CA T YU SEP 87 2/2

UNCLASSIFIED F/G 20/1 NL

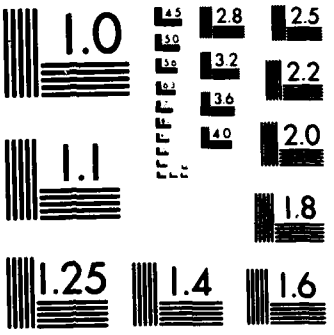

MICROCOPY RESOLUTION TEST CHART
NATIONAL BUREAU OF STANDARDS-1963-A

LIST OF REFERENCES

AMOL/Ocean Acoustics Division, NOAA, *Ross Transducer Test Report, 1979.*

Bezdek, H.F., Reflection of High-Frequency Sound at Normal Incidence from the Ocean Bottom. *Journal of Geophysical Research*, Volume 78, No. 17, June 1973.

Bunchuk, A.V. and Zhitkovskii, Yu.Yu., Sound scasttering by the ocean bottom in shallow-water regions. *Sov. Phys. Acoust.*, 26(5), Sept.-Oct. 1980.

Bradshaw, J.A., *Laboratory Study of Sound Propagation into a Fast Bottom Medium*, M. S. Thesis, Naval Postgraduate School, Monterey, CA., June 1981.

Chang, Chin-Wen, *Remote Sensing of Ocean Sediment Volume Reverberation*, M. S. Thesis, Naval Postgraduate School, Monterey, CA., December 1986.

Clarke, T.L., Proni, J.R., Seem, D.A., and Tsai, J.J., *Joint CGS-AOML Acoustical Bottom Echo-Formation Research I: Literature Search and Initial Modeling Results*, NOAA Technical Memorandum ERL-AOML, Miami, Fl., 1984.

Diaz, Frederico R., *Preliminary Study of a Technique for Measuring the Volume* Backscattering from Sediment, M. S. Thesis, Naval Postgraduate School, Monterey, CA., September 1986.

Eyring, C.F., Christensen, R.J. and Raitt, R.W., Reverberation in the Sea. *The Journal of The Acoustical Society of America*, Volume 20, No. 4, July 1948.

Facada, Joao F.F. *Volume Reverberation Measurements of Sediments in the Laboratory*, M. S. Thesis, Naval Postgraduate School, Monterey, CA., June 1987.

Ivakin, A.N. and Lysanov, Yu.P., Backscattering of sound from an inhomogeneous bottom at small grazing angles. *Sov. Phys. Acoust.*, 31(3), May-June 1985.

Jackson, D.R., Winebrenner, D.P. and Akira Ishimaru, Application of the composite roughness model to high-frequency bottom backscattering. *The Journal of Acoustical Society of America*, 79(5), May 1986.

Kinser, L. E., Frey, A. R., Coppens, A.B., and Sanders, J.V., *Fundamentals of Acoustics*, Third Edition, Wiley & sons, Inc.,New York, 1982.

Nicholet Instrument Corporation, *Nicholet 3091 Operating Manual*, 1985.

Pace, N.G. and Ceen, R.V., Seabed classification using the backscattering of normally incident broadband acoustic pulses. *The Hydrographic Journal*, No. 26, October 1982.

Urick, U.J., *Principles of Underwater Sound*, Third Edition, McGraw-Hill, Washington D. C., 1983.

Wyber, R.J., The dependence of bottom backscattering on the structure of a layered scattering medium. *The Journal of Acoustical Society of America*, 78(2), August 1985.

INITIAL DISTRIBUTION LIST

		No. Copies
1.	Defense Technical Information Center Cameron Station Alexandria, VA 22304-6145	2
2.	Library, Code 0142 Naval Postgraduate School Monterey, CA 93943-5002	2
3.	Chairman, Department of Oceanography Code 68Co, Naval Postgraduate school Monterey, CA 93943	1
4.	Dr. J.V. Sanders,Code 61Sd Department of Physics Naval Postgraduate School Monterey, CA 93943	1
5.	Dr. Stevens P. Tucker Code 68Tx, Naval Postgraduate School Monterey, CA 93943	1
6.	Dr. A.B. Coppens,Code 61Cz Department of Physics Naval Postgraduate School Monterey, CA 93943	1
7.	Library of Chung-Cheng Institute of Technology Tashih, Tao-Yuan, Taiwan Republic of China	1
8.	Director Yao, Neng-Chun Chinese Naval Hydrographic and Oceanographic Office Tsoying, Kaohsiung, Taiwan Republic of China	1
9.	Ma, Wei-ming SMC #2229, N.P.S. Monterey, CA 93943	1
10.	Dr. Von Schwind,Code 68Vs Department of Oceanography Monterey, CA 93943	1
11.	Wang, Chung-Wu	1

#22, Alley 51, Lane 375
Wu-Shing ST. Taipei
Taiwan, Republic of China

12. Yu, Ta-Te — 8
Chinese Naval Hydrographic and Oceanographic Office
Tso-Ying, Kaohsung, Taiwan
Republic of China

13. Kuo, Feng-Yu — 1
Chinese Naval Hydrographic and Oceanographic Office
Tso-Ying, Kaohsung, Taiwan
Republic of China

14. Chinese Naval Hydrographic and — 1
Oceanographic Office
Tsoying, Kaohsiung, Taiwan
Republic of China

15. Chairman, Survey Engineering Department — 1
Chung-Cheng Institute of Technology
Tashih, Tao-Yuan, Taiwan
Republic of China

16. Chairman, System Engineering Department — 1
Chung-cheng Institute of Technology
Tashih; Tao-Yuan, Taiwan
Republic of China

18. Facada, Joao — 1
Instituto Hidrografico
Rua das Trinas 49
1296 Lisboa Codex
Portugal

19. Director, Charting and Geodetic Sciences — 1
N/CG, Room 1006, WSC-1
National Oceanic and Atmospheric Administration
Rockville, MD 20552

20. John R. Proni — 1
Atlantic Oceanographic and Meteorological Laboratory
National Oceanic and Atmospheric Administration
Miami, FL 33149

21. CDR. Kurt. J. Schnebele Code 68Sn — 1
Department of Oceanography
Naval Postgraduate School
Monterey, CA93943

END

FEB.

1988

DTIC